



Norwegian University of
Science and Technology

A Study of Cultured Cells on a Nanowire-based Reverse Transfection Device

Kai Muller Beckwith

Nanotechnology

Submission date: June 2011

Supervisor: Pawel Tadeusz Sikorski, IFY

Abstract

This work builds on previous research at NTNU into the use of vertically aligned copper oxide nanowire arrays as a versatile system to deliver biomolecules into cultured, adherent mammalian cells. The background for the project and previous work on the topic is presented, including a review of relevant literature on cell transfection systems, nanowire-based transfection, cell interactions with nanowires, surface functionalization strategies and details on relevant materials. Methods and results of the current work are presented and discussed. Initially, methods to study cultured cells were investigated, including various fluorescent dyes and drying procedures for electron microscopy, and optimal procedures were found. Copper oxide nanowire arrays were grown by thermal oxidation and incorporated into functional, transparent devices by polymer processing and photolithography with PMMA, PDMS and SU-8. This led to optionally PDMS- or gold-coated nanowires protruding from an SU-8 surface patterned with wells. Surface functionalization strategies for optimal biomolecule binding were investigated, including organothiols on gold and organosilanes on glass, PDMS, SU-8 and mica. Thiols on gold were found to be challenging to study due to fluorescence quenching and substrate roughness, but aminosilanes were successfully prepared and investigated through immobilization of fluorescent quantum dots and DNA. Patterning of surface chemistry was also used to modify cell attachment and spreading, defining areas with no cell attachment or defining arrays of single cells with defined morphologies.


Transparent nanowire devices displayed limited cell attachment and spreading. Numerous model samples were tested, and it was concluded that planar substrates of PMMA, PDMS and SU-8 were biocompatible, but that the patterned SU-8 structure together with a PDMS-layer induced cell toxicity, likely due to a retainment and subsequent leakage of a process solvent. Alternative routes to produce non-toxic nanowire surfaces were found, and HeLa cells were successfully cultured and studied on such surfaces. The cells generally spread out in a way similar to flat culturing surfaces despite being penetrated by multiple nanowires. However, at high wire densities, reduced cell spreading was observed and attributed to lack of substrate contact. The HeLa cells were shown to interact with the nanowires, with cellular protrusions binding to and engulfing the nanowires regardless of nanowire surface chemistry. Preliminary experiments on delivery of a GFP-encoding plasmid showed transfection of nanowire-penetrated cells, although transfection efficiency was low. The results are compared with relevant literature, and finally future prospects of the device in delivery applications and cell microarrays are discussed.

Declaration

Trondheim, June 15, 2011

I hereby declare that this master thesis was written independently and in accordance with "Reglement for sivilarkitekt- og sivilingeniøreksamen" at the Norwegian University of Science and Technology.

Kai Müller Beckwith



(Sign.)

Preface

This work was performed at the Department of Physics, NTNU. The experimental work was performed in the biophysics lab at Department of Physics and in the cleanroom facilities of NTNU NanoLab. I would like to thank Post.Doc. Florian Mumm at the Department of Physics, who has offered invaluable help and suggestions. I would also like to thank my supervisor Associate Professor Pawel Sikorski for all helpful guidance and discussions. In addition I would like to thank the NTNU NanoLab staff for their support in using the NTNU NanoLab facilities, and Kristin Sæterbø, Christina Sæten Fjeldbo, Berit L. Strand, Sylvie Lelu, Magnus Olderløy and Minli Xie for help with cell culturing, DNA plasmids and other experiments. This thesis builds on work done in my specialization project in the fall of 2010. Although all results reported are obtained during work on the master's project, the results are in some cases compared with results obtained during the specialization project. In addition, the theoretical sections on the molecular basis of gene expression, current biomolecule delivery strategies, copper oxide nanowire growth, and SU-8 are included with some revisions for completeness, while the remaining sections are either significantly revised or entirely new. New methods of device fabrication were developed mainly by Florian Mumm, but are described here since the methods were verified and used for this project as well.

Contents

List of Figures	v
List of Abbreviations	vi
1 Introduction	1
1.1 Background	1
1.2 The current project	2
2 Theory	5
2.1 Perturbing cells by delivery of active biomolecules	5
2.2 Transfection methods	9
2.2.1 Viral transduction	9
2.2.2 Chemical transfection	10
2.2.3 Physical transfection	11
2.2.4 High aspect-ratio nanostructures for transfection	12
2.3 Culturing and studying adherent cells	13
2.3.1 General cellular reactions to material surfaces	13
2.3.2 Cells on nanowire surfaces	15
2.3.3 Methods to study cultured cells	17
2.4 Surface modification and imaging	23
2.4.1 Plasma treatment	23
2.4.2 Self-assembled monolayers	24
2.4.3 Studying material surfaces	25
2.5 Material properties	28
2.5.1 CuO Nanowires: Growth and properties	28
2.5.2 SU-8 series photoresist	30
2.5.3 PDMS	33
3 Experimental procedures	35

4	Results	43
4.1	Imaging cells	44
4.2	Progress in device fabrication	49
4.3	Surface functionalization	50
4.4	Sample toxicity and cells on model substrates	57
4.5	Cells on nanowire substrates	62
4.6	Nanowire-based delivery	67
5	Discussion	69
5.1	Device fabrication and surface functionalization	70
5.2	Device biocompatibility	73
5.3	Cells on nanowire arrays	74
6	Conclusion and future prospects	79
	Bibliography	92

List of Figures

2.1	Illustration of regular gene expression, forced plasmid expression and small interfering RNA (siRNA) silencing	8
2.2	Literature examples of cell patterning and cells on nanowire arrays.	18
2.3	Reverse transfection microarrays	22
2.4	Literature examples of surface effects, modifications and imaging	27
2.5	Copper oxide, structure and nanowire growth	31
2.6	SU-8 and PDMS chemical structures	32
3.1	A schematic overview of the process steps leading to a finished device.	35
4.1	Investigation of different visualization strategies for HeLa cells	46
4.2	eGFP-transfected HeLa cells	47
4.3	HMDS-dried HeLa cells on an SU-8 surface	47
4.4	SEM micrographs investigating the nanowire surfaces with an new fabrication procedure	48
4.5	AFM micrographs showing different attempts to produce flat gold surfaces	51
4.6	Amino-silane patterns on glass visualized by binding of quantum dots and fluorescent DNA	52
4.7	AFM micrographs of DNA immobilized on mica	55
4.8	Patterning cells by surface functionalization	56
4.9	HeLa cells on various test samples	59
4.10	Dissolved copper ions turn the solution blue and poison the cells	61
4.11	Confocal micrographs of HeLa cells grown on nanowire samples	63
4.12	SEM micrographs of HeLa cells interacting with nanowires . .	65
4.13	HeLa cells adopting different morphologies dependent on nanowire density and length	66
4.14	eGFP expression of HeLa cells on nanowire arrays	68

List of Abbreviations

AFM	atomic force microscopy	50
APTMS	(3-aminopropyl)trimethoxysilane	50
BSA	bovine serum albumin	53
calcein-AM	calcein-acetomethoxy	44
CPD	critical point drying	45
DAPI	4',6-diamidino-2-phenylindole	
DIC	differential interference contrast	
DMEM	Dulbecco's modified Eagle's medium	40
ECM	extracellular matrix	13
EDC	1-ethyl-3-[3-dimethylaminopropyl]carbodiimide hydrochloride	25
EDTA	ethylenediaminetetraacetic acid	39
eGFP	enhanced green fluorescent protein	45
FEG	field emission gun	41
FIB	focused ion beam	16
FITC	fluorescein isothiocyanate	44
GFP	green fluorescent protein	6
HEK293	human embryonic kidney cells	16
HEPES	4-(2-hydroxyethyl)-1-piperazineethanesulfonic acid	42
HMDS	hexamethyldisilazane	45
mES	mouse embryonic stem cells	16
NHS	N-hydroxysulfosuccinimide	25
NMP	N-methyl-2-pyrrolidone	38
NOA63	Norland Optical Adhesive 63	60
P11	rat embryonic dorsal root ganglion neurons	16

PBS	phosphate-buffered saline.....	40
PDMS	poly(dimethylsiloxane).....	36
PEG	poly(ethylene glycol).....	14
PGMEA	propylene glycol monomethyl ether acetate.....	58
PMMA	poly(methyl-methacrylate).....	36
PI	propidium iodide.....	44
SEM	scanning electron microscopy.....	43
siRNA	small interfering RNA.....	v
STM	scanning tunneling microscopy.....	26
TEM	transmission electron microscopy.....	76
TRIS	tris(hydroxymethyl) aminomethane.....	39
WGA	Wheat germ agglutinin.....	44
XPS	X-ray photoelectron spectroscopy.....	26

Chapter 1

Introduction

1.1 Background

Every human starts his or her life as a small vessel containing nutrition, metabolites, proteins and DNA. The information-bearing DNA plays a vital role in everything that is to come: growth and development, personality, diseases and ultimately even death. Between 20 000 and 25 000 genes encode up to 100 000 different proteins, and the relationship between the regulation of genes, gene products and how they effect humans is a vastly complicated research field busying thousands of researchers worldwide. Probing the relationship between genes and cell biology and behavior is one of the main endeavors of modern molecular biology, and it has greatly increased our knowledge of multicellular systems [1].

There are a plethora of methods available to experimentalists to probe these complex relationships, each with their benefits and drawbacks. Many of the methods rely on delivery of an *effector molecule* into the cell, i.e. a molecule that will effect the cell in some way. However, cells are surrounded by a bilayer membrane, inhibiting transport of charged or polar species such as the nucleic acids DNA and RNA, some of the most common effector molecules. Thus the molecules must be delivered in some fashion, and the various approaches involve packaging the biomolecule in lipids, viruses, cationic polymers or nanoparticles, all of which can cross the cell membrane more easily. This is termed *transfection* for non-viral methods and *transduction* if viruses are used. As all these methods rely on the biology of the cell to some extent, they are highly dependent on cell type and show a large variability in their effectiveness. Physical transfection methods offer greater possibilities as a universal delivery platform, but the standard methods need large volumes of cells and reagents and often show low cell viability after

transfection, which is problematic for limited patient samples and general low-cost approaches.

High aspect ratio nanostructures, called nanowires, nanopillars, nanorods or nanotubes [2], depending their morphology, is one field of research which has been gaining an increasing amount of attention as biomolecule delivery systems [3]. Briefly, the cells are cultured on a surface with protruding nanostructures with the effector molecules attached to the nanostructures. As the cells settle on the surface, they are impaled on the nanostructures. As the nanostructures are very small compared to the cells this occurs in a minimally invasive way, and the effector molecules are delivered into the cells. High aspect ratio nanostructures offer a physical delivery system that does not depend on the biology of the cell to any large extent, together with low cytotoxicity, spatially localized delivery and low amounts of reagent use. Thus, they are seen as possible candidates for a universal biomolecule delivery system for adherent cells (cells which grow on surfaces, as opposed to in solution).

1.2 The current project

Recently, methods for rapidly and simply producing and functionalizing large areas of nanowires have been developed at the Department of Physics at NTNU [4, 5]. Dense arrays of copper oxide nanowires that are about 100 nm in diameter and 1 μm to 10 μm in length can be rapidly grown from a thin copper foil by thermal oxidation, and the wires can be functionalized using self-assembled monolayers to modify surface properties.

We wish to develop a cell transfection array that uses nanowire impalement as a delivery vehicle, based on the above nanowire fabrication method. For such a device to be successful the nanowires must be able to bind cargo such as DNA molecules, the cells must grow relatively unperturbed on the wire array, and the wires must penetrate into the cells and deliver the cargo. In addition, there must be ways to image and study the cells, preferably in a format that is compatible with high-throughput microarray systems for rapid and quantitative cell analysis.

During my specialization project an SU-8 structure with protruding, gold-coated nanowires was produced and cells were cultured on the devices [6]. SU-8 is a negative epoxy-based photoresist known for high mechanical stability, transparency to visible light and cell compatibility [7]. Briefly, SU-8 was first applied as a thin ($\sim 4 \mu\text{m}$) layer, which buried some wires but left many protruding through the photoresist. Then a thicker ($\sim 50 \mu\text{m}$) SU-8 layer with "wells" down to the thin SU-8 layer and the nanowires was used

to produce mechanically stable samples with defined areas with and without nanowires. The copper substrate was then removed by acid etching, leaving a transparent SU-8-based structure with intact protruding nanowires. SU-8 was rendered hydrophilic and cell-compatible by oxygen plasma treatment, while the nanowires were covered in a thin (~ 4 nm) layer of sputter coated gold to allow the use of thiol-based chemistry for selective functionalization. It was shown that cells could be cultured on such a device, and were penetrated by the nanowires without apparent harm. Investigations into surface functionalization were also done, but with few conclusive results. There were also issues with the control of the acid etching step, and a relatively undefined surface with both lying and standing wires. In addition, early attempts at biomolecule delivery into cells did not show any results.

The goal of this Master's project is to further develop copper oxide nanowire-based impalement of cells as a versatile delivery platform, and improve upon some of the above issues. Specifically, certain improvements in the fabrication process are desired to improve the reliability and reproducibility of device production. Better control of surface chemistry and functionalization strategies for optimal molecule delivery are sought. Further it is desirable to investigate cell proliferation and behavior when cultured on the nanowire devices to ensure that the devices in fact can be used to study cells. Finally, solid proofs of cargo delivery via nanowire impalement would show the potential usefulness and advantages of such a system.

This thesis begins by describing the background of cellular gene expression, and how this can be controlled and studied by using DNA vectors and RNA interference. Further, the various methods that are available to deliver nucleic acids into cells are briefly described, including chemical, viral and physical methods, as well as novel techniques based on the use of nanostructured materials, since this is the field our platform operates in. As the platform that has been developed is only applicable to *in vitro* cell culture use, this will be the focus of these sections. In addition, how adherent cells react when introduced to a cell culturing surface is described, as this is very important to have in mind when designing devices for use in cell studies. Methods to study the *in vitro* cultured cells are described, including methods of confocal microscopy, microarray analysis and scanning electron microscopy. Further, as knowing the properties of the materials of the system is important for understanding how a device performs, both physically and in respect to cell culturing, an introduction to the various materials that are used is given. Methods behind altering the surface properties of materials are then described, with focus on the techniques relevant for our system. Finally, the current attempts to further develop the nanowire-based transfection device are described, including details of the fabrication, results and a

discussion concerning the current state and future possibilities of the system.

Chapter 2

Theory

2.1 Perturbing cells by delivery of active biomolecules

The flow of information in the cell, specifically the process of producing functional proteins from the information encoded in the genome, is sometimes referred to as "the central dogma of molecular biology" [8], but is more commonly known as *gene expression*. Briefly (more details can be found in e.g. [9]), cellular DNA (the genome) contains nucleotide sequences called genes, which encode functional proteins. Nearby in the genome are other sequences involved in the regulation of gene expression, such as promoter sequences. Protein complexes called transcription factors bind to the promoter sequences, allowing RNA polymerase enzymes to make an RNA copy of the gene in a process called *transcription*. This RNA copy is termed messenger RNA (mRNA), and will bind to ribosomes, which are large RNA/protein complexes. In the ribosome the information coded by the mRNA is used to produce the corresponding sequence of amino acids in a process called *translation*, which eventually results in functional proteins. The process of gene expression is illustrated in Figure 2.1a.

Cells can be forced to express a certain type of protein by introducing the gene encoding the protein into the cell. The most common method of achieving this is by using a special form of genetic construct called a *vector* [10]. Vectors can be based on viral genomes or bacterial genomes. Common to both is that they contain the gene of interest, typically introduced by recombinant DNA techniques (outside the scope of this work, see e.g. [11] for details), together with promoters and other regulatory sequences. When the vector reaches the nucleus of the cell, transcription factors bind to the promoter sequences and expression of the gene commences. This gene expression

can be either transient or stable, depending on whether the gene is incorporated into the chromosome of the cell or not [12]. Transient expression will fade over time, typically after only a few cell divisions, while stable expression will follow the cell line for multiple generations, even indefinitely. Typically a reporter gene is included in the vector [13]. A reporter gene encodes for a protein that allows some form for external readout, which can be used as an indicator for the expression level of the gene of interest. The most common reporter gene products are green fluorescent protein (GFP) and its analogues; yellow fluorescent protein, red fluorescent protein, etc. They allow fluorescent readout of gene expression, allowing both qualitative and quantitative analysis of expression levels. Luciferase, chloramphenicol acetyltransferase and β -galactosidase are other reporter proteins which allow luminescent, radioactive and colorimetric readout, respectively. An overview of the steps involved in DNA-vector based transfection is shown in Figure 2.1b.

The opposite strategy, suppressing the expression of a gene product, is called silencing the gene. This can be done by using the RNA interference system [14, 15]. Initially assumed to be a defense mechanism against viral attacks, it has later been shown that this is also a way the cell internally regulates gene expression [16]. Briefly, a 21-22 base pair double-stranded RNA molecule called a siRNA will bind to proteins in the cell to form a complex called an RNA-induced silencing complex (RISC), causing the degradation of one of the siRNA strands. RISC can bind to either mRNA or DNA that is complementary to the remaining siRNA strand, preventing the translation of the mRNA or the transcription of the gene, in both cases effectively preventing (silencing) expression of the gene. Gene silencing by siRNA molecules is illustrated in Figure 2.1c. An alternative approach to achieve silencing is the use of plasmid DNA vectors that code for siRNA strands [17]. This offers the advantage of using existing already optimized transfection protocols for plasmids, and the potential of a more sustained silencing (as each DNA plasmid gives rise to multiple RNA strands).

Both of the above techniques to modify gene expression are hugely important for biological and medical research today, already having revealed the function of numerous proteins and mechanisms in cells, the actions of infections agents and complex diseases, as well as lending hope to gene-based therapy in diseases such as HIV/AIDS, cancer or malaria (see e.g. [18, 19, 20] for some recent examples of the use of transfection in research on these diseases).

An alternative approach is the delivery of proteins into cells. This is a more direct route to studying the effects of a specific protein, and can also be used to induce specific, long-lasting changes into a cell [21]. This is the case for e.g. stem cell research, where one wishes to induce de-differentiation

of differentiated cells without altering the genome. Although few of the delivery systems available today are optimized for proteins, this will become an increasingly important field within cell biology research.

Efficient delivery of bioactive molecules to different cell types without side effects or cell toxicity represents a challenge in current molecular and cell biology [22]. There are several barriers that must be overcome until delivery is successful. DNA plasmids must reach the transcription machinery in the cell nucleus, while RNA and proteins must reach their target systems, typically in the cytosol. *In vivo* the barriers to delivery are significant, and involve the avoidance of natural defense systems such as the immune system, passage out of the blood circulation and diffusion through the extracellular matrix before even reaching the cell. *In vitro* these barriers are significantly less than *in vivo*, and only involve the barriers of the individual cell. This includes the cell membrane, which has a hydrophobic interior, efficiently inhibiting the passage of hydrophilic or charged molecules. However, the cell membrane is highly dynamic, and uptake of molecules outside the cell is a continuous process in regular cell function. The uptake occurs by several mechanisms, but common for most all of these is that the internalized molecules do not end up in the cell cytosol, but rather in separate vesicles called endosomes. As endosomes are processed in the cells the molecules inside are efficiently degraded by a lowering of pH, and the subsequent activity of multiple degrading enzymes. Thus, escaping the endosomes before degradation is a major approach in current delivery systems, and has been shown to be very important for delivery efficiency [23]. See e.g. [24] for a recent review of endosomal escape mechanisms in the various delivery systems. In the case of DNA transfection, reaching inside the nucleus is another major issue. The nuclear membrane is degraded at each cell division, which allows plasmids to enter the nucleus as the cells reform their nuclei after cell division. This is the typical strategy for most transfection systems, but lowers overall efficiency and limits transfection to relatively rapidly dividing cells.

In spite of these barriers, there are multiple systems which are able to deliver effector molecules into cells. Here follows a brief overview of the most common delivery systems together with a small discussion of advantages and disadvantages of each.

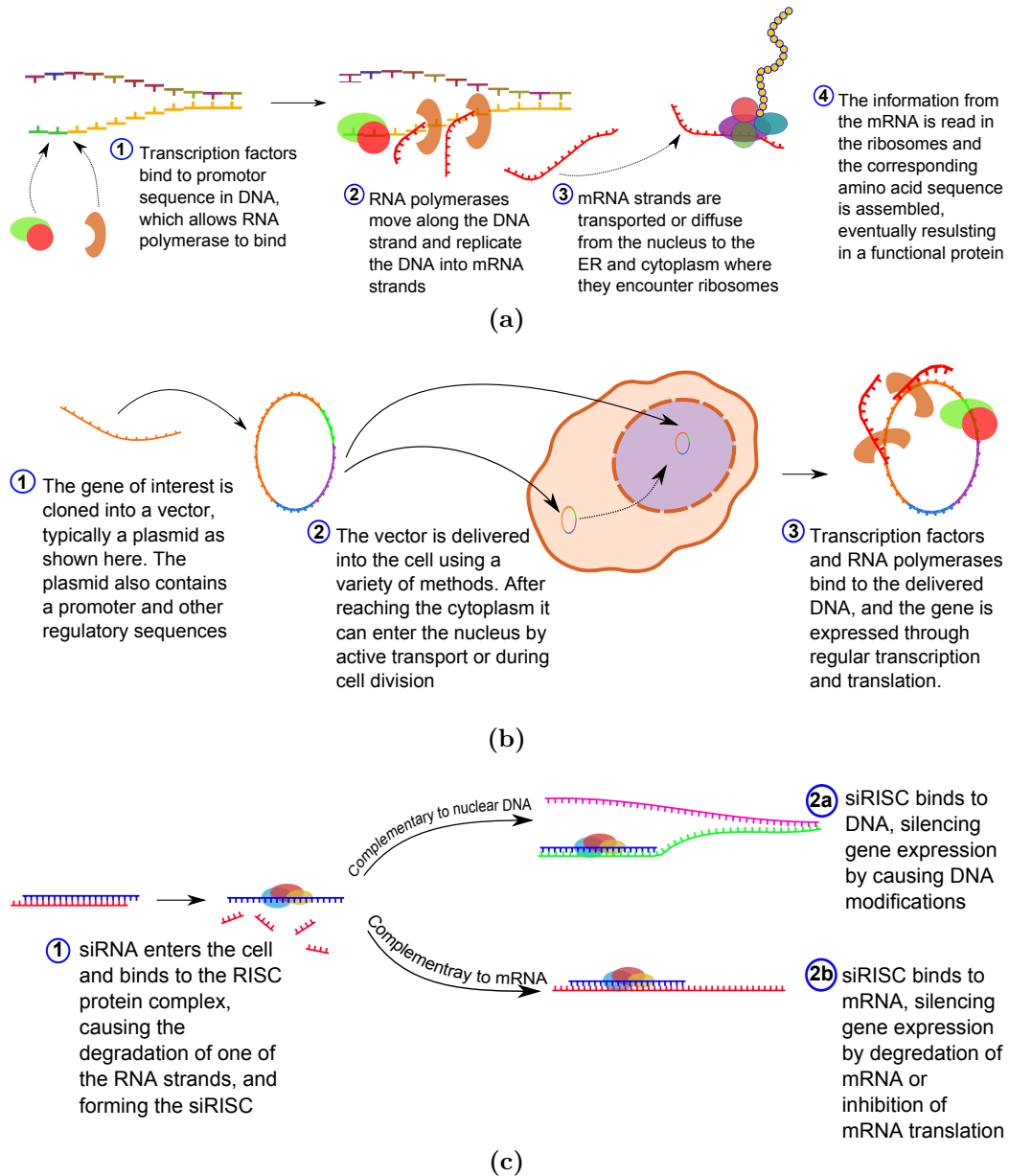


Figure 2.1: (a) The standard gene expression in a cell, including transcription of DNA to mRNA and translation from mRNA to functional proteins. (b) A DNA vector can be introduced into the cell and force the expression of specific proteins. (c) siRNA can be introduced into the cell, causing the silencing or knock-down of specific genes, either completely or partially depending on complementarity with the target gene. Illustrations are produced based on information in [9].

2.2 Transfection methods

2.2.1 Viral transduction

Viruses are advanced nanoparticles built of proteins and lipids which contain genetic material. They can only replicate through infection of a host cell, using the cellular machinery for their own benefit. Thus, viruses are nature's own specialists at getting foreign DNA into cells, they have evolved and survived using this strategy. *Transduction* is the term used to describe the deliberate use of viruses to deliver genetic material into cells. Transduction was the first [25] gene transfer method and is still widely used today. Viral gene transfer is the most effective of all delivery techniques (typically > 90% of exposed cells are transduced) [1, 26]. The most common viruses used are retroviruses (of which the popular lentivirus is one form), adenoviruses and adeno-associated viruses [27, 28]. The gene of interest and a reporter gene is introduced into the viral genome by recombinant processing. The viruses penetrate into the cells and the viral genes are expressed, either by being incorporated into the host genome or by transient expression. Viruses have mechanisms to avoid most of the cellular barriers. They show highly efficient endosomal escape after uptake by using a variety of specialized proteins [24]. Fusing plasmid DNA to viral peptide sequences that promote active DNA transport into the nucleus has also been shown to increase transfection efficiencies [29]. The original viruses are stripped of genes necessary to replicate, so they cannot destroy the target cell like a typical virus infection would. Although viruses can only deliver genome-type DNA and RNA into cells, they can be used for siRNA delivery and gene silencing experiments by utilizing the fact that certain types of DNA sequences are transformed into siRNA upon transcription [30].

Despite high transfection efficiency and ease of use once a protocol has been established, there are certain challenges in using viruses for transfer of genetic material. For *in vitro* use one of the main issues is complexity. If a new gene is to be studied, it must first be engineered into the virus. The virus must also be tailored or chosen for specific cell types, further complicating the procedure. However, commercial transduction protocols are appearing, simplifying the process [22]. Another disadvantage is the strict biosafety concerns when working with genetically modified viruses, leading researchers to hunt for alternatives which are less costly and easier to handle, such as the chemical approaches in the next section.

2.2.2 Chemical transfection

Chemical gene transfer is a form of transfection in which the negatively charged nucleic acids (i.e. different forms of DNA or RNA) are bound to one or more positively charged molecules to form a complex [31]. The complex is overall more suited to enter the cell than the nucleic acid alone. Cell entry occurs by some cell-mediated transport such as endocytosis. The first method to be developed as a non-viral form of gene transfer was (2-diethylamino)ether (DEAE)-dextran, a cationic polymer [32]. This method set the stage for many other cationic polymer systems, such as polyethylenamine, poly-L-lysine, chitosan and dendrimers [33, 34, 35, 36]. When the polymers and the nucleic acids are mixed in solution, they form nanosized complexes that may enter the cell through endocytosis. The polymers can also help protect the nucleic acids from endosomal degradation, and facilitate in endosomal escape [24]. Another widespread chemical transfection agent is calcium phosphate [37]. Calcium phosphate is co-precipitated with DNA to form nanoscale crystals, which are incubated with the cells for cellular uptake and transfection.

Although continuously developed and used due to their low cost and simplicity, both cationic polymers and calcium phosphate show cell toxicity and often low and unstable transfection efficiency. Both methods rely mainly on endocytosis to enter cells, which causes variations among different cell types. A third chemical method is *lipofection*, where the nucleic acid is packaged with synthetic cationic lipids for transfection [38, 39]. The lipids can form compact complexes or vesicular liposomes, which may enter the cells either by direct vesicle fusion, membrane integration, or via endocytosis. A general issue is the difficulty of characterizing and controlling the lipid-DNA complex, limiting the knowledge of how they function. However, reasonable efficacy together with low cytotoxicity contribute to the popularity of lipid-based techniques, and many commercial products, such as the widely used Lipofectamine and related derivatives (Invitrogen) and DOTAP (Roche), are available [33].

The above techniques have been around for 30-40 years, and continuous improvements have been made. Modern developments include combining polymers or lipids with other materials to make multifunctional nanoparticles, allowing modalities such as targeting for specific cells and controlled release [40, 41]. Examples of nanotechnology approaches are the usage of carbon nanotubes [42, 43], gold nanoparticles [44], silica nanoparticles [45] or gold or nickel nanorods [46, 47], as well as using targeting proteins with lysosomes to enhance uptake [35]. Another way multifunctionality can increase chemical transfection efficiency is photo-chemical transfection, which

enhances release of DNA from endocytotic vesicles using photosensitizers [23]. Concentration of the nucleic acids at the delivery sites, such as by tethering delivery vehicles at the cell culture substrate, has also shown promise in increasing the delivery efficiency [48, 49].

However, attempts to avoid variability among cell types together with the use of chemicals that can be toxic to cells or interfere with cellular function gives rise to another main class of delivery, termed physical transfection.

2.2.3 Physical transfection

Physical transfection mechanisms avoid certain complications of viral and chemical techniques by breaching the cell membrane directly and delivering naked (non-packaged or non-complexed) nucleic acids into the cell. The most obvious way to achieve this is by using a small syringe to inject the material directly. This method is efficient, and is often used for gene transfer to embryos, although cell damage is common [50]. Modern approaches using nanoscale needles attached to AFM tips show less cellular damage [51]. However, these techniques are still extremely labor-intensive, limiting use outside of studies on individual cells.

Electroporation is the most popular physical transfection method [52, 53]. It relies on the use of a transient electrical pulse which opens pores in the cell membrane, allowing the nucleic acid in the solution to diffuse into the cells. It is reasonably efficient, allows simultaneous transfection of large volumes of cells, and is simple to perform. However, it can only be used for cells in solution, and cell viability after electroporation is low, since membrane poration can easily cause membrane rupture, lysing the cells. Thus relatively large quantities of cells and reagents must be used, and due to different properties among cell types the protocol must be optimized for each cell type. Modern developments are improving on these disadvantages, but are not able to eliminate them completely [54]. Sonoporation is an alternative to electroporation in which transient membrane pores are induced by ultrasound bubbles [55]. Sonoporation has slightly higher cell viability, but lower transfection efficiency than electroporation [56], but the benefits and challenges remain similar.

Biolistic particle delivery (often called a *gene gun* due to the popular system from Helios) combines the directness of micro-injection with the large scale approach of electroporation, by launching a large quantity of gold nanoparticles that are conjugated with nucleic acids directly into cells. Although efficient and reliable, it is mostly used for *in vivo* DNA immunization and genetic modification of plants due to high equipment cost and a certain degree of cell damage upon delivery. The large amount of non-biodegradable

gold nanoparticles that are part of the system are also a cause of concern, but modern approaches using biodegradable alternatives of gold are being developed [57].

A combination of chemical and physical methods has led to some modern developments, such as magnetofection [58], which relies on the use of surface-functionalized magnetic nanoparticles [59, 60] or carbon nanotubes with embedded magnetic particles [61] for gene transfection. These approaches apply the chemical approach of complexing the nucleic acid with a cationic material, but similar to the gene gun, use an external force to cause higher transfection efficiencies, in this case by applying a magnetic field. These particles also offer the inherent benefit of being imaggable using magnetic resonance imaging, and are promising for both higher transfection efficiency and higher cell viability *in vitro* and for gene delivery *in vivo* due to high transfection efficiency, controllable transfection and low cytotoxicity.

2.2.4 High aspect-ratio nanostructures for transfection

The success of employing nanoscale materials for transfection has also prompted the development of techniques which use vertical arrays of silicon nanowires or carbon nanofibers to deliver biomolecules into cells in a process sometimes termed *impalification* [3, 62]. Biomolecules such as DNA, siRNA, proteins or other effector molecules can be deposited on the nanowires prior to cell culturing, either by direct adsorption, electrostatic interactions or specific covalent binding [63]. McKnight et.al. were the first to report delivery using such a system. They actively impaled cells onto carbon nanofibers (tapered, about 200 nm in diameter at the tip) by centrifugation or mechanical pressing [3]. They showed decent transfection rates (about 5%) of impaled cells, and the cells were seen to proliferate and divide up to 10 days after impalement while expressing the delivered genes. Kim et.al. successfully used silicon nanowires coated with polyethyleneimine for transfection, although transfection efficiencies were below 1% [62]. In a recent, comprehensive article by Shalek et.al. it was shown that many types of biomolecules, including DNA plasmids, RNA molecules, peptides, proteins and small molecules could be delivered into cultured cells [64]. The cells were cultured on amino-silane modified silicon nanowire arrays on which the fluorescently modified molecules had been pre-adsorbed. Delivery of biomolecules was done at very high efficiency (close to 100%), and transfection was demonstrated but not quantified, so actual transfection efficiency is uncertain. In addition, they showed delivery to and transfection of cell lines that are typically considered difficult to transfect, such as neurons. This was attributed to the physical nature of nanowire impalification, which can avoid cellular barriers to uptake. Nanowire arrays

also offer the advantage of spatially localizing the biomolecule delivery sites (as opposed to typical approaches which are solution-wide), which has shown to increase transfection efficiency in other platforms due to effector molecule concentration [48].

Since this work focuses on developing a system for transfection of cultured, adherent cells, the biochemistry of culturing cells on surfaces is described in the next sections. In addition, cells are cultured on substrates with nanowire arrays for various reasons in addition to molecule delivery, and how cells react to nanowire surfaces in general is also described. Finally, the methods used to study cultured cells are described, including fluorescence microscopy, reverse transfection arrays and scanning electron microscopy (SEM).

2.3 Culturing and studying adherent cells

2.3.1 General cellular reactions to material surfaces

It is often stated that adherent cells prefer certain types of surfaces and dislike others. This is only true to a very limited extent. A more complete picture includes serum proteins, which readily adsorb to most material surfaces [65]. It is mostly these proteins that cells sense and interact with when in contact with a surface. The most important proteins for cell adhesion to surfaces are *attachment proteins*, which include binding domains for cells, other proteins and the extracellular matrix. Two common examples are *fibronectin* and *vitronectin*, although many other proteins also play a role. *In vivo* these proteins facilitate binding of cells to the extracellular matrix (ECM). However, the ECM is typically not present in culture conditions (although sometimes surfaces are coated with e.g. collagen or laminin to mimic the extracellular matrix). Instead, these proteins mediate the binding between cells and material surfaces. Cell membranes contain proteins called *integrins* with extracellular motifs that can recognize and bind to the adsorbed attachment proteins, specifically to "cell attachment" motifs such as the RGD (Arg-Gly-Asp) sequence [66]. For most adherent cell types prolonged periods without this binding between integrins and cell attachment proteins can cause cell death, both through caspase-mediated apoptosis and through another form of apoptosis termed *anoikis* [67, 68]. However, not all surfaces with high protein adsorption support cell growth, as non-cell attachment proteins such as immunoglobulins or albumins may bind instead, or the cell attachment proteins might be denatured upon interaction with the surface, hiding or disrupting the necessary cell attachment motifs. Also, the link between cell

death and cell attachment is not completely clear-cut [69].

There are some general aspects of protein adhesion and cell proliferation on different types of surfaces [70, 71]. Proteins readily adsorb to hydrophobic surfaces due to hydrophobic interactions. However, adsorption to such surfaces often induces conformational changes in the proteins, as they rearrange to organize hydrophobic groups near to the surface and hydrophilic groups towards the solution. Thus cell growth on hydrophobic surfaces is usually limited, although not completely absent. This can also vary greatly depending on the specific treatment of the surface before cell culturing. An example of this is two articles in which nearly identical self-assembled octa- and hexadecanethiol monolayers are produced on gold. In the case where the functionalized surface was only exposed to serum during cell culturing it was cytophobic (hindering cell attachment), while if the surface was pre-treated with a fibronectin solution was cytophilic (promoting cell attachment) [72, 73]. This difference could also stem from different cell types, or different preparation procedures, but in general this illustrates how variable and important surface treatment can be for cell growth (see section 2.4 below for more details on surface modification methods).

Hydrophilic surfaces generally do not cause large conformational changes in serum proteins, so here it is rather a question of how much protein adsorbs to the surface. Certain proteins are also able to replace less tightly bound proteins over time, a phenomenon called the Vroman effect [74]. On hydrophobic surfaces proteins tend to bind more irreversibly [70]. Charged hydrophilic surfaces generally have significant protein adsorption and good cell growth, with electrostatic attraction and counter-ion dissociation upon protein adsorption as major driving forces. However, highly charged proteins do not adsorb to like-charged surfaces, as electrostatic repulsion will dominate here. Finally, uncharged hydrophilic surfaces can often resist protein adsorption, especially in the case of extended hydrophilic chains such as poly(ethylene glycol) (PEG) [75]. This is thought to be due to a reduced hydrophobic interactions together with effects of chain compressibility resisting adsorption of larger molecules. As cells do not attach and spread on surfaces without adsorbed attachment proteins, PEG is a widely used surface modification to inhibit cell growth.

Most surfaces do not contain a single functionality, but rather a mix of several functional groups. Here the relation between surface properties, protein adsorption and cell proliferation is more complicated [76]. In addition, the (nano)topography of the surface also plays an important role in how proteins adsorb and change conformation and subsequent cellular responses [77]. These complications make designing surfaces for good cell adhesion and growth challenging, but do indicate some general rules that are important

to consider when modifying surface properties. For a recent, comprehensive review of the current research on cell-biomaterial interactions, see [78].

On the intracellular side, integrins have binding sites for the cytoskeleton (especially the actin microfilament) and many signaling molecules [9]. Once the integrins bind to the attachment proteins, signaling cascades commence, resulting in integrin clustering, rearrangement of the actin filament so the cell spreads out, and the formation of *focal adhesions*, which are the primary contacts between cells and the extracellular matrix (or culturing surface) [79]. These are all factors necessary for the proliferation of adherent cells, and thus a rough measure of proliferation in such cells is the extent of cell attachment and spreading. In mobile cells, actin-containing protrusions called *lamellipodia* and *filopodia* extend from the main cell body as protrusions, and form new focal adhesions in the direction of cell movement. The cell cytoskeleton is able to react very specifically to certain types of input from the extracellular matrix or culturing surface [80]. This has been employed to e.g. pattern single cells on surfaces, define areas favorable to cell growth or specifically modify cell morphology, as shown in image Figure 2.2a. This can allow well-defined cells for quantitative studies, but can also alter cell behavior and growth in e.g. stem cell studies [72].

2.3.2 Cells on nanowire surfaces

As mentioned above, cells are not only sensitive to surface chemistry, but also the topography of the surface. Recently, there has been an increasing amount of research on producing well-defined nanotopographies to investigate how cells react to such structures (see [81] for a review). In relevance to this work, there have been some studies on how cells react to high aspect ratio nanostructures, such as nanopillars or nanowires.

Hällström et.al. showed that neurons cultured on gallium phosphide (GaP) nanowire surfaces showed similar viability and growth as cell on glass, significantly better than on planar GaP [82]. The wires had a surface coverage of $\sim 1 \mu\text{m}^{-2}$, a height of $2.5 \mu\text{m}$ and a diameter of $\sim 45 \text{ nm}$. The cells grew completely on top of the wires, and it could be seen that the wires penetrated into the cells to some extent. An image of a neuron cultured on GaP nanowires is shown in Figure 2.2b. In a similar study Zhao et.al. found the complete opposite. Using titanium carbide and titania nanowires of 70 nm in diameter, lengths of several micrometers and a density of $\sim 1 \mu\text{m}^{-2}$, they effectively repelled osteoblasts, with cells showing little attachment, low proliferation and high degree of apoptosis on the nanowire substrates [83]. This is not linked to surface chemistry or protein adsorption issues. The large difference between the results of Hällström et.al. and Zhao et.al. are

not clear, but might be tied to the use of different cell types, which might have different requirements for adhesion and proliferation, despite both being adherent cells. Lee et. al. also showed significant cell repulsion using a high-density ($\sim 126 \mu\text{m}^{-2}$) array of ZnO nanowires that were ~ 50 nm in diameter and ~ 500 nm long [84]. They attribute the reduced cell spreading and proliferation to the fact that the cells on the nanowire array are not able to produce focal adhesions, as they do on planar substrates. The same group found similar results for SiO₂-coated ZnO nanowires, indicating that it is not a surface chemistry, but rather a topological effect that causes the reduced spreading [85].

Berthing et.al. showed that human embryonic kidney cells (HEK293) and rat embryonic dorsal root ganglion neurons (P11) had similar proliferation when penetrated by indium arsenide (InAs) nanowires and on planar InAs surfaces and glass [86]. The nanowires were $1 \mu\text{m}$ to $3 \mu\text{m}$ in length, 100 nm to 300 nm in diameter, and the average density of the NW arrays was $0.3 \mu\text{m}^{-2}$. In this study it appeared that the cells were mostly in contact with the surface, with the nanowires penetrating into the cell interior. This is different from the systems above with a higher nanowire density, which likely makes a significant difference in cellular reactions to the surface. Berthing et.al. also showed that membrane integrity, protein expression and cell maturation occurred in a typical fashion despite being impaled by nanowires. An image of a cell impaled in this way is shown in Figure 2.2c. Although Berthing et.al. did not indicate any dependence between nanowire dimensions and cell proliferation, a study by Kim et.al. on HEK293 and mouse embryonic stem cells (mES) showed that for nanowires with a diameter of 400 nm and a length of $3 \mu\text{m}$ to $6 \mu\text{m}$ with a similar density (2-3 per cell, i.e, roughly $0.2 \mu\text{m}^{-2}$ to $0.3 \mu\text{m}^{-2}$) cells did not attach and died after 1 day, but on wires with a smaller diameter (90 and 30 nm) cell survival was reasonable ($\sim 80\%$) [62].

With platinum, silicon (Si) and silica (SiO₂) nanowires precisely defined by focused ion beam (FIB) milling Xie et.al. showed that neurons were effectively pinned to areas with nanowires, but that cell growth was otherwise unperturbed for nanowires of diameters of 75 nm to 400 nm and lengths of $0.7 \mu\text{m}$ to $2 \mu\text{m}$ in height [87]. The effects were similar for all three types of nanowires, so the pinning was assumed to be a geometrical effect and not a material-specific effect, with a proposed explanation that the wires served as focal adhesion points anchoring the cells more strongly than a flat surface. Neurons pinned on such a nanowire surface are shown in Figure 2.2d. All of the above articles and more (see section 2.2.4) state that the nanowires interact closely with the cells, and demonstrate by using SEM and confocal fluorescence imaging that it is likely that the wires penetrate inside the cells.

A recent article by the same group as above (Xie et.al.) showed elegantly that their silica nanowires were indeed in contact with the cytoplasm of PC12M neural cells and COS-7 fibroblasts, as antibodies conjugated to the nanowires were able to recruit and bind intracellular GFP [88]. In addition, they showed that the cells preferentially had outgrowths towards and ending at the nanopillars.

Apart from the article by McKnight et.al. [3], the cultured cells in the cited articles were allowed to passively settle on the nanowires, but the subsequent nanowire penetration mechanisms has not been described in detail. Shalek et.al. showed that the cultured cells were resting on top of their silicon nanowire array 15 minutes after plating, but the nanowires had penetrated into the cells by 1 hour after plating [64]. Rough calculations give a gravitational force of less than 1 pN for an average cell due to the density difference between the cells and the medium, while even very small nanowires (30-40 nm in diameter) have been shown to need a force of 100-200 pN to penetrate the cell membrane directly, although they can do so without perceivable harm [51]. However, factors such as cell adherence to the underlying substrate could significantly increase the downwards force of the cell, allowing penetration [89]. There also seems to be some wire penetration on substrates with a high wire density, but to what extent these actually penetrate into the cell cytoplasm has not been fully elucidated. In light of the literature above it seems likely that the nanowires to some extent directly penetrate the membrane, avoiding typical uptake mechanisms of the cells, although this needs to be studied in more detail. It is also likely that surface treatments, nanowire dimensions and morphology will effect nanowire penetration and cellular reactions to nanowires.

2.3.3 Methods to study cultured cells

The two main methods of directly imaging objects that are too small to see with the naked eye are optical microscopy and electron microscopy. In the case of *in vitro* studies on cultured cells, the most used techniques are (confocal) fluorescent microscopy and SEM. In the next sections, a brief introduction to these techniques together with typical sample preparation procedures and imaging possibilities are given. Examples of images of cells imaged by the methods described here have already been shown in Figure 2.2 above. In addition, high-throughput methods are becoming more and more important as both processing power and study complexity increases. High-throughput cellular microarrays are presented as an increasingly important method for qualitative cell studies.

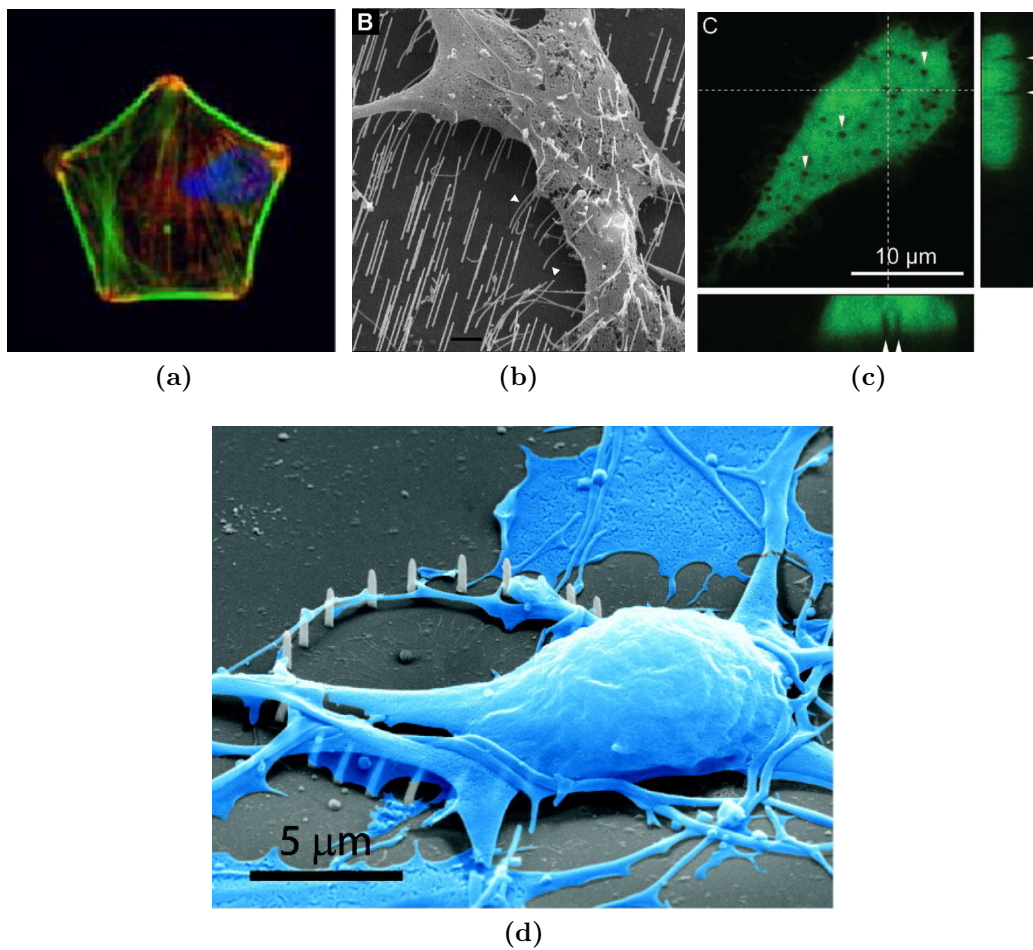


Figure 2.2: (a) Mesenchymal stem cells patterned by pre-adsorbing fibronectin to a patterned hydrophobic monolayer on gold. The image is a typical confocal fluorescence overlay, with the nucleus stained with DAPI (blue), the actin filament with Alexa488-phalloidin (green) and vinculin (a focal adhesion-specific protein) by an anti-vinculin antibody (red). Image from reference [72]. (b) Scanning electron micrograph of adult mouse dorsal root ganglia neurons cultured on a dense array of gallium phosphide nanowires. The cells adhere and spread, but gain little contact with the surface. The bent wires indicate cell interaction with the nanowires, but drying artifacts are difficult to rule out. Image from reference [82]. (c) Confocal micrograph of HEK293 cells stained with calcein-AM (the "live" stain in a typical live/dead staining kit), with black dots showing the volume excluded by penetrating InAs nanowires. Image from reference [86]. (d) Scanning electron micrograph of embryonic cortical neurons cultured on well-defined silicon nanowires used to pin individual neurons in place. Notice how the cell's extensions closely interact with the nanowires. This was shown to be largely independent of surface chemistry, and is attributed to geometry alone. Image from reference [87].

Confocal microscopy

Fluorescent microscopy is a light microscopy technique that relies on the use of fluorescently active molecules, called *fluorophores*, to obtain information-rich images of biological samples [90]. The microscope is typically set up in a reflection system, in which the objective lens also functions as a condenser lens. High intensity lasers are focused onto the sample, exciting the fluorophore to an electronically excited state. Upon relaxation, photons of a longer wavelength than the incident ones are emitted, due to the Franck-Condon and solvation effects. The light from the sample passes through an emission filter, which can be set so that it blocks reflected laser light but is transparent to the longer wavelength light emitted from the fluorophores. A scanning confocal microscopy system is similar, but in addition a pinhole (confocal) aperture is placed in a conjugate image plane, which filters out light that originates from fluorophores that are excited outside the focal plane. As this limits the focus area to a small point (diffraction limited to about half the wavelength of the light used), the laser needs to be raster-scanned across the surface, and the image is assembled point-by-point on a computer. This results in high contrast, high resolution images in both axial (along the optical axis, perpendicular to the sample) and lateral (parallel to the sample) directions. Small axial optical sections of some hundreds of nanometers can be viewed independently of one another, or reconstructed for a three dimensional rendering of the sample.

There exists a large variety commercial fluorophores, available with excitation and emission wavelengths in the whole visible spectrum and slightly outside. The standard fluorophores are small organic molecules with extended conjugated aromatic rings. These are provided with a number of functional groups, allowing them to bind to e.g. proteins, polymers or DNA. Quantum dots are a newer form of fluorophores, made of nanosized semiconductor crystals, with excellent excitation and emission properties [91]. Finally, fluorescent proteins such as GFP are in wide use as they are produced by the cells themselves.

Live cells can be imaged quite easily, although having environmental chambers which maintain temperature, CO₂ concentrations and humidity is an advantage for long-term studies. Membrane-binding or membrane-permeable dyes can be used directly. A common assay is combining a membrane-permeable dye that is rendered membrane-impermeable by intracellular enzymes with an membrane-impermeable dye, which is a relatively good assessment of whether a cell is dead or alive (the membrane of dead cells is usually compromised) [92]. An example of this is the live/dead kit with calcein-acetomethoxy (calcein-AM) and ethidium homodimer that is

used in the current work. For many dyes, especially those conjugated to proteins, antibodies or other larger molecules, the cell interior is not accessible in live cells. Instead, the cells are first fixed, typically using an aldehyde such as paraformaldehyde, which cross-links proteins in the cell. Then, the membrane is permeabilized either by lipid extraction in an (ice-cold) organic solvent or with a detergent/surfactant. Now the cell interior is accessible to e.g. dyed antibodies, allowing many specific intracellular structures to be visualized. The cells can also be maintained for a long time in this state, as long as they do not dry out.

Scanning electron microscopy

Although powerful for visualizing specific intracellular structures and live cells, the resolution of typical fluorescent microscopy systems is limited to about half the wavelength of the light used, i.e. some hundreds of nanometers. By using electrons instead of light for imaging, substantially better resolution can be obtained, typically down to a few nanometers or less [93]. Briefly, in an electron microscope, electrons are generated from a source and accelerated through vacuum by a strong electric field towards the sample. As the electrons impede on the sample the energetic collisions cause scattering of the incident electrons and generation of new, low-energy electrons and x-rays. All of these can be detected for high resolution imaging with material contrast and identification of elements. Similar to the scanning confocal system above, the electrons are focused into a small point, although in this case the point is limited by system design to a few nanometers or less. As the beam is raster-scanned across the sample, a computer stores the data from each point and assembles a complete image.

As the electron system needs to be in vacuum, biological samples must first be fixed and dehydrated, otherwise the water contained in cells will boil and evaporate, collapsing the cells and contaminating the microscope [94]. An alternative to dehydration is freezing, but this requires specialized microscopes and is not widely used in routine investigations of cultured cells. Fixation is similar to fixation for fluorescent microscopy, but usually glutaraldehyde is used in the place of paraformaldehyde, as it preserves structure to a higher extent after dehydration, but due to its high autofluorescence it is less used for fluorescent microscopy. Secondary fixation is often performed using osmium tetroxide, which stabilizes both proteins and the lipid membrane, in addition to providing increased contrast since osmium is a comparatively heavy element.

To dehydrate a biological sample the water must be gradually replaced by an organic solvent such as ethanol or acetone, as water has such high

surface tension that direct evaporation of water will collapse the cell. The sample can be air-dried from the organic solvents, but these still have quite high surface tension, so fine cellular details will be lost. The most common method of completing the drying is by critical point drying (CPD) [95]: The organic solvent is replaced first by liquid CO₂ under high pressure, then the CO₂ is brought past its critical point by raising the temperature. Finally, the pressure is reduced, allowing the CO₂ to evaporate without having crossed the liquid-vapor phase boundary, so no surface tension is induced. A simpler alternative to critical point drying is hexamethyldisilazane (HMDS) drying: After dehydrating the specimen with an organic solvent it is replaced with HMDS, which is allowed to evaporate in air. HMDS has a favorable blend of properties for such drying as it shows a low surface tension when interfaced organic materials, can rapidly infiltrate samples and is quite volatile. HMDS drying has been reported to provide similar structure preservation to CPD, at least for animal cells [95].

Finally, since biological samples are non-conductive, they must typically be coated with a thin layer of metal to avoid building up electronic charge, which interferes with the imaging. Gold, platinum or palladium are most used, since when sputter coated these give homogeneous thin films with small grain sizes and high electron yields, which gives a good signal.

Reverse transfection microarrays

Microarrays are a method to increase the throughput in studies where several effects or situations are to be studied simultaneously and automatically. In some fields, such as DNA and protein analysis, high throughput microarray approaches are commonplace, but microarrays for studying whole cells have only been developed more recently, the first example being from 2001 [96]. The typical approach uses the concept of *reverse transfection*, which means that the effector molecule is localized on a site before the cells are cultured. This is typically realized by using robotic spotters, where each type of effector molecule is patterned in one or more sub-millimeter sized spots [97]. After the effector molecule solution has dried out, the cells are seeded, and the effects of each effector molecule can be studied in an automated fashion using specially developed microscope systems, as exemplified in Figure 2.3a. This allows a highly quantitative analysis of transfection effects, easy comparison under identical conditions and high throughput. However, the cost of the equipment can be high, which, together with the difficulty and cost involved in assembling a library of multiple effector molecules, has limited widespread adoption. When such a system first is available it can be used very advantageously, which has been done locally at NTNU [98]. Single cells

can also be defined and analyzed in such a high-throughput way, which further reduces the variability typically seen when attempting to quantitatively analyze cells [99].

Transfection in microarrays is typically performed using chemical transfection reagents, so the issues associated with chemical methods still apply. Since chemical methods are dependent on cellular biology for uptake of the DNA or RNA, this limits the types of cells that are possible to transfect, and protocols have to be tailored for every cell type. Here the nanowire arrays show a large potential as they, as surface-based transfection techniques, should be easily converted to a microarray format. Indeed, in the already described article by Shalek et. al. this was successfully performed by using a standard microarray printer on the silicon nanowire array, as shown in Figure 2.3b [64].

This concludes the background for the cell-related methods in this work. Another important aspect is the properties of the materials that are used, and how these can be altered and studied. This is described in the next sections, starting with methods to specifically study and alter surface chemistry and study surfaces, moving on through the copper oxide nanowire arrays themselves, before finally describing properties, lithographic patterning and structuring of the most important polymer materials that are used.

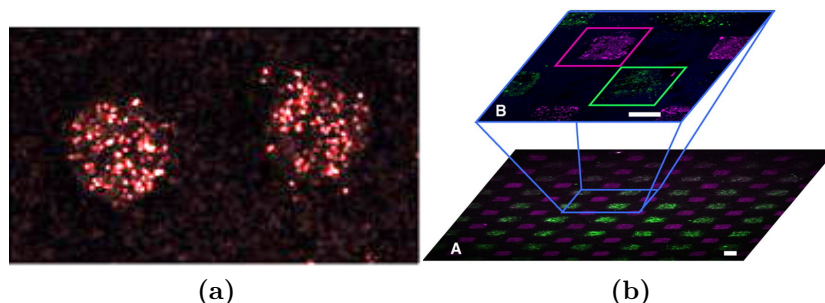


Figure 2.3: (a) Two spots ($\sim 800 \mu\text{m}$ each) of HEK293 cells transfected with DsRed (a red fluorescent protein analog of GFP) in a typical reverse transfection microarray set-up. Image from reference [98]. (b) A cell microarray printed with two kinds of siRNA (the two siRNAs are bound to each their fluorescent dye) on a silicon nanowire array surface with cultured HeLa cells. Image from reference [64].

2.4 Surface modification and imaging

Being able to modify surface chemistry is a key aspect of device production for biological applications, as this can drastically change how biomolecules and cells react to a given surface [100]. Many useful, but bio-incompatible materials can become more bio-compatible using relatively simple methods. Two common methods in widespread use are plasma treatment and various forms of self-assembled monolayers, and will be presented here.

2.4.1 Plasma treatment

Plasma is another name for an ionized gas, in which the electrons are continuously stripped from their molecules, forming reactive species and releasing UV radiation upon recombination [101]. To create a gaseous plasma, which is the most common form used for surface modification applications, a cyclic electric field (typically at radio frequency (RF), 13.56 MHz) is applied across a chamber filled with the gases to be ionized, often at reduced pressure. These gases can be air, oxygen, argon or many others. As the molecules are ionized, they form radicals which can react with molecules of the sample surface. High energy UV radiation is generated when free electrons recombine with ionized molecules, which can also introduce modifications in the sample by breaking bonds and forming radicals. Organic materials introduced into the chamber will typically undergo many surface modifications through these processes [101]. A common modification is plasma oxidation, where the surfaces are exposed to an oxygen plasma and incorporate a range of oxygen-rich organic functionalities including hydroxyl (-OH), carbonyl (-C=O) and carboxyl (-COOH) groups. Anisotropic removal of material (as it reacts with the plasma to form volatile species) typically increases the surface roughness, although this can vary from material to material.

As protein adsorption from serum is typically more favorable on hydrophilic, mixed functionality surfaces (as described in section 2.3.1), oxygen plasma modification is a very common method of making most polymeric surfaces cell compatible, including the production of e.g. tissue culture polystyrene [69]. In relevance to the current work, poly(dimethylsiloxane) (PDMS) as well as poly(methyl-methacrylate) (PMMA) and SU-8 undergo well studied changes in surface chemistry, increasing surface energy and cell compatibility upon exposure to oxygen RF plasma [102, 103, 104].

2.4.2 Self-assembled monolayers

Certain functional groups have high affinities for certain types of surfaces, and molecules with these functionalities can form well-ordered and dense films on the surfaces of materials to which they bind. Such self-assembled monolayer chemistry is a very important method to modify surface properties, as it allows the simple introduction of arbitrary functional groups to many types of surfaces by using bi-functional molecules [105]. The most common bi-functional molecules for monolayer formation are organosilanes, which bind to multiple surfaces, including silicon, glass and PDMS, and organosulfurs, which bind to many metallic surfaces such as gold and copper. These are described in further detail below. In addition there are many other functional groups that can bind to surfaces and induce functionalities, including phosphides, phosphates and phosphites, which bind to many oxides and semi-conductors, carboxyl groups which bind to certain oxides and metals, and amines, which bind to some metals and oxides [106]. A schematic of a generic self-assembled monolayer is shown in Figure 2.4b.

Silanes

Silanes are reactive compounds which have the general formula $X-Si-Y_3$, where X is a functional group and Y is a good leaving group, such as ethoxy or methoxy ethers or chloride (in order of increasing reactivity) [105]. These molecules react with surface silanol ($Si-OH$) groups, forming strong $-Si-O-Si-$ bonds to the surface of e.g. glass or plasma oxidized PDMS [107, 108]. It has also been shown that they react well with other $-OH$ groups, such as $-C-OH$ groups present on many (plasma) oxidized polymeric surfaces, such as SU-8 [109]. Figure 2.4e shows an example of a silane reaction with a hydroxylated surface. The assembly of high quality monolayers can be challenging, since the reaction is very sensitive to the amount of water present in the solution, and the silane molecules easily inter-polymerize [110]. Many deposition techniques exist, with most working to a certain degree, but requiring optimization to obtain defect-free, high density monolayer films.

The main methods to produce silane monolayers are [111]: Concentrated vapor phase, dilute vapor phase, organic liquid phase and aqueous phase deposition. Vapor phase deposition can be done either by heating in a closed chamber or in a vacuum desiccator, in both cases introducing the silane into the vapor phase where it will react with the surface. In liquid phase deposition the sample is immersed directly in the silane solution, and allowed to react. Typical incubation times to produce well-ordered films are 18-24 hours, although much shorter incubation times are also used [112]. Many

functionalities can be introduced through the silane molecule, and the type of functionality determines the reactivity of the surface towards molecules. This includes proteins and other biomolecules, which greatly effect the way cells react to a surface, as described above [113]. One typical use of silanes is to modify a negatively charged surface containing hydroxyl groups (this includes most plasma oxidized surfaces) with positive charges, allowing binding of negatively charged biomolecules. Examples are immobilization of DNA on amino-silanzed mica for AFM imaging [114] or binding of proteins to SU-8 [115].

Organosulfides

Silanes can generally not be used on metals, whereas molecules with sulfide functionalities (typically -SH, S-S or similar) have been shown to have a high affinity to many noble metals, including Au, Ag, Pt and Cu [106]. The most common are thiols (R-SH), which form well-ordered monolayers on the metal surface, and are simpler and more reliable than silanes as they hardly inter-react. The standard method of preparing monolayers on surfaces is by incubating the surface in a ~ 1 mM solution of the thiol in ethanol for 18-24 hours. However, if lower quality monolayers are acceptable incubation times can be reduced significantly, as monolayers of 70-80% of full coverage are formed upon the first few minutes of immersion [116]. As with silanes, most organic functionalities are available, although for most applications the standard functionalities of alkyl (-CH₃), hydroxyl (-OH), carboxyl (-COOH) and amine (-NH₂) are used. These cover the standard surface states of hydrophobic, uncharged but hydrophilic, negatively charged and positively charged (in solution), respectively. In addition, these groups allow many coupling reactions, such as the very common 1-ethyl-3-[3-dimethylaminopropyl]carbodiimide hydrochloride (EDC) and N-hydroxysulfosuccinimide (NHS) coupling reaction that allows the covalent binding of amine groups to carboxyl groups, often used for immobilizing proteins to surfaces. Other common functional groups include fluorosubstituted alkanes, which have a higher hydrophobicity than regular alkanes, and PEG, which is highly resistant to protein adsorption and cell adhesion. Another common strategy is to functionalize biomolecules with thiols so they can be directly immobilized on the metallic surface [117].

2.4.3 Studying material surfaces

Although the surface of a material is a very important feature, studying the surface exclusively is challenging, as the surface usually constitutes only

a minor fraction of the total material. This is especially the case for e.g. self-assembled monolayers and potentially attached biomolecules. In the biological sciences, fluorescent imaging is the major method of closely studying samples. On some commonly used surfaces, such as glass, this is not an issue. However, if e.g. thiol chemistry is used to bind molecules on metallic surfaces, this becomes more challenging due to the electrical activity of such surfaces. If fluorescent molecules are in close proximity to metallic surfaces, the fluorescence is typically quenched, reducing the observable signal significantly [118]. This is especially true for thin metallic films, as illustrated in Figure 2.4a. Depending on the situation, the mechanisms that usually lead to quenching can also increase the fluorescence of molecules, which is widely studied in well-defined systems such as with gold nanoparticles [119]. However, as the situations that lead to enhancement are often more specific and need to be more precisely controlled, quenching near metallic films is the norm. Scanning electron microscopy is not a well-suited technique either, as it lacks both the resolution and contrast to be able to specifically analyze surface species. However, many other techniques are available that are much better suited to study surface chemistry and molecules, including scanning probe systems such as atomic force microscopy (AFM) and scanning tunneling microscopy (STM), and spectroscopy systems such as X-ray photoelectron spectroscopy (XPS), auger electron spectroscopy and ellipsometry [93]. Only AFM will be described, as this is the only surface characterization technique used in this work.

AFM

Scanning probe systems work by raster-scanning a small tip across a surface and detecting a signal as a function of the position [93]. In an AFM the tip is attached to a cantilever which is oscillating near its resonance frequency. A laser is reflected off the cantilever, and the position of the laser is precisely detected using a quadrant (4 squares) photodiode detector. Near or on the surface the tip starts interacting with the surface, which causes a physical deflection and a change in the oscillating frequency of the cantilever, both of which can be detected with the laser. The system is extremely sensitive to such interactions, allowing height mapping in the sub-nm range, although the lateral resolution is limited by the tip size and scanning equipment to a few nm. Other measurements are possible, such as detecting forces between the tip and the surface or the hardness of the surface, and imaging can be performed both in air and in liquid. AFM has been widely used to study self-assembled monolayers, DNA, proteins, cells and combinations of these [106].

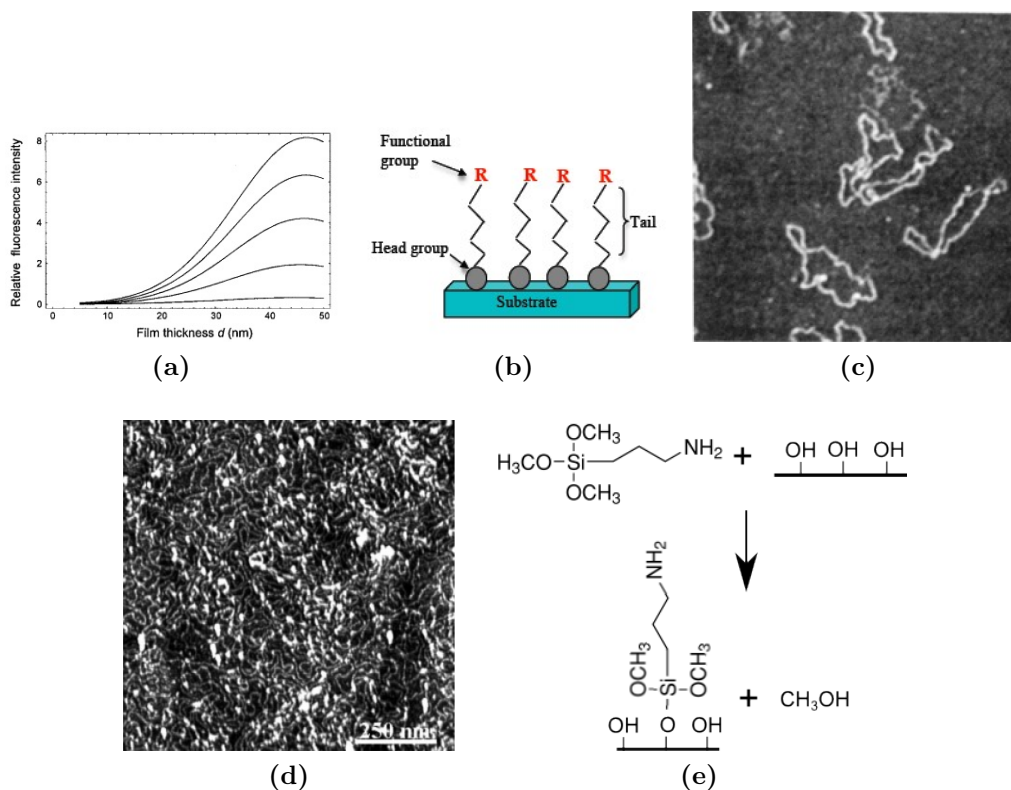


Figure 2.4: (a) Theoretical model of the influence of the thickness of a thin gold film on the fluorescent intensity of a fluorescent molecule near the surface, specifically 5-25 nm in 5 nm steps for curves from bottom to top. The excitation light in this case is at 633 nm. Image from reference [118]. (b) Schematic of a generic self-assembled monolayer film. Image released to public domain through Wikimedia Commons. (c) AFM image of plasmid (circular) DNA immobilized on a mica surface functionalized with an aminosilane. Scan size is 1 μm , image from reference [120]. (d) AFM image of DNA immobilized onto an ultraflat gold surface prepared by annealing and functionalized with cysteamine (gives a positive surface charge). The concentration of DNA is relatively high compared to (c), so the number of adsorbed molecules is much higher. Image from reference [121]. (e) An example of a silane reaction with a surface, in this case (3-aminopropyl)trimethoxysilane (APTMS).

One aspect of AFM imaging is that unless the surface is homogeneous and flat, distinguishing surface-bound molecules such as DNA or monolayers from intrinsic surface structure can be very challenging. Therefore, the most common substrate for imaging biomolecules with AFM is mica, a group of silicate minerals. Large sheets of mica can be easily cleaved off along atomic basal planes, leading to atomically flat substrates. The surface of mica is negatively charged and contains hydroxyl groups, so both electrostatic binding and silane functionalization is possible. The two most common methods of immobilizing e.g. DNA to mica are by using divalent cations, which form a bridge between the the anionic DNA and mica, and silanizing mica with an aminosilane to get a surface containing cationic amino groups [120]. An example of DNA molecules bound to mica is shown in Figure 2.4c. Other substrates common for AFM imaging include glass, which is flat enough for larger molecules and cells, but not DNA and small proteins, and silicon, which can be flat enough also for DNA [122]. Due to the widespread use of thiol functionalities, gold surfaces are also studied frequently in AFM, but more advanced techniques must be used to prepare gold surfaces that are flat enough. Typically, thin gold films are evaporated onto a flat substrate such as silicon or mica. Then, the gold film can either be annealed at high temperature [123], or glued to another substrate and stripped from the initial substrate, leading to flat gold by using the initial substrate as a template [124]. An example of DNA immobilized on a thiolated flat gold surface is shown in Figure 2.4d.

2.5 Material properties

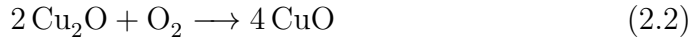
2.5.1 CuO Nanowires: Growth and properties

High aspect ratio nanostructures are emerging as one of the main fields of nanotechnology [125]. The structural materials include metals, semiconductors and insulators, and the growth methods range from filling porous templates to epitaxial growth. One of the simplest and most scalable techniques for nanowire growth is the direct thermal oxidation of a metallic film, resulting in the growth of nanowires perpendicular to the interface due to high surface strain between the metal and the metal oxide. This is the case for several metals such as iron [126], zinc [127], gallium [128] and tin [129], but the most common is perhaps the growth of CuO nanowires from metallic copper [130].

As metallic copper is heated in air, cuprous oxide (Cu_2O) is formed by the following reaction: [130]



However, as the thickness of the cuprous oxide layer increases, the availability of copper decreases, and oxidation occurs according to:



If the oxidation process occurs on copper substrates under favorable conditions, dense arrays of CuO nanowires can be formed in a three-layer structure as shown in Figure 2.5a [131].

Vapor-solid [130] and stress relaxation [132] growth mechanisms have been proposed, as these are typical for formation of metal oxide nanowires by thermal oxidation, but the current consensus is leaning towards a grain-boundary diffusion model [133], illustrated in Figure 2.5b.

Several factors can effect the growth of the nanowires. Depending on the temperature, the diffusion path of the copper can vary between grain boundary diffusion, dislocation diffusion and lattice diffusion. Nanowire growth only occurs in the temperature range where grain boundary and dislocation diffusion dominate, between about 400°C and 700°C [134]. Under these conditions the length of the nanowires follows a parabolic relation with time and increases with temperature [135]. The average diameter of the nanowires also increases with increasing temperature but the areal density (number of nanowires per surface area) decreases with increasing temperature, since higher temperature will anneal the grains in the cuprous oxide. Regulating the availability of oxygen can also affect both the diameter, length and density of the nanowires [136]. Since the growth appears to be related to a local electric field, an external electric field can also effect growth parameters such as length and diameter [137]. Thermally grown nanowires are polydisperse with regards to length and diameter, but are typically between 50 and 300 nm in diameter and from one to tens of microns in length. Surface coverage can range from essentially zero up to around $10 \mu\text{m}^{-2}$.

Stress appears to be an important factor if high quality arrays are to be produced, with higher surface tension leading to denser arrays of wires [5]. The large surface mismatch between cuprous oxide and copper can easily cause flaking of pieces of the copper oxide, making it hard to produce large, continuous arrays. However, this can be mitigated by using thin ($\sim 25 \mu\text{m}$) copper foils, under the hypothesis that a thin sheet copper is more compliant and thus some interfacial stress can be released through bending of the foil [5]. Such a large non-flaking sheet with a dense array of nanowires is shown in Figure 2.5c.

Current research on the applications of CuO nanowires involve sensors [131], photovoltaics [138] field emission [139, 140] and as electro-optical components [141], but so far little research has been done on interfacing CuO nanowires with biological systems. Although copper is essential as a cofactor to many enzymes, larger amounts of copper ions are reported to be toxic [142]. The primary mechanism involves catalyzing the formation of reactive oxygen species, which leads to widespread cell damage and toxicity. However, copper oxides are not soluble in water, which limits toxicity, although they readily form complexes with several ions [143]. Such factors are important to be aware of when interfacing inorganic and biological systems.

2.5.2 SU-8 series photoresist

Photoresists have typically been used in the semiconductor manufacturing industry to allow high resolution patterning of multiple layers of semiconductors and metals [144]. Photoresists are monomer solutions which can be selectively polymerized (negative resists) or dissolved (positive resists) by exposing them to high intensity UV light. Patterning is done by projecting the light through a mask, which allows the selective exposure of certain areas. More recently, photoresists have also been associated with microfluidic and lab-on-a-chip applications, although their primary use in this field are as temporary molds for PDMS systems (see below) [145]. However, one photoresist, SU-8, is also used as a structural component in many applications.

SU-8 series negative tone photoresist was developed by IBM to yield well defined high-aspect ratio structures [146]. SU-8 is an epoxy-based resin dissolved in a solvent, gamma-butyrolactone (GBL) for SU-8 standard series, and cyclopentanone for SU-8 2000 series. SU-8 comes in many concentrations, which means different viscosities and thus different film thicknesses upon spin casting. A higher number indicates increased viscosity, e.g. SU-8 5 is more viscous than SU-8 2. To the SU-8 solvent mixture a triaryl sulfonium antimony salt is added as a photosensitizer. When exposed to UV-light, preferably with a wavelength of 365 nm (the *i-line* of a mercury lamp) the photosensitizer releases a proton, which initiates an acid-catalyzed crosslinking between the epoxy groups of the SU-8 resin, causing the formation of a highly stable bisphenol polymer. The chemical structure of unreacted SU-8 is shown in Figure 2.6a. Each SU-8 molecule contains 8 free epoxy groups, any of which may react with other SU-8 molecules during the crosslinking reaction. Unexposed SU-8 can be removed in many organic solvents, the most common being propylene glycol monomethyl ether acetate (PGMEA).

Cured SU-8 is in principal transparent at visible wavelengths (above 360 nm), but shows some autofluorescence at high light intensities in the green

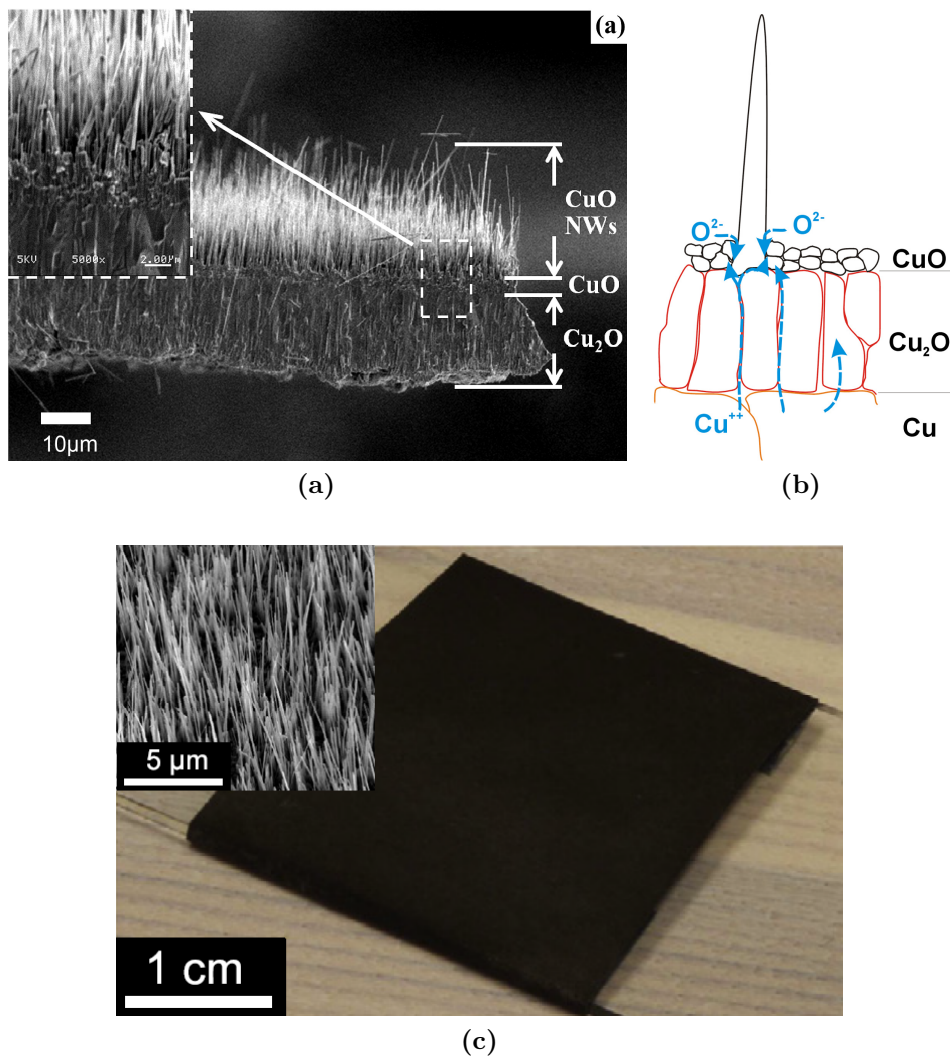


Figure 2.5: (a) Overview of copper oxide structure that is formed upon thermal oxidation of a copper substrate, with a thicker layer of cuprous oxide with long, narrow grains, a thin, highly defective cupric oxide layer and CuO nanowires protruding on the top. Image from reference [131]. (b) Schematic of the process of grain boundary diffusion in the formation of CuO nanowires. Oxygen atoms adsorb and ionize at the air-solid interface, creating an electric field that drives the diffusion of copper ions along the grain boundaries in the Cu_2O layer. Copper ions and oxygen combine at the bottom of the CuO layer, and crystallize to form a CuO nanowire. Illustration from reference [133]. (c) Digital photograph of a large, non-flaked array of copper oxide produced by thermal oxidation. A scanning electron micrograph of the nanowires on such a surface is inset. Images adapted from reference [5].

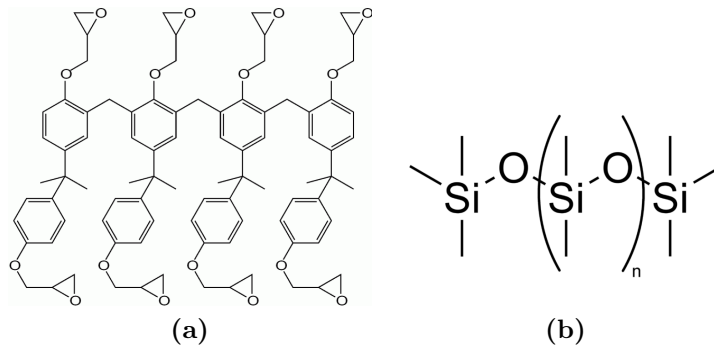


Figure 2.6: (a) The SU-8 monomer contains 8 free epoxy groups which may react with other SU-8 monomers during the photo-induced crosslinking reaction. (b) PDMS repeating unit consists of a siloxane backbone with methyl groups protruding from each silicon atom and is usually thermally cured using a catalyst. Images released to public domain through Wikimedia Commons.

(~ 500 nm) range [147]. Cured SU-8 shows good chemical stability, biocompatibility and gives the possibility of high aspect ratio structures, and has therefore seen increased use in bio-MEMS applications [7]. However, cured SU-8 is moderately hydrophobic due to the presence of aromatic, methyl and epoxy groups on the surface, with a contact angle of about 90° . For biological and microfluidic applications a hydrophilic interface is often required. The most common approach to achieve this is by activating the surface using an oxygen plasma treatment. This treatment causes the partial oxidation of the SU-8 surface, introducing carboxyl and aldehyde groups, and reducing the contact angle of water from 90° to under 10° , showing only moderate hydrophobic recovery over several months [148]. Oxygen plasma treatment also increases the surface roughness and concentrates antimony from the photosensitizer on the surface, probably due to preferential removal of carbon-containing species. Oxygen plasma treatment of SU-8 has also been shown to have a positive effect on cell proliferation [149]. This is associated with the chemical changes on the surface, and not the increased surface roughness. The increased antimony concentration on the surface could not be seen to have a detrimental effect, despite antimony being a known toxin, probably due to it easily being washed away during rinsing steps before cell culturing.

Two other techniques have been used to render the SU-8 surface hydrophilic: by grafting it with a hydrophilic co-polymer [150] or modifying the surface in a two-step process with cerium ammonium nitrate (CAN), nitric acid and ethanolamine [151]. It is well known that amines react with epoxy groups [152], which was initially assumed to be the reason the ethanolamine treatment caused a more hydrophilic surface. However, later investigations

showed that the ethanolamine treatment did not work unless the surface was pre-activated with CAN and nitric acid, although the ethanolamine does reduce the contact angle significantly more than CAN and nitric acid does alone [153, 154]. The proposed model is that ethanolamine binds to nitric acid groups incorporated into the surface after CAN and nitric acid treatment, although the actual mechanisms remain unclear.

2.5.3 PDMS

PDMS is a versatile and widely used silicon-based polymer, especially in lab-on-a-chip and other biomaterial systems [145]. This is mainly due to PDMS being impermeable to aqueous liquids but permeable to gases, transparent and bio-compatible. PDMS structures are produced by combining vinyl-terminated dimethylsiloxane oligomers with a curing agent consisting of more reactive siloxane hydride molecules and a platinum-based catalyst, after which the cross-linking reaction will commence. The repeating unit of PDMS is shown in Figure 2.6b. A wide variety of different PDMS types are available, but the most common completely cross-link in about 24 hours in room temperature. The cross-linking rate increases with temperature, down to about 10 minutes at 120 °C. PDMS is quite flexible and shows highly viscoelastic properties, easily molding itself to surfaces over time. Fabrication of PDMS structures usually occurs by cast molding and curing on a template, which often is made by photo patterning a material such as SU-8. PDMS easily flows into nanoscale features, making it very useful for reproducing a wide variety of surface features. However, due to a low Young's modulus (around 1-3 MPa depending on monomer to crosslinking agent ratio, curing temperature and geometry [155]), it does not have the mechanical strength to form high-aspect ratio features.

Native PDMS is hydrophobic due to the methyl functionalities, with a static contact angle of about 100° [156]. Mild oxygen plasma treatment replaces methyl groups with oxygen-rich groups such as hydroxyls (-OH), rendering the surface hydrophilic. When brought into contact with another plasma activated PDMS surface or glass and cured at elevated temperatures, a condensation reaction between the hydroxyl groups on each surface occurs, covalently binding the two surfaces through strong -Si-O-Si- linkages. More extensive oxygen plasma treatment forms a (SiO_x)-rich surface layer of up to 150 nm [157]. This layer is similar to silica glass, is somewhat brittle and typically contains cracks. It is also highly hydrophilic, like glass, as opposed to native PDMS. The hydrophobic character of PDMS typically recovers quickly due to diffusion of un-cross-linked monomers to the surface, reforming a methylated surface. This can be alleviated using a variety of

techniques, including storage in water [158] or thermal aging [159], however a rapid plasma treatment before device use is usually sufficient. Hydrophobic recovery typically takes a few hours, while bonding activity disappears within about 30 minutes [157].

Due to the hydrophobic nature of PDMS, cell adhesion to native PDMS can be quite low, but this depends on cell type, culture conditions, possible pre-adsorption of protein to the surface, etc [160]. Plasma activated PDMS surfaces typically show good cell compatibility.

Chapter 3

Experimental procedures

An overview of the processing steps from a freshly made nanowire surface to a finished device is given in Figure 3.1.

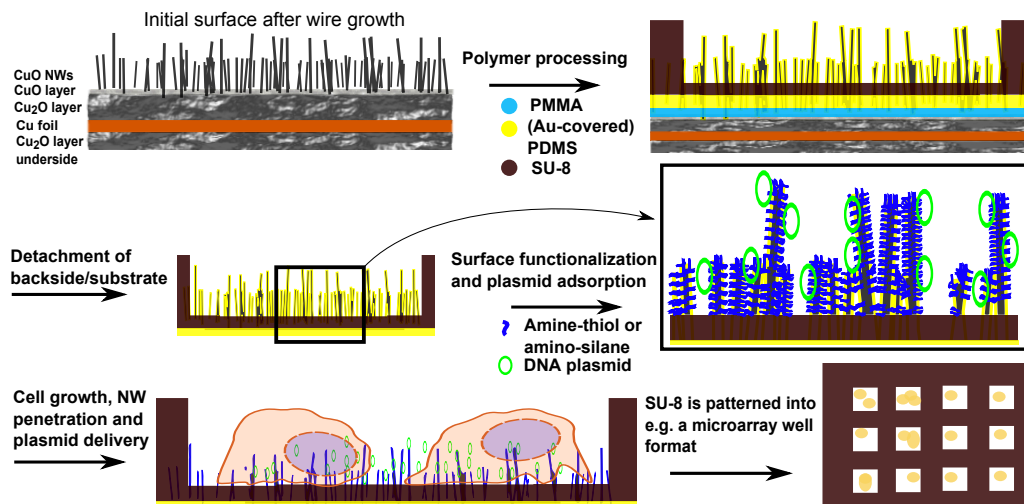


Figure 3.1: A schematic overview of the process steps leading to a finished device.

Nanowire growth

Copper foil (25 μm , 99,98% purity, Sigma Aldrich) was ultrasonicated for 1 minute in 2M HCl (Merck Chemicals, Germany), rinsed in water and ultrasonicated in acetone and ethanol (96%) or isopropanol for 1 minute each. The foil was then dried using a Kimtech wipe and stretched around a glass slide to obtain a flat surface with some tension, and smoothed with a rumpled tissue. The glass slide with the foil was put in a high temperature laboratory

oven (Carbolite CWF1200) at 500 °C for 120 minutes. The samples were removed from the oven and allowed to cool to room temperature.

Polymer structuring and processing

An overview of the polymer materials that are used and approximate thicknesses is presented in Table 3.1.

Table 3.1: The polymers that are used in device fabrication and associated properties. Given by order of application in the fabrication process.

Polymer	Approximate thickness	Structure
PMMA	1 μm	Planar
PDMS	1 μm	Planar, thin layer around nanowires
SU-8 2	2 μm	Planar
SU-8 2100	50 μm	Patterned with 500 μm wells down to the SU-8 2/nanowire layer

A sacrificial layer of poly(methyl-methacrylate) (PMMA) (PMMA-A9, MicroChem) was spun on the sample in a spin coater at 4000 rpm for 90 s, and baked on a hot plate at 180 °C for 5 minutes. An intermediate layer of poly(dimethylsiloxane) (PDMS) was then applied. PDMS (Sylgaard 184, Dow Corning) was prepared by mixing 9 parts of the monomer with 1 part of the catalyst solution, mixing thoroughly and dessicating under vacuum for 15 minutes. The PDMS was then diluted to 10% in hexane or tert-butanol and applied to the sample by spin coating at 6000 rpm for 90 s. The sample with PDMS was then cured at 80 °C for 20 minutes. On some samples a 4 nm gold layer was applied to the PDMS in a Cressington 208 HR sputter coating system.

Before further processing, a 50W, 12 s plasma treatment was then performed in an oxygen atmosphere of 0.4 mbar in a Diener Electronics Femto 13.56 MHz plasma system to increase the PDMS surface energy.

SU-8 2 (MicroChem) was then dispensed with a pipette on the sample until the entire sample was covered. The sample was spun in a spin coater at 6000 rpm for 90 s. All baking procedures were performed on contact hotplates. The sample was soft baked at 65 °C for 1 minute and at 95 °C for 3 minutes. The sample was flood exposed without a mask with an exposure dose of 300 mJ/cm² in a Karl Suss MJB3 mask aligner with an i-line (365 nm) mercury source. The sample was post-exposure baked at 65 °C for 1 minute and at 95 °C for 1 minute, before being allowed to cool to room temperature.

At this point some samples (i.e. non-transparent samples with an intact back side) either were used directly, or more commonly glued to a 15x15 mm cover glass slide by applying a thin layer of Norland Optical Adhesive 63 (NOA63), then exposing to 4J of UV-light in a Karl Suss MJB3 mask aligner.

Other samples were further processed without gluing by applying SU-8 2100 (MicroChem) using a plastic stick due to very high viscosity. This was done to ensure a layer covering the entire surface. Alternatively, structures were made using SU-8 2100 thinned 4:1 in SU-8 thinner (cyclopentanone) for simpler processing, parameters for thinned SU-8 are in parenthesis. The sample was spun at 3000 (1000) rpm for 90 s. A soft-bake was performed at 65 °C for 5 (3) minutes and 95 °C for 25 (12) minutes. The sample was then moved back to the 65 °C hot plate, and the mask (see below) was pressed onto the SU-8 photoresist. The sample was then exposed at 300(150) mJ/cm² through the adhered mask and post-exposure baked for 5 (3) minutes at 65 °C and 12 (7) minutes at 95 °C. The sample was then immersed in acetone, which partly dissolves the PMMA and swells the PDMS, which allows the copper oxide substrate to be separated from the SU-8 structure using mild agitation. In some cases the substrate could be separated without acetone immersion, either directly or by the use of Scotch tape to gently pull off the substrate.

Finally, the sample was developed in mr-Dev 600 (propylene glycol monomethyl ether acetate (PGMEA), Micro Resist Technology GmbH) for 10 (5) minutes with light agitation, rinsed in isopropanol and dried under a nitrogen gas flow.

A series of experiments was designed to test and verify the applicability and toxicity of the different materials and structures that were used (see section 4.4 for an overview). In these cases fabrication methods identical to those above were used, except the substrates were 15x15 mm cover-glass slides instead of oxidized copper foils, and in many cases only one or two layers of the device were made (e.g. only PDMS and SU-8 2). It was not possible to detach the glass slides from the rest of the structure as with the copper foil, so these samples simply underwent the same solvent treatment without substrate removal.

Fabrication of flexible masks

Masks for patterning SU-8 were designed in CleWin 4 (PhoeniX Software) and were made using two methods, as standard chrome masks on glass were too stiff to allow patterning of the somewhat uneven samples. For lower resolution masks, typically containing a lattice of squares with sides

of 300 μm to 700 μm , the masks were printed on a transparency foil using a standard laser printer (HP Laserjet 2200) at 1200 dpi. For higher resolution masks, PDMS slabs (about 2x2 cm, 1 mm thick) were prepared similar to the PDMS above. After curing, the slabs were plasma treated (100W, 10 minutes, 0.8 mbar oxygen atmosphere) to increase the surface energy, and placed on a glass slide for mechanical stability during further processing.

The positive photoresist S1813 (Shipley) was applied by spin coating at 3000 rpm for 30 s, baked at 115 $^{\circ}\text{C}$ for 1 minute, exposed through a commercial high resolution chrome mask on borosilicate glass at 150 mJ/cm^2 , and developed in MF-26 developer (MicroChem) for 1 minute. An 80 nm layer of chrome was applied using a Cressington 308R DC-magnetron sputter coater, as measured by a quartz crystal thickness monitor. Finally, lift-off was performed by sonicating the sample for 5 minutes in Remover PG (50-100% N-methyl-2-pyrrolidone (NMP), MicroChem). To protect the chrome features from detachment when the mask was applied to samples, a thin protective (~ 500 nm) PDMS layer was added by briefly plasma activating the mask surface (50 W, 12 s, 0.4 mbar oxygen atmosphere), spinning on 10% PDMS with crosslinking agent in tert-butanol at 3000 rpm for 60 s, before leaving to cure at room temperature over night.

Sample surface treatment and functionalization

Prior to further functionalization and cell culturing all samples were exposed to an oxygen plasma, typically 100W, 10 minutes, 0.8 mbar oxygen atmosphere, but in some cases a milder treatment of 50W, 5 minutes at 0.6 mbar of oxygen was used.

Standard sample

If gold had been sputter coated onto the PDMS layer, the sample was incubated in 1 mM cysteamine ($\text{SHCH}_2\text{CH}_2\text{NH}_2$) in ethanol for 30 minutes to produce amine groups on the surface.

If no gold was sputter coated, an amino-silane monolayer was applied instead by one of two methods:

Vapor phase deposition: The sample was placed in a vacuum dessicator together with 50 μL of (3-aminopropyl)trimethoxysilane (APTMS) (Sigma-Aldrich) on a glass slide for 1 hour, then rinsed well in ethanol and MQ-water (milli-Q water, 18 $\text{M}\Omega\text{ cm}^{-1}$, sterile filtered) and blow dried with nitrogen.

Aqueous phase deposition: The sample was immersed for 1 to 5 minutes in 1% APTMS in MQ-water, rinsed thoroughly in MQ-water and blow-dried with nitrogen.

Simplified, model samples

Test patterns of gold on glass were made by a standard lift-off process. Briefly, a layer of S1813 photoresist was patterned as when producing PDMS-masks. 10 nm of gold was then applied in a Cressington 208R sputter coating system, before finally lifting off the photoresist in Remover PG, leaving a gold pattern on the glass surface. If small features (e.g. 25 μm wells) were produced, the final lift-off was performed for 10 minutes in a sonicator. The gold patterns were then functionalized as above.

To validate the surface functionalization and discover optimal deposition parameters, fluorescent quantum dots or DNA were deposited. For quantum dot deposition experiments a 10 nM solution of carboxylated Qdot 605 ITK quantum dots (Invitrogen) in a 10 mM borate buffer (pH=8) was used. For DNA deposition experiments a solution of 50 $\mu\text{g mL}^{-1}$ salmon testes DNA (Sigma-Aldrich) in a buffer made of 10 mM tris(hydroxymethyl) aminomethane (TRIS), 2 mM ethylenediaminetetraacetic acid (EDTA) and 10 mM NaCl at pH=8 was used. If fluorescent DNA was needed 50 $\mu\text{g mL}^{-1}$ of propidium iodide (PI) (Sigma-Aldrich) was added to the DNA solution. A drop ($\sim 20 \mu\text{l}$ to $50 \mu\text{l}$) of DNA solution was applied to the sample, incubated for 20-30 minutes and rinsed off in MQ-water. The sample was dried in nitrogen before imaging.

Fluorescent imaging was performed using an Olympus CX21HAL fluorescence microscope with the appropriate filter sets (typically FITC or TRITC). AFM imaging of deposited species was also attempted using a Veeco Nanoscope II AFM with a silicon nitride tip in tapping mode at a scan rate of 1 Hz and a resolution of 512x512 pixels.

Ultra-flat gold surfaces were made to facilitate AFM imaging. The first method was by annealing. Briefly, freshly cleaved muscovite mica was inserted into a Pfeiffer Vacuum Classic 500 e-beam evaporator, warmed to 300 $^{\circ}\text{C}$ and left at 10×10^{-7} mbar for 1 hour. Then, 150 nm of Au was evaporated at a rate of 0.5 \AA s^{-1} . The sample was moved to a rapid thermal processing unit (Jipilec JetFirst 200) and annealed at 600 $^{\circ}\text{C}$ in an N_2 atmosphere for 5 minutes, then allowed to cool to room temperature. The second method of producing flat gold surfaces was template stripping. An identical evaporation procedure as above was performed either on silicon or mica. Then, a small piece of a glass microscopy slide was attached to the gold surface using a two-component epoxy glue and allowed to dry overnight. Stripping was performed by using a razor blade at the edge of the piece of glass until it loosened and could be lifted off together with the gold film. Deposition of monolayers and DNA was done as on the sputtered gold samples.

As there were difficulties involved in validating and investigating deposi-

tion of quantum dots and DNA on gold surfaces, silane-based surface chemistry was investigated instead. For fluorescent imaging tests, native cover glass slides or cover glass slides with a PDMS or SU-8 2 layer applied on top were fabricated using the same methods as when producing the standard device. 500 μm square patterns of S1813 photoresist were made on the samples, and silanization was performed using either aqueous or vapor phase silanization with APTMS, as above. Then quantum dots or DNA were deposited and imaged fluorescently in the same way as on the gold samples. For AFM imaging freshly cleaved muscovite mica was silanized by a 1 minute aqueous phase APTMS deposition before immersion in DNA solutions consisting of salmon testes DNA or eGFP plasmids ($10 \mu\text{g mL}^{-1}$ to $50 \mu\text{g mL}^{-1}$) for 20 minutes, rinsing and drying under nitrogen.

For experiments involving cell patterning patterned gold samples were produced as above. They were rendered hydrophobic by incubating the samples for 1-24 hours in a 1 mM solution of octadecanethiol (Sigma-Aldrich) in ethanol. For successful cell patterning the gold surface was blocked by incubating the sample for 1 hour in 1% bovine serum albumin (BSA) in MQ-water, rinsed in ethanol for sterilization and allowed to dry before cell culturing. Other rinsing procedures were also attempted, including rinsing in MQ-water, rinsing in phosphate-buffered saline (PBS) or directly placing the sample in serum. PDMS samples with an APTMS pattern were produced as above and also used in an attempt to pattern cells. The patterned samples were incubated in 1% BSA for 1 hour, rinsed with ethanol and dried before cell culturing.

Cell culturing

HeLa cells were cultured in 25 cm^2 culture dishes in growth medium (Dulbecco's modified Eagle's medium (DMEM) with 4.5 g L^{-1} D-glucose, 10% fetal bovine serum, 1% minimum essential medium non-essential amino acids and 0.5% L-glutamate). At 70-90% confluence they were removed from the culture dish by incubation in a trypsin/EDTA (0.25%/0.02%) solution for 3 minutes. Trypsination was halted by adding DMEM, and the cell suspension was centrifuged at 1500 rpm for 5 minutes. The supernatant was removed and the cells were resuspended in DMEM to a density of 50 000 cells/mL. The samples were sterilized by incubating for at least 15 minutes in ethanol, then allowed to dry in a laminar flow hood, or alternatively directly rinsed in MQ-water and PBS. 1 to 1.5 mL of the cell suspension was then added to a 12-well tissue culture plate containing the samples, typically giving $\sim 13\,000$ cells/ cm^2 (50 000 cells per well), although other seeding densities were also sometimes used. The cells were incubated at 37°C at 5% CO_2 for typically 2-3 days, but

also up to 9 days before imaging. In attempts to deliver cargo into the cells, the negatively charged species (PI ($50 \mu\text{g mL}^{-1}$ in MQ-water), quantum dots (10 nm in borate buffer) or plasmid DNA (eGFP, $50 \mu\text{g mL}^{-1}$ in PBS) were incubated for 30 minutes on the samples, which were either dried before use, rinsed in MQ-water and dried, or used directly without rinsing or drying.

Imaging of samples and cells

Electron microscopy

A Hitachi S-5500 field emission gun (FEG) SEM was used for all electron microscopy imaging at acceleration voltages of 10-20 kV. The secondary electron detector was used for all images. For non-processed nanowires and samples no preparation was done before imaging. For samples which had undergone SU-8 processing steps the sample was sputter-coated with 8 nm of Au or 8 nm of Pt/Pd before imaging to reduce charge buildup. When cells were imaged the samples were rinsed in PBS and fixated in 4% glutaraldehyde in PBS either over night at 4°C or for 2 hours at room temperature. After fixation they were rinsed in PBS and dehydrated in a graduated series of ethanol (30%-50%-70%-90%-96%-100%-100%, 5 minutes each) and either dried in a critical point drying system or transferred to 100% hexamethyldisilazane (HMDS) (two incubations) then removed and allowed to dry in a fume hood. Notice: HMDS is corrosive and harmful if inhaled, so all work with HMDS must be performed in a fume hood. Before imaging the samples were sputter coated with ~ 8 nm of Au or Pt/Pd.

Fluorescent microscopy of cells

Several fluorescent labels were used to study the cells: CellTracker Red (Invitrogen), live/dead kit with calcein-acetomethoxy (calcein-AM) and ethidium homodimer (Invitrogen), fluorescein isothiocyanate (FITC)-dextran (Invitrogen), fluorescein (free acid, Sigma-Aldrich), Alexa Fluor 488/Phalloidin (Invitrogen) and propidium iodide (PI). All were prepared according to the manufacturers protocols. Briefly, the following staining procedures were used:

CellTracker: The cells were rinsed in PBS and incubated in a $10 \mu\text{M}$ solution of CellTracker in DMEM for 30 minutes at 37°C , before incubation in growth medium for 30 minutes.

Live/dead kit: The cells were rinsed with PBS, then incubated in a solution of $2 \mu\text{M}$ calcein-AM and $4 \mu\text{M}$ ethidium homodimer in serum-free DMEM for 45 minutes, then rinsed again in PBS.

Exclusion staining: 100 μM stock solutions of fluorescein or FITC-dextran was added to the cell medium until a concentration of 10 μM was reached.

Actin staining: The cells were rinsed in PBS, fixed in 4% *para*-formaldehyde in PBS, permeabilized in Triton X-100 (0.1%) in PBS, and incubated with 6.6 μM of Alexa488-Phalloidin in PBS for 15 minutes. Finally, the samples were rinsed in PBS and transferred to fresh PBS for imaging.

Propidium iodide: 25 $\mu\text{g mL}^{-1}$ PI was added either directly to the cell medium during cell incubation or used together with actin staining.

eGFP transfection: HeLa cells were seeded in a 8-well Labtek confocal well plate at a density of 20000 cells per well ($\sim 30\,000\text{ cells/cm}^2$) and cultured for 24 hours. eGFP plasmids were diluted to 20 $\mu\text{g mL}^{-1}$ in PBS and Metafectene Pro (cationic lipid based transfection agent, Biontexas Laboratories GmbH) was diluted 1:10 in PBS, both after being brought to room temperature. The Metafectene solution was carefully added to the plasmid solution and incubated for 15 minutes at room temperature, giving a final plasmid concentration of 10 $\mu\text{g mL}^{-1}$ and a lipid:plasmid ratio of about 6:1. Finally, 3.3 μL of the transfection solution was added to each of the wells, and the cells were cultured for 2 days before rinsing in prewarmed PBS and imaging.

For fluorescent imaging of the cells and nanowires a Leica TCS SP5 II confocal microscope was used. This microscope has acousto-optic tunable filters (AOTF) that give band-pass filter characteristics in a user-selected interval. For each fluorophore, appropriate lasers and filter settings were determined from excitation and emission spectra given by the manufacturer. Typical settings were excitation at 488 nm and emission at 500-550 nm for "green dyes", and excitation at 543 nm and emission at 580-630 nm for "red dyes". For live (i.e. non-fixed) imaging the cells were transferred to pre-warmed 37 $^{\circ}\text{C}$ DMEM with 25 mM 4-(2-hydroxyethyl)-1-piperazineethanesulfonic acid (HEPES) to maintain appropriate pH at atmospheric CO_2 concentrations. Fixed cells were imaged in PBS.

Chapter 4

Results

This work has focused on several sub-topics which are not intrinsically connected, but form important parts of reaching the overall goal of producing a nanowire-based delivery platform. For clarity, a brief summary of this section is in order:

This section starts out by presenting methods that have been tested to study cells through fluorescence microscopy and scanning electron microscopy (SEM) on various substrates. Although these can be considered standard methods, the large number of methods available for such studies lends value to finding optimized methods appropriate for our system. Further, new progress in device fabrication is presented (see chapter 5 below for how this compares to device fabrication during my specialization project). It was found that some aspects of the new device fabrication process led to severe cell toxicity, and attempts to pin-point the source of the toxicity and how to avoid it are described. Then, investigations to find optimal surface functionalization strategies for molecule deposition and delivery are presented, together with ways surface functionalization can be used to control cell behavior. This was done on model systems that could be studied more simply than the final device. Using the methods and knowledge gained in these attempts, cells were cultured on nanowire devices and studied using fluorescence microscopy and SEM. The effects of surface functionalization and nanowire length and density are described together with a general analysis of cell-nanowire interactions. Finally, delivery of fluorescent molecules and DNA plasmids is presented.

4.1 Imaging cells

Although the procedures are mostly routine, there are very many different ways to image and investigate cells. To find the best suited procedures different fluorescent labels and methods were tested, including a live/dead kit with calcein-acetomethoxy (calcein-AM) and ethidium homodimer, CellTracker Red, propidium iodide (PI), Alexa 488-WGA, Alexa 488-phalloidin and fluorescein isothiocyanate (FITC)-dextran.

A common method of investigating cell viability is through the use of a live/dead stain, described in section 2.3.3. Using HeLa cells grown on glass the live/dead kit was tested with good results, as shown in Figure 4.1a. High selectivity was observed, with mutual exclusion between the live (green) and dead (red) cells in live cell samples. Staining by calcein-AM was homogeneous throughout the cell, with no apparent preference for organelles, while ethidium homodimer clearly shows the structure of the condensed DNA in the nucleus. Similar to calcein-AM, CellTracker Red is also dependent on active intracellular esterases for retainment. However, it was shown that CellTracker was not a reliable marker of live cells, as it also stained cells that were dead according to the live/dead kit, as shown in Figure 4.1b. Although both CellTracker Red and ethidium homodimer have fluorescence emission maxima around 605 nm, they could be separated by their different excitation spectra, by exciting with laser lines at either 488 nm (ethidium homodimer) or 543 (CellTracker). Despite not being useful for identifying live cells, CellTracker was still a good dye for brightly and simply labeling cells for general visualization of cells and cell morphology.

PI was investigated as an alternative to ethidium homodimer for labeling dead cells in a non-fixed cell sample, and gave similar results. As these dyes are cell membrane impermeable, they are effectively excluded from live cells. Thus these dyes could also be added to the cell growth medium without apparent harm to the cells, allowing quick identification dead cells in an otherwise unstained cell sample.

Wheat germ agglutinin (WGA) is a lectin with high affinity for carbohydrates, specifically sialic acid and N-acetylglucosamine sugar residues which are present on the plasma membrane. This should allow membrane-specific labeling of cells. A fluorescent conjugate of WGA and Alexa488 was investigated, and upon initial incubation it showed good membrane labeling properties, but it was quickly internalized into live cells, where it could be seen in vesicles in the cytoplasm, as shown in Figure 4.1c. For fixed but not permeabilized cells, membrane labeling properties were also good.

For cell structure investigations Alexa488-phalloidin, which binds strongly to actin filaments in the cell, could be used to provide insights into cell mor-

phology, allowing e.g. lamellipodia, filopodia and stress fibers to be visualized in detail. Cells had to be fixed and permeabilized to use this staining. This also allowed the advantageous use of PI as an additional stain for simple identification of individual cells, as it stains the nucleus and partly the cytoplasm (due to mRNA) of all permeabilized cells. Such labeling of HeLa cells is shown in Figure 4.1d.

Another method to investigate cells by confocal microscopy was exclusion staining. The solution was stained with a cell-impermeable molecule, which allowed visualization of the cell by negative contrast. Exclusion staining was investigated using PI, fluorescein (free acid) and FITC-dextran (70 kDa molecules). It was not possible to visualize PI in solution (fluorescence of PI increases strongly when bound to DNA), while fluorescein was seen to permeate cells to a certain extent, differing somewhat from cell to cell. However, dextran was excluded by the cells, allowing efficient visualization of cells by exclusion, as shown in Figure 4.1e.

Transfection of HeLa cells was performed using a cationic lipid based transfection reagent (Metafectene) and an enhanced green fluorescent protein (eGFP)-encoding plasmid. 2 days after adding the transfection reagent to the cultured cells, eGFP expression was visible in some cells as indicated by green fluorescence, although the transfection efficiency was only about 1% (this is a rough estimate and was not precisely quantified). eGFP-transfected cells were usually present in small clusters, which is likely due to that if the plasmid first reaches the cytoplasm, the cells need to divide for the plasmid to access the nucleus. When the cells divide the plasmid will be available in both nuclei, and thus expression is seen in several neighboring cells (that originally stemmed from the same cell). Another explanation is that the eGFP protein is transferred to daughter cells after cell division, the reality might be a combination of these. Expression levels also varied somewhat between the eGFP-expressing cells. An example of an eGFP-expressing cell cluster is shown in Figure 4.2.

The most commonly used methods to prepare biological samples for SEM were presented in section 2.3.3. Drying via hexamethyldisilazane (HMDS) is a simple alternative to the standard method of critical point drying (CPD). Although not thoroughly investigated, initial comparisons between HMDS-drying and CPD showed that cell shrinkage was not significantly different, and small structural details such as filopodia were clearly visible, as shown in Figure 4.3. In comparison with drying from 100% ethanol (as performed in previous work [6]) the improvements in cell preservation using HMDS are large.

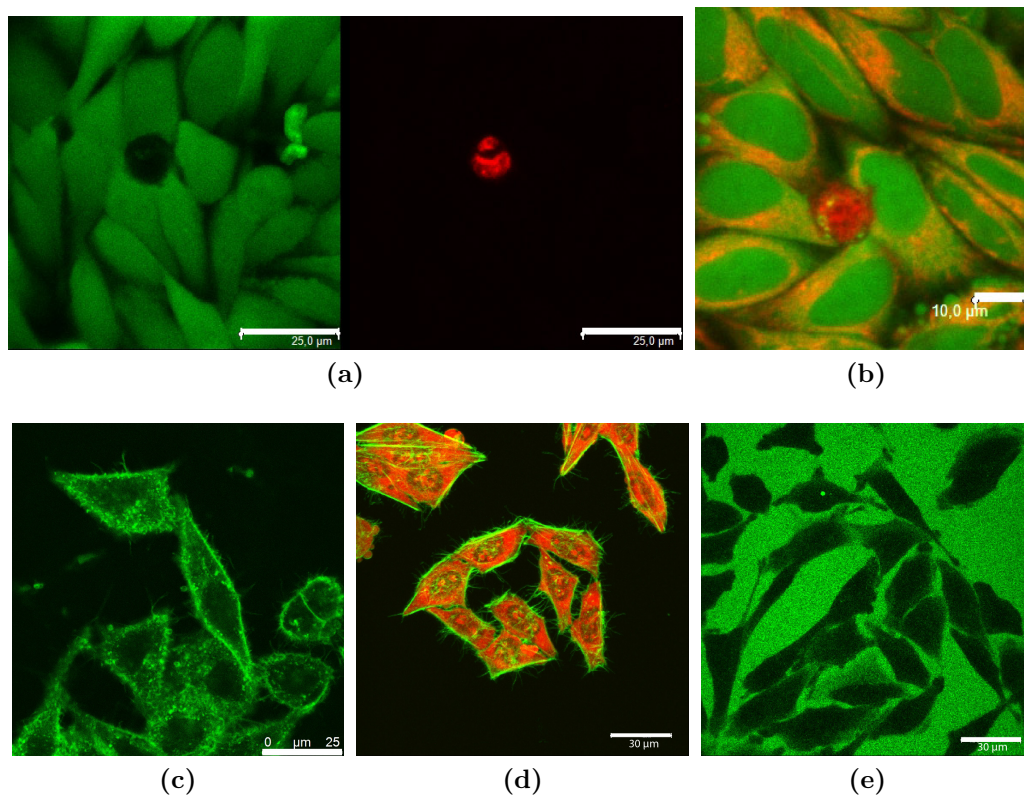


Figure 4.1: (a) Live cells are stained green with calcein-AM, while the dead cell shows no green signal but is labeled red by ethidium homodimer. (b) Live cells are stained green and orange (combined signal of green and red) by calcein-AM and CellTracker. However, dead cells were stained by CellTracker, but not by calcein-AM, indicating that CellTracker is not a reliable indicator for cell viability. (c) WGA (green) shows high affinity for the cell membrane. Cells are also stained red with CellTracker. (d) Maximum intensity projection of fixed and permeabilized HeLa cells cultured on glass, where the actin filament has been stained with Alexa488-phalloidin (green) and the RNA (cytoplasm) and DNA (nucleus) had been stained with propidium iodide (red). (e) Solution stained by $10 \mu\text{g ml}^{-1}$ 70 kDa FITC-dextran, which is not directly internalized by the cells.

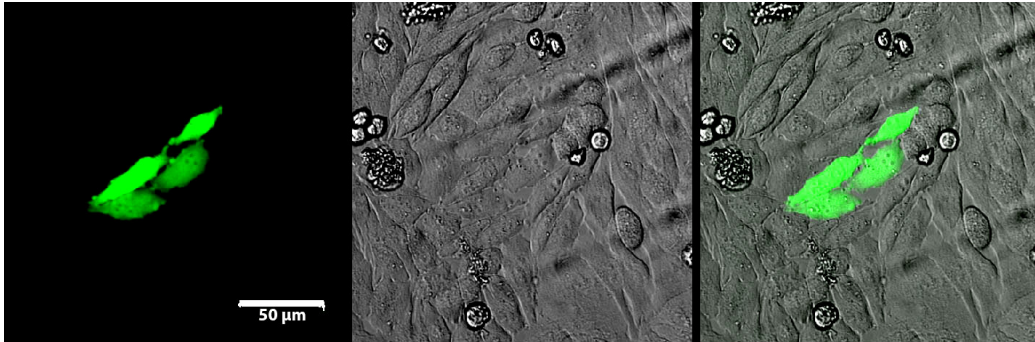


Figure 4.2: Confocal fluorescence (left), DIC (center) and overlay (right) images of HeLa cells expressing eGFP 2 days after transfection using Metafectene Pro. Note the clustering of the eGFP-expressing cells, and the varying expression level.

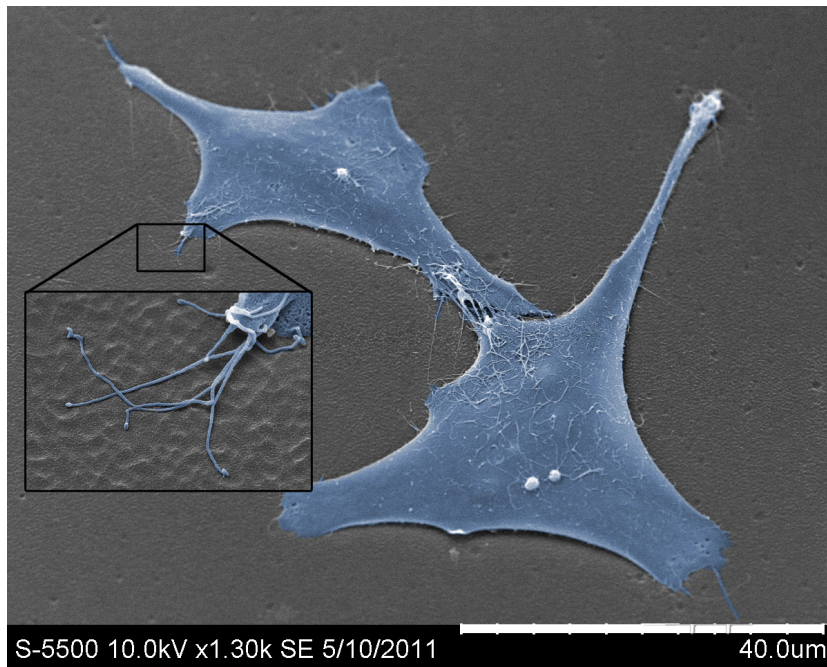


Figure 4.3: SEM micrograph of HeLa cells on SU-8, fixed and dried using the HMDS drying procedure. Inset: Closer view of some filopodia extending from the HeLa cells, indicating good structural preservation. Cells are false-colored blue for clarity in this micrograph.

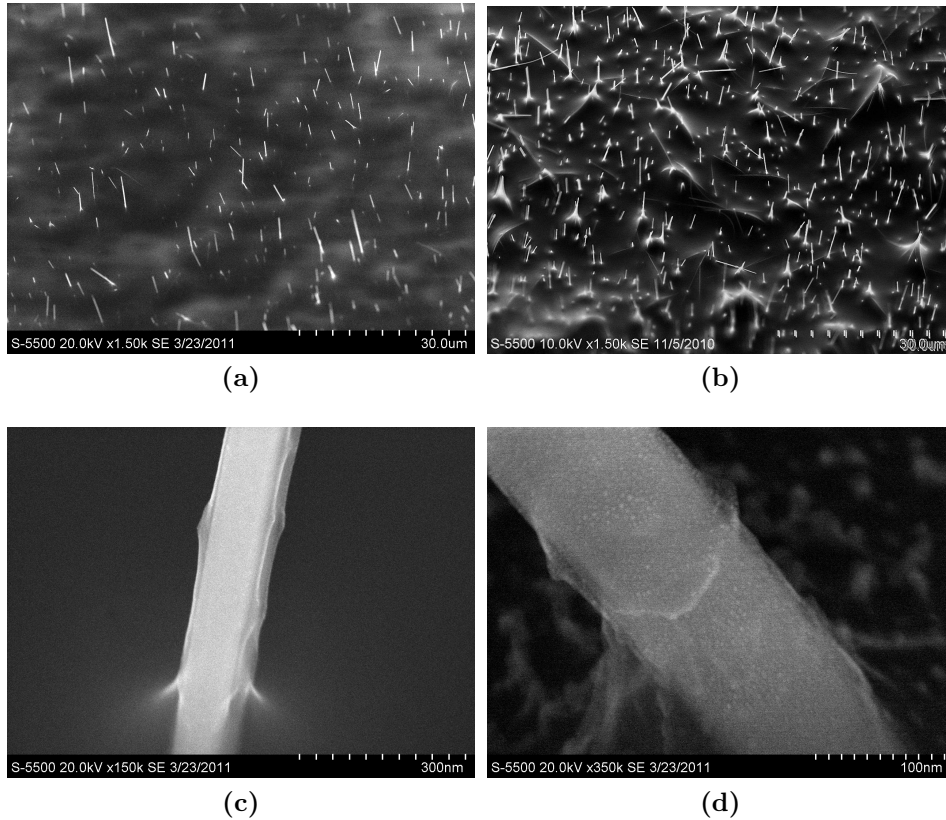


Figure 4.4: (a) SEM micrograph of nanowires protruding from the surface of the standard device, i.e. a three layer structure of PMMA, PDMS and SU-8 2, showing a satisfactory wire density and height. (b) A nanowire surface with only an SU-8 2 layer applied, which gives a much less homogeneous surface than if the PMMA layer is applied in addition. (c) Magnification of a single nanowire on the standard device showing a polymeric layer surrounding the nanowire. (d) Further magnification of a single wire where gold grains can be visualized on the surface of the wire. This indicates that the wire is covered in a thin layer of PDMS (as opposed to SU-8), since the gold was sputter coated after applying PDMS but before applying SU-8. This sample was imaged after plasma oxidation.

4.2 Progress in device fabrication

As a transparent device which is compatible with inverted fluorescent microscopy systems is desired, the copper oxide substrate needs to be removed while leaving the wires protruding from a transparent material, such as SU-8. In previous work [6], this was done by first peeling off the un-oxidized copper foil from the device (which could easily be separated from the cuprous oxide layer), then etching the remaining cuprous and cupric oxide in hydrochloric acid. However, this treatment was prone to remove the nanowires themselves at the same time, unless carefully controlled, so a new method to separate the nanowires from the oxidized copper substrate was developed.

The current device fabrication process is described in section 3 and illustrated in Figure 3.1. Briefly, a four-layer polymer structure was made on top of the nanowire array, consisting of PMMA, PDMS and SU-8 (a thin, covering layer, and a thick, patterned layer). By exploiting the fact that PMMA dissolves and PDMS swells in acetone, a softer layer with low adhesion is formed between the copper oxide and the SU-8 structure upon exposure to acetone. This allowed the copper oxide substrate to be removed quite easily, with the nanowires remaining firmly bound in the SU-8 structure. In many samples this could also be done without acetone treatment, as the adhesion between the layers was quite low even before acetone treatment. SEM investigations revealed that after this treatment a satisfactory wire surface coverage and protrusion height was preserved (see Figure 4.4a). However, this depended on the initial wire density and the thickness of the PMMA and PDMS layers. Thicker layers allowed simpler removal of the oxidized copper substrate, at the cost of decreased wire density. It also appeared that the four-layer structure, in particular the PMMA-layer, beneficially interacts with the wires, effectively burying longer, more flexible wires, while leaving straight, intact wires protruding. In contrast, SU-8 alone less effectively buried such wires, leading to a rougher, less homogeneous surface with multiple semi-buried, lying wires and other structures that could potentially harm cells (see Figure 4.4b).

Closer investigation revealed that the nanowires were covered in a low-density polymeric both before and after oxygen plasma treatment, as indicated by the reduced, but not absent electron signal (Figure 4.4c). The layer was likely PDMS, as it was not visible after only PMMA application. This is also supported by the gold grains that were visible on the surface of this layer (Figure 4.4d). This gold was sputter coated onto the PDMS before SU-8 was applied, although a very thin layer of SU-8 covering this again would not be visible and can thus not be ruled out. It must be noted that for the close-up investigation of the wires in the two last images the oxidized copper substrate

was not removed, as this would have broken electrical contact between the wires and ground, making high resolution imaging impossible without sputter coating, which would hide the features under investigation. However, it can reasonably be assumed that the removal of the oxidized copper substrate is unlikely to change the surface of the wires.

4.3 Surface functionalization

To optimize conditions for biomolecule attachment and delivery using nanowires, the surface chemistry of the nanowires must be controlled. The initial approach used a sputter coated gold layer on the wires for thiol-based surface functionalization (such surface functionalization is described in section 2.4.2). As verifying monolayer presence on the nanowires themselves was challenging, monolayers consisting of cysteamine were produced on test samples with a thin (~ 10 nm) layer of gold sputter coated on glass. Using contact angle measurements the monolayers appeared to form easily (data not shown). However, further investigations trying to visualize negatively charged, immobilized fluorescent quantum dots or DNA did not succeed, as little or no signal was observed, likely due to the strong surface quenching effects of thin gold films. As an alternative, atomic force microscopy (AFM) imaging was used to image sputter coated gold-cysteamine surfaces with deposited DNA molecules. Unfortunately, due to the roughness of sputter coated gold, the possibly immobilized molecules were obscured. Thus, attempts were made to produce ultra-flat gold films, which could facilitate the AFM imaging of deposited molecules. Several such approaches were attempted, with the results outlined in Figure 4.5. Briefly, evaporated gold films (which are generally less rough than sputter coated gold films) were either annealed at high temperature or template stripped from silicon or mica. Despite large improvements over sputter coated gold, none of the methods gave flat enough surfaces to visualize the self-assembled monolayers or potentially bound quantum dots or DNA.

Due to the issues with gold coating, which in addition to the difficulties mentioned above also rendered the entire sample less transparent (even a few nm of gold reduced transmitted light intensity by 50% or more), alternatives to gold/thiol-based surface functionalization were investigated. By using silane monolayers a variety of functional groups can be formed on any surface containing hydroxyl (-OH) functionalities (see section 2.4.2). Such groups are natively present on glass and PDMS after plasma oxidation. Using standard photoresist patterning, a $500\ \mu\text{m}$ square grid pattern was produced on glass. The surface was silanized with (3-aminopropyl)trimethoxysilane (APTMS)

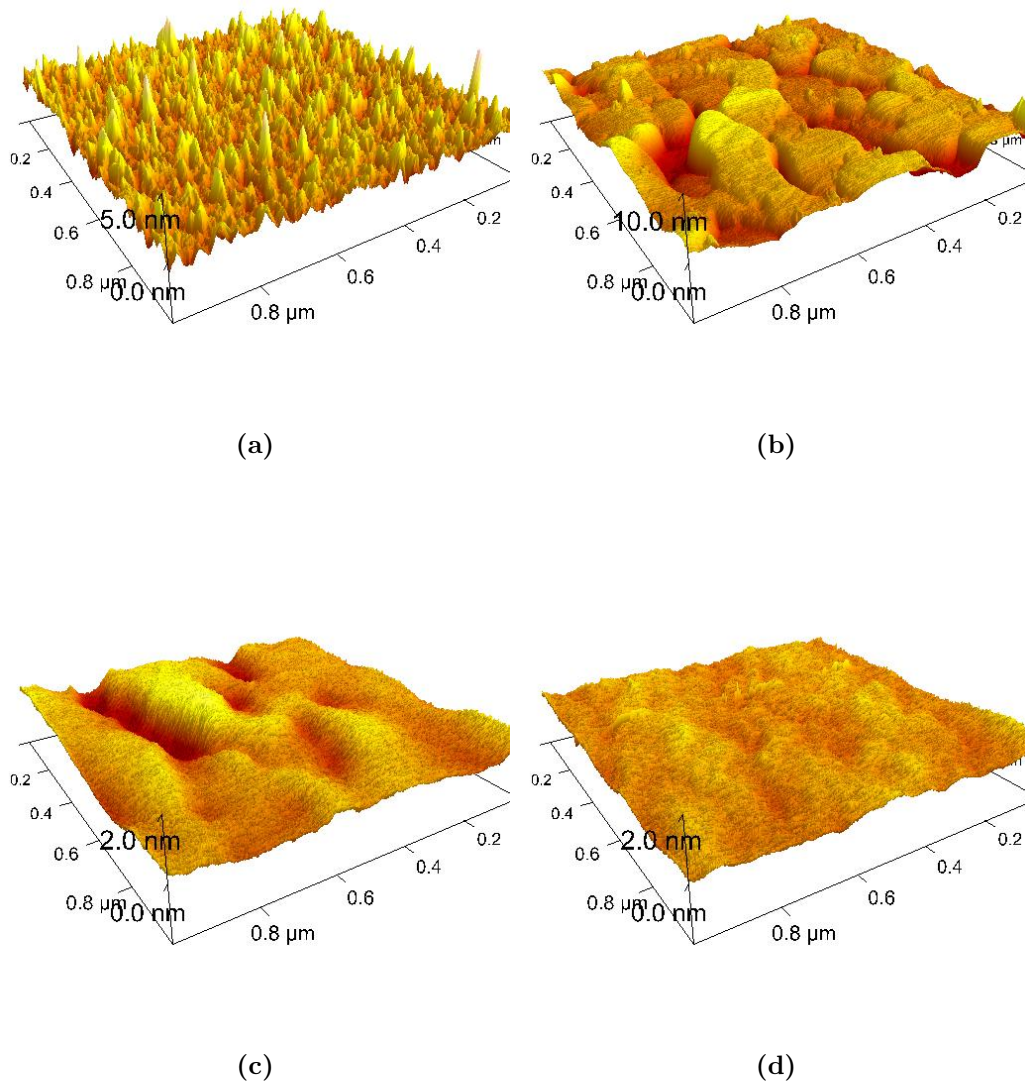


Figure 4.5: 3D renderings of AFM micrographs of gold thin films on glass, produced by (a) sputter coating, (b) evaporation, (c) evaporation followed by annealing at 600 °C for 5 minutes and (d) template stripping by gold evaporation onto a silicon wafer, followed by attachment of a glass piece via epoxy gluing and finally detachment. All scans are 1 $\mu\text{m} \times 1 \mu\text{m}$, and the z-ranges are 5 nm, 10 nm, 2 nm and 2 nm for (a) to (d) respectively.

using either a concentrated vapor phase deposition or a dilute aqueous phase deposition, after which the remaining photoresist was removed in a solvent. Since APTMS contains amino groups the surface should contain positive charges in solutions at $\text{pH} \leq 10$ (pKa of propylamine groups is about 10.7 [161]). Solutions of carboxylated quantum dots and DNA bound to PI, both of which are negatively charged and fluorescent, were incubated on the samples, rinsed and imaged in a fluorescent microscope. The square grid pattern with defined APTMS areas is clearly visible due to the immobilized fluorescent molecules in both cases, although the quantum dots gave a brighter signal, as shown in Figure 4.6. No square grid pattern was visible in a similar sample without DNA or quantum dots, indicating little or no auto-fluorescence from the silane itself. Both silane deposition methods were also attempted on planar PDMS and SU-8 substrates. Similar results were obtained, but both PDMS and SU-8 had to be activated with oxygen plasma before silanization could occur, and longer plasma treatment (increased from 12 seconds to 5 minutes at 50W) gave significantly better quantum dot immobilization results.

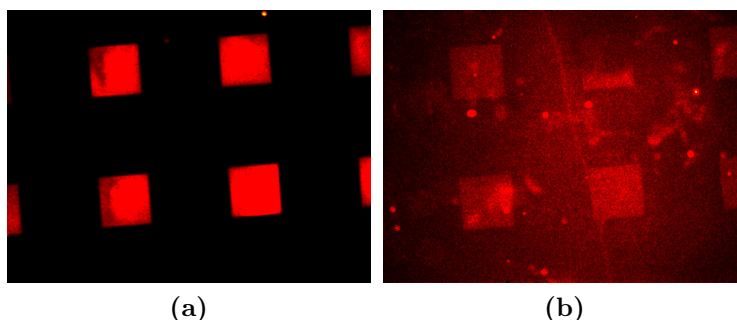


Figure 4.6: Vapor phase deposited (3-aminopropyl)trimethoxysilane (APTMS) patterned in a square grid pattern on glass by photolithography. Samples were incubated with (a) a 10 nM solution of carboxyl-modified quantum dots or (b) $50 \mu\text{g ml}^{-1}$ DNA solution with $50 \mu\text{g ml}^{-1}$ PI. In both cases the aminosilane pattern is clearly visualized by binding of the fluorescent molecules, although the signal from the quantum dots is significantly stronger. The DNA background signal is partly noise from the camera, so how much the DNA binds to the unmodified glass is unknown. The squares are $500 \mu\text{m} \times 500 \mu\text{m}$.

Another substrate for investigating silane modification is mica, which has surface hydroxyl groups and a layered structure that is easily cleaved to produce large, atomically flat surfaces. Figure 4.7a shows an unmodified mica surface, while Figure 4.7b shows some DNA strands adhered to an unmodified mica substrate. To investigate the effect of a positively charged

surface group, the mica was silanized by incubating in a 1% aqueous APTMS solution for 1 minute. This somewhat increased the surface roughness, as shown in Figure 4.7c. Longer (up to 5 minutes) APTMS incubation times lead to much rougher substrates, likely indicating the formation of multilayer films on the mica surface (not shown). Finally, DNA was deposited on the APTMS-modified surface. AFM micrographs showed drastically increased amount of bound DNA compared to the unmodified surface (Figure 4.7d). Concentrations of $50 \mu\text{g mL}^{-1}$ salmon testes DNA (highly polymerized, i.e. long strands) were used in Figure 4.7d. Tests were also performed with concentrations down to $10 \mu\text{g mL}^{-1}$ and with incubation times of 10 minutes of both salmon testes and eGFP plasmid DNA. These showed similar results, indicating that high surface coverage is achieved quickly at these concentrations on APTMS modified surfaces.

The above investigations into surface functionalization are related to the "delivery" part of the device, investigating necessary surface modifications and biomolecule concentrations, rinsing procedures and incubation times. However, surface functionalization could also be used to control cell growth and spreading. Gold was patterned on glass using a standard photolithography lift-off process, and rendered hydrophobic using an octadecanethiol monolayer as hydrophobic surfaces often show reduced cell attachment (described in section 2.3.1). The contact angle with water was greatly increased after monolayer deposition, and due to the surface stresses induced in contact with water delamination of the gold could occur, especially at longer monolayer incubation times (24 hours). Upon culturing cells on the samples, the hydrophobic surface alone supported similar cell attachment as the glass surface. To increase cell repellence on the hydrophobic surfaces, the sample was blocked using 1% bovine serum albumin (BSA), which should bind irreversibly to the hydrophobic areas. Indeed, this prevented cell attachment on the areas of hydrophobic gold, but not on the areas with glass. The patterning was in many cases not absolute. It was found that rinsing the samples with ethanol then drying before use gave the best results. Cell seeding density also played a role, where higher cell seeding density reduced patterning efficacy. This method was used to define both large scale-areas which prevented cell attachment (as shown in Figure 4.8a), but it could also be used to localize cells to well-defined spots on the sample, as shown in Figure 4.8b. In addition to patterning cell positions, small features such as this could control cell morphology, with most cells becoming square to match the pattern, limiting cell spreading area (e.g. compared to cells on unpatterned glass, above). As HeLa cells divide rapidly, many of the squares in the pattern contained more than one cell, although in such cases the cells still conformed to the pattern, as shown in the inset in Figure 4.8b.

A similar approach was used on planar PDMS on a glass slide, with the cytophobic regions represented by hydrophobic, aged PDMS blocked with BSA and cytophilic regions represented by APTMS-modified PDMS. This patterning worked to some extent, with increased cell growth in the APTMS modified areas, although specificity was lower than on the gold-patterns above.

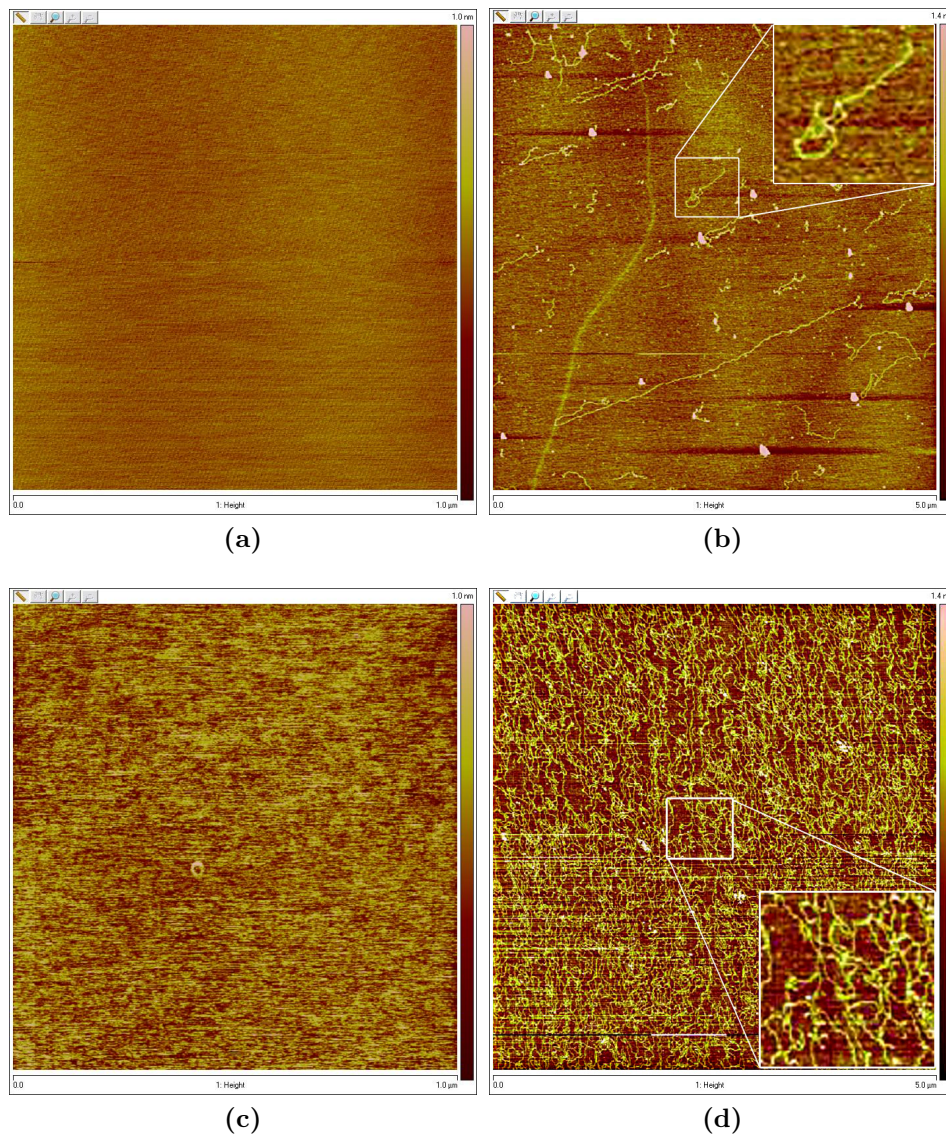


Figure 4.7: (a) Native mica, atomically flat, measured rms-roughness 0.0428 nm. (b) DNA deposited on native mica. (c) APTMS-modified mica showing increased rms-roughness of 0.147 nm compared to native mica, but this is still very flat. (d) DNA deposited on APTMS-mica, showing a large increase in binding affinity compared to DNA on native mica. For APTMS modification the samples were incubated for 1 minute in a 1% solution of APTMS in MQ-water. The DNA used was $50 \mu\text{g mL}^{-1}$ salmon testes DNA in a pH=8 TRIS-buffer. (a) and (c) are $1 \mu\text{m} \times 1 \mu\text{m}$ scans with a 1 nm height scale, while (b) and (d) are $5 \mu\text{m} \times 5 \mu\text{m}$ scans with a 1.4 nm height scale.

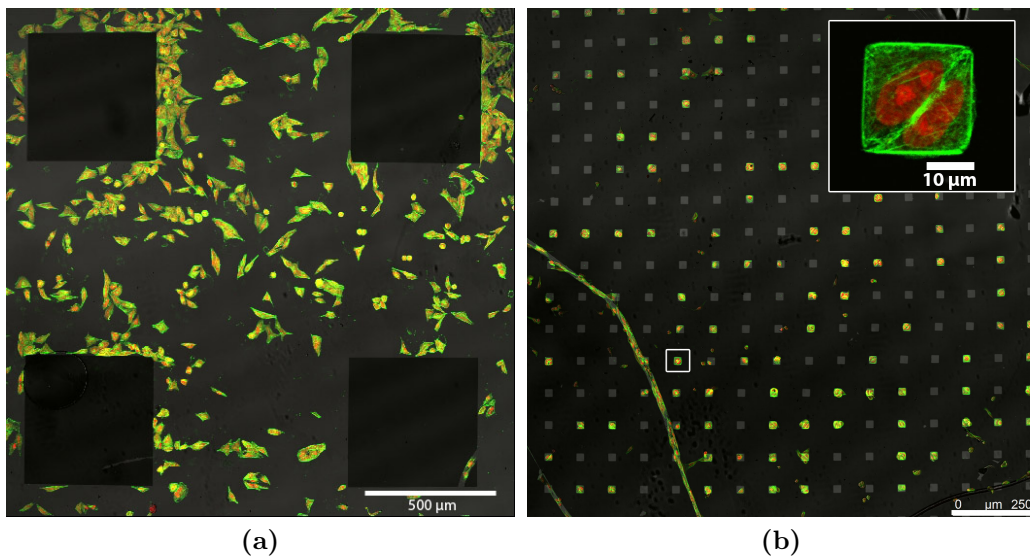


Figure 4.8: HeLa cells growing on (a) glass with a 500 μm square gold pattern and (b) 25 μm glass square pattern surrounded by gold. The gold is rendered hydrophobic and blocked with BSA, effectively hindering cell attachment. Cells in (b) can be seen to largely adopt their morphology to the pattern, as shown clearly for the cells in the inset (the position of the inset image is indicated by the white square in (b)). The line in the lower left of (b) is a scratch in the gold layer, which the cells can be seen to tightly fill. The images are confocal overlays visualizing the gold patterns (darker gray, brightfield), cellular actin filaments (green) and the cell nuclei (red).

4.4 Sample toxicity and cells on model substrates

The fabrication method described in section 4.2 using a sacrificial PMMA layer and PDMS together with an SU-8 structure provides a well-controlled way to produce a transparent device with protruding nanowires. Unfortunately, HeLa cells showed significantly reduced surface spreading and proliferation on and near (i.e. on the glass surface in the vicinity of the device, up to about 1 mm away from the device) these samples, as shown in Figure 4.9a. If such reduced cell spreading was observed, there was no difference inside and outside the SU-8 wells. Cells which showed reduced spreading were labeled with calcein-AM and ethidium homodimer, and it was seen that despite most of the cells being rounded and not spread out, they were still alive. After 9 days of culturing on such samples the cells could be seen to proliferate somewhat, as shown in Figure 4.9b. In contrast, after only 3-4 days a confluent layer of cells was formed on a typical non-toxic or control sample (e.g. samples where the old fabrication method of acid etching was used).

As described later this was not linked to the nanowires themselves. Therefore, more detailed investigations were done into which materials and processing steps could cause the cellular toxicity. A number of different test-samples were produced on 15x15 mm cover glass slides in order to easily grow and investigate cells. An overview of the most representative samples that were tested are shown in Table 4.1.

At first it was suspected that either SU-8 formulation (i.e. SU-8 2, SU-5 or SU-8 2100, which are essentially the same except for casting solvent type and concentration) or surface treatment might play a role. However, this did not seem to be the case, as cells were shown to grow well on planar SU-8 substrates and SU-8 substrates with SU-8 well patterns on top, for surface treatments from 0-10 minutes of oxygen plasma and ethanolamine and cysteamine incubation (ethanolamine might react with surface epoxy groups on the SU-8, while cysteamine was used for gold functionalization, and could also react with surface epoxy groups). A typical example of cell growth after 2 days of culturing on such an SU-8-only sample with wells is shown in Figure 4.9c. Investigations on cell morphology using actin staining together with PI showed no significant differences between cells on SU-8 samples and glass controls, as shown in Figure 4.9d and Figure 4.9e. The electron micrograph in Figure 4.3 shows two HMDS-dried HeLa cells inside a well on such an SU-8-only sample, similarly indicating typically spread HeLa cell morphology.

Table 4.1: An overview of the most representative test-samples that were used to pin-point the source of cell toxicity that arose as part of the new fabrication scheme. Sample material is given in order of fabrication (from a clean glass surface). Cell attachment was investigated by inspection in an optical microscope, and is a qualitative assessment divided into three categories: "No attachment" indicates a large majority of rounded cells and very few spread out cells, "reduced attachment" indicates some cell attachment and growth, but lower than glass controls, while "good attachment" indicates spreading and growth similar to glass controls.

Sample material	Cell attachment	Comment
SU-8	Good	SU-8 2, 5 and 2100, planar, unmodified
SU-8	Good	SU-8 2, 5 and 2100, planar, oxidized 50W, 3 minutes, 7W, 5 minutes and 100W, 10 minutes
SU-8	Good	SU-8 5, 2100 and thinned 2100 in 500 μm well patterns (developed in propylene glycol monomethyl ether acetate (PGMEA))
PDMS	No/reduced	Native, increased attachment over time (1-4 days)
PDMS	Good	Native and exposed to solvents (acetone and/or PGMEA for 5 minutes each). Plasma oxidized (12 s - 10 minutes, 50-100W)
PMMA	Good	Native and exposed to solvents (acetone and/or PGMEA for 2 minutes each). Plasma oxidized (5 minutes, 50W).
PMMA + PDMS	Good	Exposed to solvents (acetone and/or PGMEA for 5 minutes each). Plasma oxidized (5 minutes, 50W).
PMMA + PDMS + SU-8 2	Good	Native and exposed to solvents (acetone and/or PGMEA for 5 minutes each). Plasma oxidized (5 minutes, 50W).
PDMS + SU-8 2 + SU-8 2100 well pattern	Reduced	Exposed to acetone and/or PGMEA for 5 minutes each. Plasma oxidized (5 minutes, 50W).
PMMA + PDMS + SU-8 2 + SU-8 2100 well pattern	No/reduced	Exposed to acetone and/or PGMEA for 5 minutes each. Plasma oxidized (5 minutes, 50W).
PMMA + PDMS + SU-8 2 + SU-8 2100 well pattern	No/reduced	Solvent exposure, then incubated for 2 hours in ethanol. Plasma oxidized (5 minutes, 50W).
PMMA + PDMS + SU-8 2 + SU-8 2100 well pattern	Reduced	Solvent exposure, then incubated for 1 hour in 95 $^{\circ}\text{C}$ MW-water. Plasma oxidized (5 minutes, 50W).
PMMA + PDMS + SU-8 2 + SU-8 2100 well pattern	Good	Solvent exposure, then baked for 2 hours at 120 $^{\circ}\text{C}$. Plasma oxidized (5 minutes, 50W).

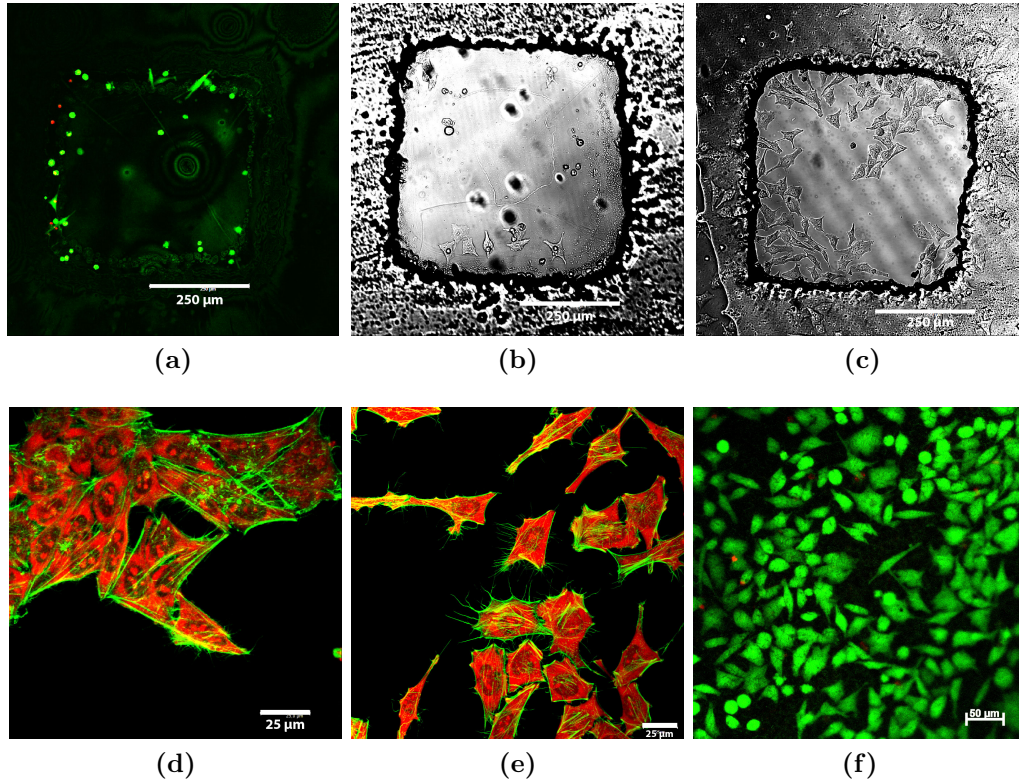


Figure 4.9: (a) HeLa cells in a single 500 μm well produced using a layer of PDMS together with the thin and thick SU-8 structures and developed in acetone, showing significantly inhibited cell growth. The cells were stained with calcein-AM (live cells, green) and ethidium homodimer (dead cells, red), showing that despite being rounded, the cells are mostly alive. (b) DIC micrograph of a sample produced using the standard procedure after 9 days of cell culturing, showing a certain amount of proliferation, although less than in (c): a typical sample which contains only SU-8 after 2 days of cell culturing. (d) Morphological investigations of cultured cells on glass using actin filament staining (green) and PI staining (red). (e) Same as (d), but the substrate is planar SU-8 instead of glass, showing no significant difference in cell morphology between the two substrates. (f) Live (green) / dead (red) stained cells growing on a planar substrate glued onto a glass slide, i.e. no thick, patterned SU-8 layer. Cell proliferation is high on such substrates, similar to planar glass and SU-8.

Thus it appeared that one of the other materials which recently had been implemented into the process was to blame, i.e. either PDMS or PMMA. However, planar (i.e. no well structures, only thin polymer layers on glass) samples containing PDMS, PMMA, SU-8 or combinations of these showed similar cell proliferation as glass controls as long as they had undergone a brief oxygen plasma activation. As none of the polymer materials themselves seemed to negatively effect the cells, it was suspected that one of the solvents in the process could play a role, which included acetone for detachment of the oxidized copper substrate, PGMEA for development of SU-8, isopropanol for rinsing or ethanol for sample sterilization before cell culturing. However, regardless of solvent treatment the planar samples showed similar cell proliferation as glass controls. The exception was samples which were not sterilized in ethanol, these were severely contaminated by bacteria during culturing.

Thus, cell toxicity must have been caused by something specific for the entire device processing procedure. Indeed, once the thick SU-8 structure was introduced together with an underlying planar SU-8 and PDMS layer, samples again showed significantly reduced cell proliferation after solvent treatment with acetone (which also functions as an SU-8 developer), PGMEA or both. Thus, it appeared the issue was a solvent retainment effect in the PDMS layer which occurred as the solvent was "trapped" beneath the thick SU-8 well structure, although the precise mechanism is uncertain. Possible solutions to this issue were investigated, including 1 hour incubation in ethanol or in 95 °C water for solvent extraction, or baking at 120 °C for 2 hours. Ethanol incubation showed little effect, incubation in hot water showed somewhat better proliferation, while baking at 120 °C for 2 hours appeared to improve cell spreading in many cases. Unfortunately, in regular nanowire samples that underwent this treatment, some cell toxicity was still observed on certain samples, so the issue remains partially unresolved.

The reason the thick SU-8 structure is needed is for mechanical support, as the thin layers of PMMA, PDMS and SU-8 were not rigid enough to support the device alone. Alternative methods were found to work around this. The simplest alternative to SU-8 structuring is simply not removing the oxidized copper substrate, at the cost of device transparency. However, on such samples culturing cells did not succeed, as a blue coloring of the growth medium indicated dissolved copper (see Figure 4.10). Cell proliferation was significantly reduced in such blue-colored growth medium. This was resolved by protecting both sides of the sample: The top side by the standard PMMA+PDMS+thin SU-8 processing (i.e. no thick SU-8 or solvent treatment), and the back side by gluing the samples to a cover glass using Norland Optical Adhesive 63 (NOA63), a solvent free, biocompatible, inert, transparent UV-curable adhesive. On such samples, with protruding

nanowires, cell growth and spreading was good, similar to glass controls, as shown in Figure 4.9f. These samples could be used for SEM investigations of cells on nanowire substrates and preliminary delivery experiments (presented below). Inverted confocal fluorescent microscopy of such samples could be performed by turning them upside-down inside a confocal imaging dish with a thin glass bottom.

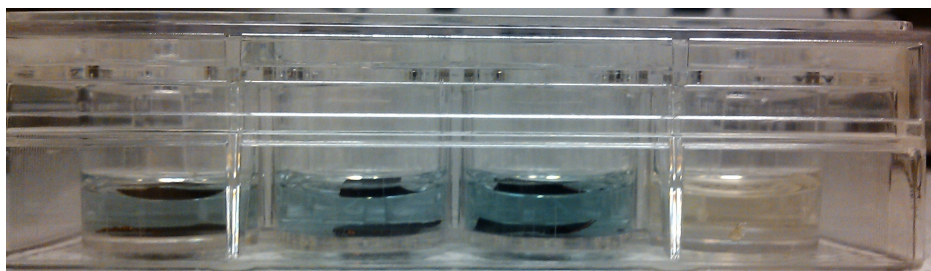


Figure 4.10: Side view of a 12-well plate showing the effect of samples with exposed copper oxide surfaces. The right-most well contains standard growth medium and no samples, while the three wells on the left contain samples with a thin SU-8 layer on one side and unmodified oxidized copper on the other side. The blue color is a typical sign of Cu^{2+} ions present in solution.

4.5 Cells on nanowire substrates

Using either the method of baking a sample at 120 °C for 2 hours or gluing samples with an intact backside to a cover glass slide, cells could usually be successfully cultured without apparent toxic effects. In well samples which were baked out cell proliferation was quite good, as shown in Figure 4.11a, although this varied from well to well. Similar variations were seen across planar samples, and was most likely caused by inhomogenous seeding of cells. As shown in previous work and used in the literature [6, 86, 62], wire penetration can be visualized by "negative staining", i.e. by exploiting the fact that the non-fluorescent volume of the wires, and possible quenching effects, give a local drop in signal compared to the surroundings inside a cell, thus allowing visualization of the wires. Closer inspection of the cells inside the wells of Figure 4.11a, which were fixed and stained with Alexa488-phalloidin (actin filament, green) and propidium iodide (nucleus and cytoplasm, red), showed that the cells were penetrated by wires, as indicated by the black, elongated areas in the orthogonal section view in Figure 4.11b. No particular actin structures were associated with the penetrating nanowires. Cells on nanowire substrates were also investigated using the live/dead stain. An overview of HeLa cells cultured on a planar sample with protruding, APTMS modified nanowires was already presented in Figure 4.9f, showing high cell proliferation. Closer investigation of such cells is shown in Figure 4.11c, where numerous black dots in each cell indicate the penetration of nanowires. As the cells are only stained with calcein-AM (green) and not with ethidium homodimer (red), this indicates that cells are viable and have intact membranes despite the penetration by nanowires. HeLa cells were cultured up to 5 days on such nanowire surfaces and produced confluent layers, indicating continued cell viability.

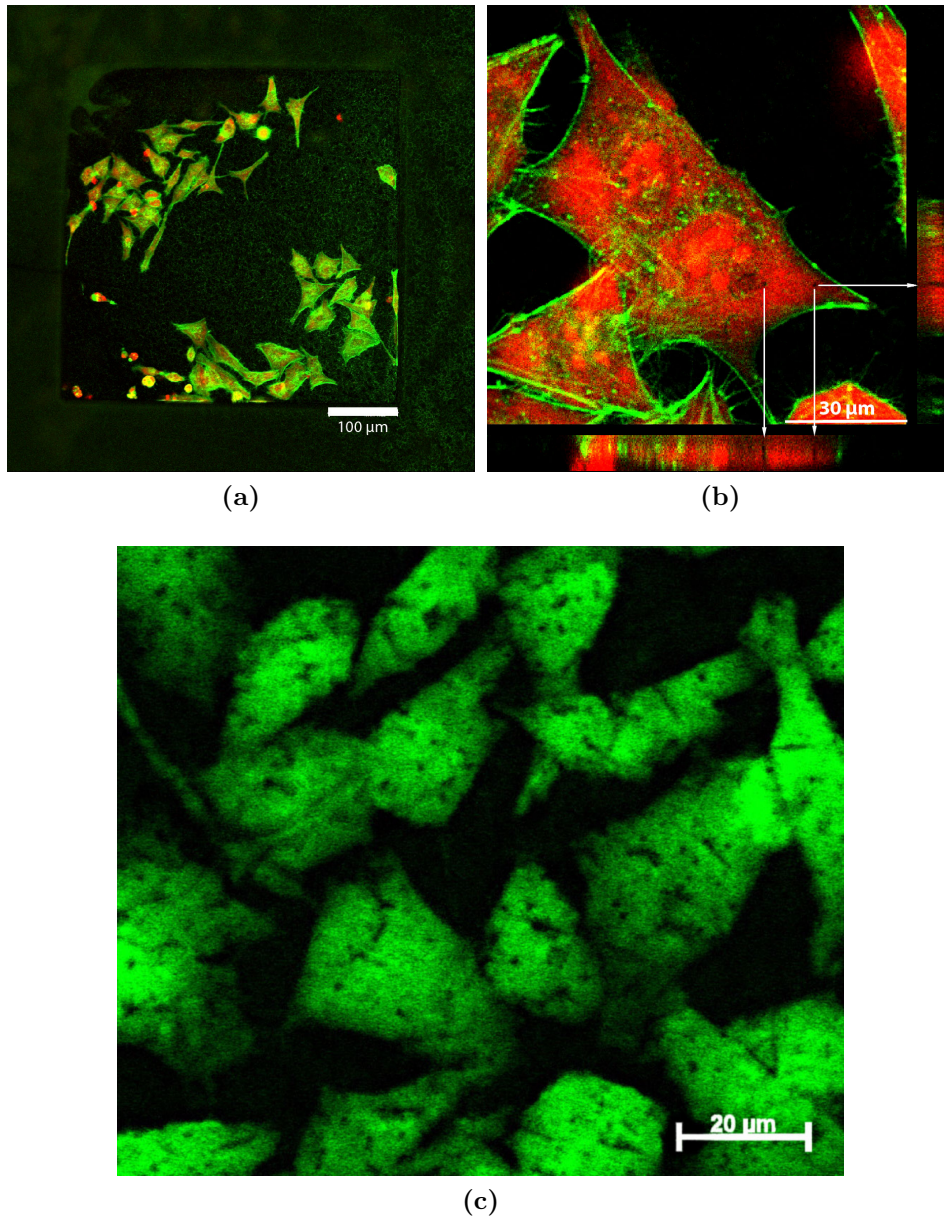


Figure 4.11: HeLa cells cultured for 2 days on a transparent nanowire sample and imaged in a confocal microscope. The sample has PDMS-covered wires, but without the gold layer. The cells are fixed, permeabilized and stained by Alexa488-phalloidin (green) and PI (red). **(a)** An overview of the HeLa cells in a moderately populated well showing good spreading and growth. **(b)** A slice from a stack of images of a closer view of some cells in the well. Side-views of the stack are presented below and to the right of the image, showing how the two wires indicated at the start of the arrows penetrate through the cell. **(c)** HeLa cells stained with live/dead kit, showing only live cells with intact membranes (green) despite being penetrated by multiple nanowires (black dots).

Scanning electron microscopy was used to investigate the interactions between the cultured HeLa cells and the nanowires. It was shown that HeLa cells spread out on nanowire-decorated surfaces as shown in Figure 4.12. The investigations showed that the cells were indeed penetrated by the nanowires, which in some cases could be seen directly by long wires penetrating through the entire cell (Figure 4.12a). It must be noted that as some cell shrinkage occurs during dehydration, drying artifacts may be present, although this is probably not significant for the results (see discussion below). Penetration by nanowires also occurred in cell areas which were not originally in contact with the nanowires, such as the lamellar extension shown in Figure 4.12b, which grows out after the cell adheres to the surface. Direct nanowire interaction was also observed, where filopodial extensions actively bound to the nanowires, as shown in Figure 4.12c. In some cases such attachments were seen to bend the wires, but it is not clear if this occurred while the cell was alive or due to shrinkage during drying. Filopodial extensions could also engulf wires as they extended from the cell, as shown in Figure 4.12d.

On most nanowire surfaces the cells spread out to a large extent, although not as much on planar substrates such as glass or SU-8. To investigate critical parameters for wire surface density and length on cell spreading, different non-standard substrates were produced. Figure 4.13a shows cells on a wire surface covered in only SU-8 2. This left long, protruding wires together with many bent, broken or otherwise misshaped wires. Cells on this sample were seen to be mostly rounded with a low degree of spreading. Many cells were also apoptotic, as identified by apoptotic blebs in the membrane (clumpy structure, see inset in Figure 4.13a). The rounded cells could be seen to be resting mostly on top of the wires, with little or no contact with the substrate. In addition, a PMMA surface with protruding nanowires was made. PMMA interacted differently than SU-8 with the nanowires, burying the longer and bent wires, leaving a relatively uniform surface of shorter, protruding wires (as shown above in section 4.2). The final wire density was similar or somewhat lower than that produced by the SU-8 2 layer above, and the cells could be seen to spread to a much larger extent, as shown in Figure 4.13b. The cells here were in much more contact with the substrate, instead of resting on top of the wires. Finally, a typical sample with the standard three-layer (PMMA, PDMS and SU-8) structure which had a lower wire density and length was investigated. Here the cells spread out to an even larger extent than on the PMMA substrate, similar to cells on planar substrates (see Figure 4.13c).

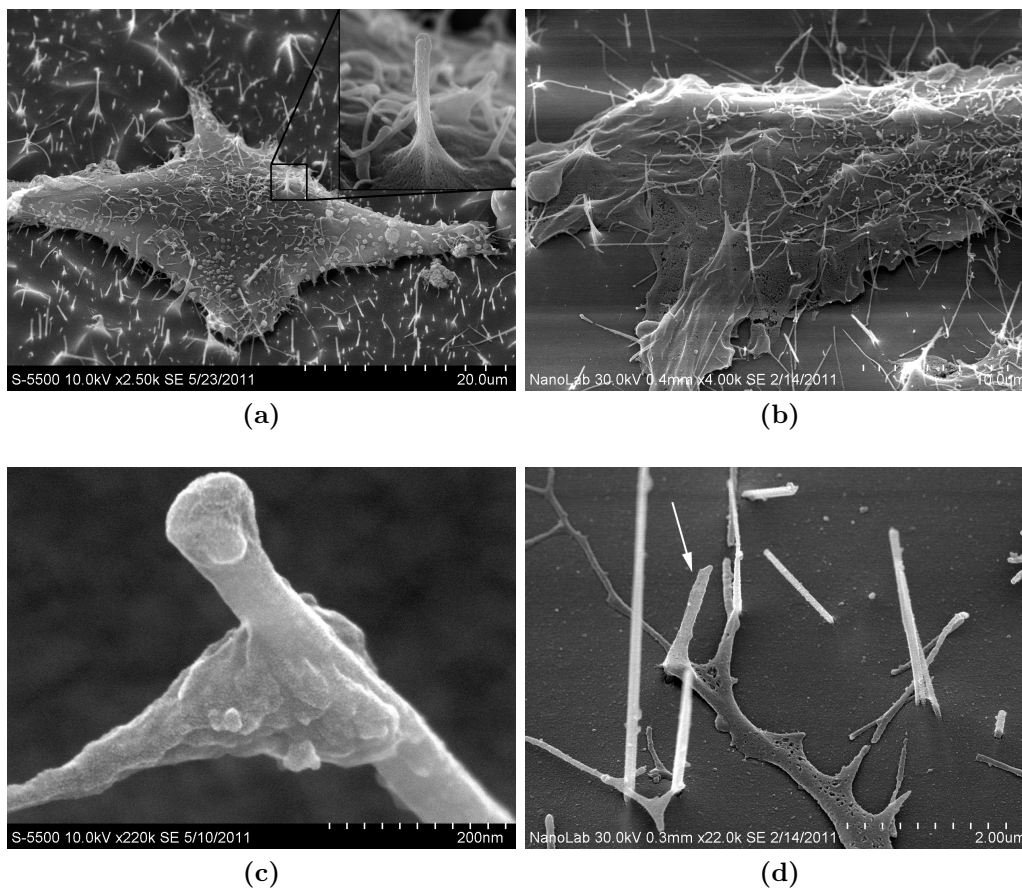
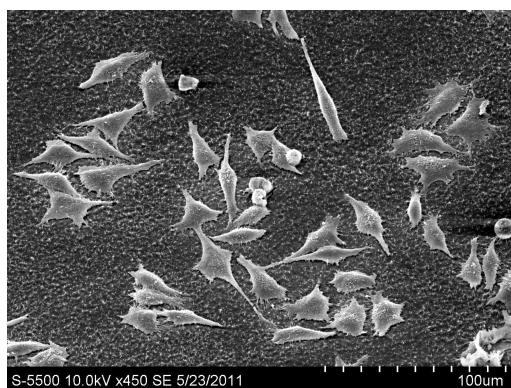


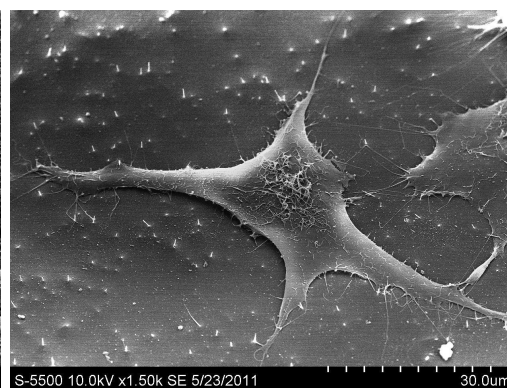
Figure 4.12: HeLa cells were cultured for 2 days on SU-8-covered substrates with protruding nanowires, either coated in gold (b and d) or plasma activated PDMS (a and c). Cells were fixed in glutaraldehyde and dehydrated by critical point drying (b and d) or HMDS drying (a and c). **(a)** A cell spread on a surface showing typical spread morphology, but being pierced all the way through by several wires, as shown in the inset. Notice how the wire appears to be covered in a material that is continuous with the cell membrane. **(b)** Large cellular extension being penetrated by multiple nanowires. **(c)** Filopodial extension from cell binding tightly to a single nanowire, with a thickening close to the nanowire, which could be due to protein clustering at the adhesion point. **(d)** Small extension from the cell moving along the surface and completely engulfing an encountered nanowire (indicated by an arrow).



(a)



(b)



(c)

Figure 4.13: (a) Cells grown on an SU-8 2-covered substrates with a high density of protruding, longer nanowires. Only a few cells are spread, most are rounded. The inset shows a close-up of two cells, one apoptotic (lower left). Notice how both cells are impaled on nanowires and in fact appear to be resting on top of the wires. (b) Cells on a PMMA substrate with a similar wire density to (a), but with shorter, more uniform wires, spreading out to a larger extent. (c) Cells cultured on a PMMA, PDMS and SU-8 substrate with a lower wire density, showing similar morphology as when cultured on flat SU-8 (see Figure 4.3).

4.6 Nanowire-based delivery

As the nanowires clearly penetrated into the cultured cells, it should be possible to use the nanowires to deliver attached cargo into cultured cells. Three types of cargo were used: PI, which is a negatively charged, cell impermeant small molecule, negatively charged fluorescent quantum dots, and plasmid DNA encoding eGFP. These molecules were predeposited on the nanowires using the same methods that were seen to be successful on the model, APTMS-modified mica, glass, PDMS and SU-8 surfaces. After depositing the cargo, HeLa cells were cultured on the samples for 2 days and then imaged using fluorescence microscopy to detect molecules inside the cells, or expression of eGFP. As PI fluorescence increases 20-fold upon binding of DNA or RNA, but is generally not cell permeant, if PI was delivered successfully then live cells (as labeled with calcein-AM from the live/dead kit) should also contain red nuclei (usually this is mutually exclusive, as shown in section 4.1). No such double-labeled cells were seen, indicating either that no such delivery took place, or that PI interferes to such an extent with DNA transcription in the cell that cells with PI died and were thus not labeled with calcein-AM. No particular increase in cell fluorescence was observed as cells were cultured on nanowires with deposited quantum dots either. However, in many cases a significant background signal was observed, which made it challenging to distinguish a certain amount of intra-cellular fluorescence due to possibly delivered quantum dots from quantum dots immobilized on the surface.

Finally, eGFP-encoding plasmids were deposited on the nanowires and HeLa cells were cultured on the samples. After 2 days a few cells were seen to clearly express eGFP as indicated by their bright green fluorescence. Close investigation of eGFP-expressing cells showed that they were clearly penetrated by nanowires, as shown in Figure 4.14. However, transfection efficiency was very low, only a few cells of several thousand (this was not precisely quantified) showed eGFP expression.

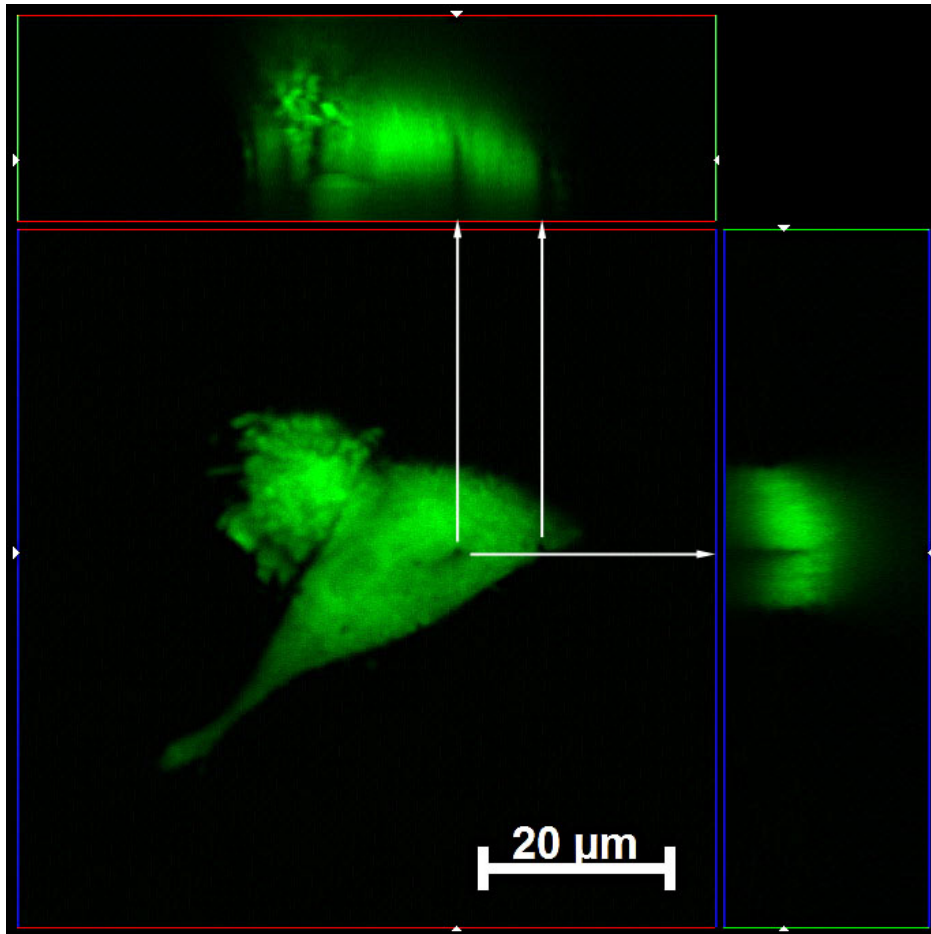


Figure 4.14: Confocal micrograph of two HeLa cells, the one to the left appearing apoptotic, expressing eGFP after culturing on nanowires with pre-deposited eGFP plasmids. The cells are penetrated by nanowires, as shown in the orthogonal views at the areas indicated by arrows.

Chapter 5

Discussion

To reach the overall goal of developing a versatile, biocompatible device in which a range of biomolecules can be effectively delivered into cells via nanowire penetration, several sub-goals have to be reached. Thus this work has focused on improving several aspects of the device, including optimized methods to study the cells using confocal microscopy and scanning electron microscopy, device fabrication, manipulation of surface chemistry both for optimized biomolecule delivery and cell manipulation, studies of cells on the nanowire devices and delivery via the nanowires. More specifically, the following are the different criteria that must be met, which form the basis for the discussion below:

- The devices must be made in a low-cost and up-scalable way so fabrication is not a major limitation for actual device use. In addition it must be possible to use standard methods to study the cells on the devices without significantly changing established procedures.
- The cargo must adhere to the nanowires through some form of deposition technique and surface interaction.
- The device must be biocompatible and not interfere significantly with cell behavior and proliferation, apart from the desired perturbation caused by the cargo delivered through the nanowires.
- The nanowires must penetrate into the cells and make the cargo accessible for the interior of the cell.

5.1 Device fabrication and surface functionalization

In the literature involving cell growth on nanowires (described in section 2.3.2), nanowire fabrication techniques are significantly more complex than ours, but they have the advantage of having better control over nanowire parameters such as length, diameter and density. The thermal oxidation method to produce wires is simple, low-cost and rapid, but suffers from sensitivity to contamination and growth conditions. Samples could also be somewhat inhomogeneous. Most of these issues are being resolved as better understanding and subsequent control over growth conditions emerges, and using e.g. patterns of electro-deposited nickel to produce more reliable and homogeneous samples is currently being investigated with promising results [5].

The new methods of device fabrication, which employ intermediate layers of PMMA and PDMS, offer numerous advantages over the previous method which only used SU-8 structuring and acid etching. Despite the growth of the nanowires being difficult to control, the polymer processing gave relatively homogeneous nanowire arrays where nanowire density and average length could be controlled by tuning the thickness of the polymer layers. Thicker PMMA and PDMS layers made it simpler to remove the oxidized copper substrate, but at a cost of lower wire density. In most cases satisfactory density was reached in any case (the preliminary goal is to have at least several wires penetrating each cell), as long as wire growth proceeded without issue.

A layer of a light-weight material could be seen to cover the nanowires. This was most likely PDMS, as no such layer was visible after only PMMA application, while oxygen plasma is reported to remove SU-8, although at a low rate (around 250 nm min^{-1} at equivalent settings as those used in this work [162]). As the layer that was observed was still present even after 10 minutes of oxygen plasma treatment, it was likely not SU-8. PDMS is not removed by oxygen plasma, but rather oxidized to form a silica-like structure [157]. The PDMS layer around the nanowires is likely highly oxidized, as thicker (30 nm) layers have been shown to be mostly oxidized at much milder air plasma treatment [156]. Thus the surface chemistry is likely to be similar to that of glass. Such a layer has many advantages. It isolates the nanowires from the cells, likely eliminating the toxicity issues that are associated with copper ions and possible nanowire dissolution, although it has not been investigated in detail if the layer is porous or contains cracks. By subjecting the samples to hydrochloric acid, unprotected nanowires should be

rapidly removed, this could be used to verify the properties of this surrounding layer in future experiments. PDMS-covered wires also give the option for two main methods of surface functionalization that were investigated in this work: thiol-based and silane-based, which allow functionalization of gold and hydroxyl-rich surfaces, respectively.

Thiol-based gold chemistry is considered more reliable than silanization due to the low inter-reaction between the monolayer species [105]. By gold-coating the PDMS layer prior to SU-8 processing a layer of gold could be formed on the nanowire surface. In theory, this should allow the introduction of surface chemistry optimized for attachment and delivery of biomolecules, while the SU-8 surface could be modified independently for cell attachment and spreading.

However, in practice the introduction of gold into the system had some disadvantages, at least during device development and testing. In addition to reducing overall device transparency, the gold layer was observed to severely quench the fluorescence of nearby fluorophores, making it challenging to test different biomolecule deposition strategies. This is an expected result [119], although reports within the nanowire-based delivery field sometimes do report fluorescent labeling of gold structures [64, 46]. However, it is possible that this is due to the different sizes and morphologies of the gold structures, as this is also reported to be a great import [119]. AFM imaging of molecules deposited on gold was also very challenging, due to the inherent roughness of most gold films. This is a well-known issue, and many methods, usually quite complex, are described to produce ultra-flat gold films [124, 163, 164]. Two of these (annealing and template stripping) were attempted, but sufficient flatness was not obtained as AFM imaging of e.g. deposited DNA was not successful. Despite these issues with studying molecule deposition on gold surfaces, this does not mean molecule deposition does not work. Thus, for future applications gold functionalization remains a viable approach, but for current device development incorporating multiple, uncertain steps within gold functionalization and subsequent molecule deposition is not beneficial.

Directly using the PDMS-coating on the nanowires for silane functionalization was investigated as a promising alternative. Deposition of molecules onto silanized surfaces could be studied more simply, as shown both by AFM imaging of DNA deposited on silanized mica and fluorescence images of quantum dots and DNA deposited on silanized glass, SU-8 and PDMS. Using silanes to immobilize biomolecules on all these surfaces is well reported in the literature [115, 165, 166]. The investigations in this work indicate that deposition of an aminosilane such as APTMS, performed by both concentrated vapor phase and dilute aqueous phase deposition, seems to function rather well, binding both DNA and negatively charged quantum dots. This

allowed some investigations of optimal deposition conditions (i.e. buffers, molecule concentrations, rinsing steps, etc.), which likely are transferable to similarly silanized PDMS/silica nanowires.

A disadvantage of silanization is that the difference in surface chemistry between SU-8 and PDMS is not as large as between SU-8 and gold (both contain hydroxyl groups after oxygen plasma treatment), so silanization will likely alter the surface chemistry of SU-8 in a similar manner to PDMS [167]. Chemically, non-plasma oxidized SU-8 does not have hydroxyl groups (SU-8 should consist of ether and aromatic functionalities [148]), so if PDMS is plasma activated prior to SU-8 application, silanization of only the hydroxyl-rich oxidized PDMS might still be possible. However, to increase wettability and cell compatibility it is desirable to plasma oxidize the SU-8 surface, but this would simultaneously remove the silane on the PDMS. These factors reduce selectivity and control over the system when using silanes, but in practice this is not of a large concern at the current device state, as amino-silane modified surfaces are in general reported to be highly cell compatible (e.g. [113]).

Covalent immobilization of DNA to nanowires has been investigated as an alternative to electrostatic adsorption for delivery purposes, using e.g. the reducing environment in the cell cytoplasm to trigger release [63]. The major disadvantage is that this reduces device versatility, as all molecules that are to be delivered must first be modified with covalent linking groups (e.g. amine groups or thiol groups), thus such approaches should be avoided unless necessary, but might be beneficial for increasing general delivery efficiency.

A common issue in standard cell biology investigations is the variability between different cells, making automated analysis difficult [99]. Patterning cells in microarrays of cell clusters or even single cells is proposed as a promising approach [96, 99]. This was achieved by functionalizing gold patterns with a hydrophobic monolayer and subsequently blocking these areas with BSA, allowing patterning of cells both in larger areas and defining single cells. This is a common approach in literature (see e.g. [73]), and offers the possibility of precisely defining cell position and morphology. The observed results are similar to that of the literature, although there is room for optimization [168]. Applying a thin adhesive layer of e.g. chrome or titanium between the gold and the glass should avoid delamination of the gold layer [169]. Reducing cell density and applying a rinsing step to remove non-adhered cells after allowing attachment for a few hours should improve patterning specificity [73]. Patterning of silanes was also done directly on the SU-8 surface, so it could be possible to adapt approaches on glass to SU-8 for direct cell patterning on our devices [170]. This was briefly investigated on PDMS with APTMS patterns as a model substrate, and some selectivity was

observed. This would have to be combined with a more reliable approach to avoid cell attachment on the native PDMS (or SU-8) regions of a real sample, because although these regions showed reduced cell growth, cell growth is not absent, as shown both in this report and described in the literature [149, 160]. Higher specificity and better patterning on both the gold-patterns and on SU-8/PDMS might be obtained by using a PEG-like modification to resist protein adsorption, as this is a very common approach to avoid cell attachment in certain areas [171]. Combined with a nanowire-based versatile biomolecule delivery system this is a powerful approach to quantitatively study cells under standardized conditions.

5.2 Device biocompatibility

Some issues were encountered with device biocompatibility using the new fabrication procedures, despite that PMMA, PDMS and SU-8 are reported to be biocompatible in themselves [149, 69]. Studies on multiple model surfaces were performed, and it was concluded that exposing a device which included at least a PDMS layer with a thick SU-8 well structure to either acetone, the SU-8 developer (PGMEA) or both induced the toxicity. The precise mechanism is not known, although an important clue is that it was seen that cells both on and near the device were affected, indicating something occurring in solution and not only on the SU-8 surface. This could be leakage of the solvent itself, but it could also be leakage of uncured PDMS monomers or oligomers, facilitated by PDMS-swelling due to the solvents. Such leakage is reported to be common, even into aqueous solutions, and can be toxic to cells [172]. A possible explanation for why this does not occur on planar substrates is that here the area for solvent/monomer escape is much larger (i.e. not buried under a thick patterned SU-8 layer), and thus escape occurs naturally during the fabrication procedure. Extended heat treatment seemed to alleviate the issue, which could be due to solvent removal or further cross-linking in the PDMS-layer. These issues are likely completely fixable if investigated further, but alternative approaches could also be beneficial.

If non-transparent devices are acceptable, no solvent processing is needed, and such samples indeed had no toxicity issues. However, transparent devices are beneficial due to ease of investigation and better compatibility with analysis systems. Avoiding organic solvent use could also be possible on transparent devices. Acetone can be avoided by ensuring thick enough layers of PMMA and PDMS together with homogeneous samples, as the oxidized copper substrate can be removed directly in this case. SU-8 development can be avoided by some larger alterations in the device fabrication: Instead

of having a self-supported structure with a thick layer of SU-8 with wells for mechanical strength, the sample can be glued directly to a glass slide after removal of the oxidized copper substrate, providing an entire surface of only nanowires. This can also have several other advantages, e.g. allowing patterning of wire functionality (as opposed to patterning of wire presence in the case of wells) to control cell growth in a similar way as that done on glass and gold above, or direct integration into a typical microarray spotter system without potential alignment issues. The only challenge is that another strong support layer must temporarily be in place so the oxidized copper substrate can be removed and the sample can be glued to glass, as the PMMA, PDMS and thin SU-8 layer are not mechanically rigid enough to support the device by themselves. This is currently being investigated through the use of heat curable, water soluble glues.

For the investigations of cell proliferation on various surfaces only qualitative optical inspections were performed. Not considering the toxicity issues above, the results roughly coincide with the literature, showing cell proliferation similar to glass on plasma treated PDMS and PMMA [69]. One exception is that plasma oxidation of the SU-8 surface could not be seen to have a particular effect on cell proliferation as opposed to literature reports [149], but this could also be due to the qualitative nature of our investigations or the differences between the cell lines that were used (HeLa cells are considered a robust cell line with reduced sensitivity to many factors [173]). There are several methods available to quantify cell proliferation, including counting cells after live/dead staining, a colorimetric MTT assay [174] or through flow cytometry analysis. For the current system this was not necessary, as the difference between non-toxic and toxic samples was easily visible, but can be of interest for future investigations into e.g. different surface chemistries or a quantitative analysis of nanowire influence on cells (see below).

5.3 Cells on nanowire arrays

Nanowire arrays with a PMMA layer were shown to be more homogeneous and planar than nanowires with an SU-8 2 layer, probably due to differences in the viscous properties of the polymer solutions. These differences were seen to impact cell proliferation and spreading, and are attributed to two alternate modes of cell-substrate interaction: At high wire density and with longer wires, i.e. with an SU-8 2 layer, the cells landed on the wires, but were only to a small degree able to form focal adhesions and spread out, mostly remaining balled up and often entering apoptosis (or anoikis) [68]. If the wires on average were shorter, and/or had a lower surface density (with

the PMMA layer or PMMA, PDMS and SU-8 2 layers), the cells are able to interact both with the nanowires and the surface, forming much more focal adhesions, and spreading out to a higher degree. Indeed, at low wire densities it was observed that cells spread in a manner similar to planar substrates.

A direct comparison with the literature is challenging, as other studies have used different cell lines, different materials and different wire fabrication methods. However, the general trends appear to be the same, with most studies showing cell attachment and spreading on the surface while being penetrated by the wires [62, 64, 86, 87, 88]. In cases where cells grew on top of the wires, articles mostly (the one exception is Hällström et.al. [82] the reason is not known for the discrepancy) report reduced cell spreading and apoptosis, similar to what was observed in this work [83, 84]. In the studies reporting cell spreading while the cells were penetrated by wires, the wire density was typically below $1 \mu\text{m}^{-2}$, while in those reporting reduced cell spreading, higher wire densities were used, indicating the existence of a critical wire density for if cells were able to spread or not. Due to sample variability and inhomogeneities, a good estimate for our final wire density is difficult to make, although it is usually considerably below $1 \mu\text{m}^{-2}$. It would seem that when using only SU-8 2 as a coating on samples which also have a high initial wire density, the critical value is exceeded. This could also be due to wire length, as the protruding wires in this case are longer than those protruding from the PMMA layer, up to several microns. For the complete device fabrication process, which also includes the beneficial PMMA flattening and homogenizing of the wires, the critical value does not seem to be reached, indicating a good wire density and length for minimally invasive delivery of biomolecules. In earlier work during my specialization project, a coating of only SU-8 5 ($\sim 5 \mu\text{m}$) was used, which gives somewhat thicker layers than SU-8 2 ($\sim 2 \mu\text{m}$). Such layers showed good cell spreading and growth while the cells were being penetrated by the nanowires, so this can be regulated in several ways.

Cells were also shown to closely and actively interact with the nanowires, which is in agreement with reported literature [87]. Filopodia seemed to have a preference for nanowire binding as opposed to binding to nearby flat surfaces, and filopodia were also seen to engulf nanowires. Nanowires could be seen penetrating into cells, both into cell bodies and cellular extensions formed after the cells settled on the surface. This together with the fluorescent and viability investigations of cells growing on nanowires indicate that the penetration by nanowires is not itself harmful for the cells. Spreading rates are reported to be somewhat perturbed when cells are cultured on nanowires [64], but this was not investigated.

The exact nanowire penetration mechanism still remains uncertain. Ob-

ervation of the way the nanowires penetrate the cells in the SEM micrographs makes it seem unlikely that the outer cellular membrane is engulfing the entire nanowire inside the cell. It could be possible that the nanowires are maintained in a vesicle-like structure, although such a structure would be very different from typical vesicles, so this seems unlikely. Cell shrinkage and other drying artifacts may play a role in these observations, as cell shrinkage of around 30% is reported for both HMDS and CPD dried cells [175]. This could at least be the cause for the observed bending of filopodia-bound nanowires, but also wires significantly protruding through the cells and out the other side. However, the drying would likely not cause the wires to penetrate into the cells in the first place. Other articles investigating cell growth on nanowires conclude that the wires penetrate through the outer membrane and into the cell cytoplasm (e.g. [62, 64, 86, 87, 88]). This is also supported by the investigations of direct penetration of single nanowires or other nanostructures into cells by applying an external force (e.g. a nanowire attached to an AFM tip) [51, 61, 176]. In these studies the membrane bulges to a certain extent, and typically indentation depth is significantly less than a micron before membrane penetration (e.g. 0.6 μm for 200 nm silicon nanowires, or 0.1 μm for 40 nm carbon nanotubes). Based on the SEM and confocal penetration investigations, drying artifacts notwithstanding, it seems likely that the nanowires in this work similarly penetrate into the cell cytoplasm.

Closer investigations on the interaction between nanowires and cells could be done by optimizing methods to visualize single wires, e.g. by quantum dot conjugation, together with immunostaining methods to visualize focal adhesions and actin filaments [79]. Optimally, the use of a pure polymer-based device (as opposed to the semi-conductor devices used in literature) could allow sample embedding and subsequent slicing of the sample to prepare sections for transmission electron microscopy (TEM), which would likely provide clear insights into how the wires penetrate into the cells, as cell membranes and organelles can be visualized at high resolution in TEM [9].

Three types of molecules were used for delivery experiments: propidium iodide (PI), quantum dots and plasmid DNA encoding for eGFP. Initial results seem promising, but naturally leave a large room for optimization. The results for PI and the quantum dots are not very surprising. Even though PI is a negatively charged molecule, it is unlikely to significantly bind to the positively charged nanowires, as entropy works against such association. Thus it is unlikely that significant amounts of PI could be delivered into the cell via the nanowires, and the PI delivery experiments mostly indicate that live cells penetrated by wires have largely intact membranes, similar to the live/dead assays. For quantum dots the background signal originating from surface-bound quantum dots is the main issue, as the amount of quantum

dots inside a given cell cannot be significantly higher than that on the surface in general, as the entire surface is expected to have approximately the same positive charge after silanization. The solution to this would be to attempt something similar to Shalek et.al., who showed delivery of fluorescent molecules by first culturing the cells on nanowire arrays, then re-plating the cells on glass after trypsin treatment for observation [64]. The observed background signal from non-delivered molecules is likely a major reason they performed such re-plating of the cells. This is assuming that re-plating in fact is possible and that the cells are not interacting so closely with our nanowires that trypsination fails to release them.

The delivery of plasmid DNA and subsequent expression of eGFP observed in some cells is very promising. Such delivery is relatively simple to verify directly on the device, as concerns about background fluorescence (as is the case with direct delivery of fluorescent molecules such as quantum dots) are absent. Unfortunately, transfection efficiency was low, with only a few cells being transfected of several thousand on each sample. Naked plasmids are reported to induce a small amount of transfection [46], so this can not be ruled out as the transfection mechanism in this case. However, even transfection with Metafectene Pro, a commercial transfection agent, is reported to have quite low (about 6%) transfection efficiencies in HeLa cells [177], and transfection efficiencies observed with Metafectene Pro in the current work were even lower. In addition, bright transfection occurs in even fewer cells than those defined as "transfected" in the literature, many cells are only weakly fluorescent and flow cytometry analysis must be performed to actually quantify this. Thus these preliminary observations of transfection are in fact quite promising, as they have not been subject to any specific optimization so far. An important point is that it was demonstrated that transfection, regardless of plasmid delivery route, is possible while the cells are penetrated by nanowires, and that typical cellular functions are thus intact, which is also the main point of a recent article on this field by Berthing et.al. [86]. In further studies plasmid DNA could be added into solution after cell seeding to serve as control experiments, and naturally attempts must be made to generally increase delivery efficiency to at least rival that of the current, commercial techniques.

Chapter 6

Conclusion and future prospects

A system for delivery of exogenous molecules into cultured HeLa cells based on arrays of vertical CuO nanowires grown by thermal oxidation was further developed and investigated. Methods to observe HeLa cells using fluorescent and electron microscopy were investigated, and several procedures and fluorescent labels were found suitable for obtaining useful and complementary information. Polymeric spin-casting and photolithography of PMMA, PDMS and SU-8 was used to create a transparent surface with protruding, PDMS- or gold-covered nanowires in a thicker SU-8 structure with wells down to the nanowire surfaces. Toxic effects were observed on cells on these devices, which was finally linked to retainment or influence of organic solvents used during processing. However, planar substrates without SU-8 wells, even if they underwent solvent treatment, did not show cell toxicity, indicating some mechanism related to the thick SU-8 structure. Toxicity could be significantly reduced by baking the samples at elevated temperatures. Alternatively, non-transparent samples with protruding PDMS-covered nanowires and an intact oxidized copper substrate could be glued to a glass slide and used for cell culturing, as such samples did not show any cell toxicity.

Surface modification strategies for optimal biomolecule deposition were investigated. Although thiol-based self-assembled monolayers on gold are usually considered reliable, it was challenging to study these, as gold strongly quenched the fluorescence of nearby molecules, and gold films were typically too rough for AFM imaging of deposited molecules. Silane-based surface modification was investigated as an alternative, and it was shown that negatively charged fluorescent DNA and quantum dots could be selectively bound to an aminosilane monolayer. Both vapor-phase and aqueous phase silanization methods were shown to be suitable. The silane could be patterned using

photolithography processing, and patterns of quantum dots bound to the silane could be visualized on glass, PDMS and SU-8. Deposited DNA could also be visualized using AFM by modifying mica with the same aminosilane. Hydrophobic surface modification of gold patterns on glass was used to pattern cells, both defining areas with and without cell growth and defining the morphology of single cells.

HeLa cells were cultured on samples with protruding wires, and in general showed good proliferation and spreading. However, reduced spreading was observed at higher nanowire surface densities and longer nanowire lengths. On standard nanowire samples the nanowires appeared to penetrate into the cells as shown by both confocal fluorescent and scanning electron microscopy. The cells could also be seen to interact with the nanowires, with cellular protrusions binding to and engulfing the nanowires. Finally, preliminary delivery of plasmid DNA coding for eGFP and subsequent expression of eGFP in HeLa cells penetrated by nanowires was demonstrated, although delivery efficiency was low.

A major goal for further work on this system is proving its suitability as a delivery system. This could be investigated through delivery of fluorescent molecules in addition to further experiments with reporter plasmids. If difficulties with cell toxicity on transparent-type samples and background fluorescence still are present, detachment and re-plating of cells on glass after culturing on nanowires is a possible alternative. However, fabrication avoiding the toxicity-related process steps should also be pursued, as a transparent device would enable more rapid and direct cell visualization and simpler integration into current imaging systems. Cell-wire interactions should also be further investigated as insights into this are both of a fundamental interest and important to understand the nanowire delivery mechanisms. Cell viability and behavior on the nanowire arrays should also be compared more thoroughly with standard substrates, as actual device usage will depend on minimal wire invasiveness.

As one of the main foreseen application areas for this device is for high-throughput analysis, attempts should be made to use standard microarray techniques to spatially define delivery sites on nanowire arrays. This could be combined with the early attempts of cell patterning to provide well-defined systems for quantitative cell analysis. As a physical transfection system with direct access to the cell cytoplasm, and possibly cell nucleus, nanowire-based delivery should allow transfection of non-dividing cells and other cells that are typically hard to transfect. Thus once delivery is shown to be reliable for common immortal cell lines such hard-to-transfect cell lines should be investigated on the nanowire arrays.

Bibliography

- [1] RECILLAS-TARGA F. *Multiple strategies for gene transfer, expression, knockdown, and chromatin influence in mammalian cell lines and transgenic animals.* Mol Biotechnol, 34(3):337–354, Nov 2006.
- [2] PEARCE ME, et al. *Multi-functional nanorods for biomedical applications.* Pharm Res, 24(12):2335–2352, Dec 2007.
- [3] MCKNIGHT T, et al. *Tracking gene expression after DNA delivery using spatially indexed nanofiber arrays.* Nano Letters, 4(7):1213–1219, 2004.
- [4] MUMM F, et al. *Easy Route to Superhydrophobic Copper-Based Wire-Guided Droplet Microfluidic Systems.* ACS nano, 3(9):2647–2652, 2009.
- [5] MUMM F et al. *Oxidative fabrication of patterned, large, non-flaking CuO nanowire arrays.* Nanotechnology, 22:105605, 2011.
- [6] BECKWITH KM. *Surface-functionalized CuO nanowires in an SU-8 epoxy as a platform for biomolecule delivery into cells.* Specialization Project, 2010.
- [7] ABGRALL P, et al. *SU-8 as a structural material for lab-on-chips and microelectromechanical systems.* Electrophoresis, 28(24):4539–4551, 2007.
- [8] CRICK F. *Central dogma of molecular biology.* Nature, 227(5258):561–563, Aug 1970.
- [9] BECKER W, et al. *The world of the cell.* Benjamin Cummings, 7th edition, 2008.
- [10] COLOSIMO A, et al. *Transfer and expression of foreign genes in mammalian cells.* Biotechniques, 29(2):314–331, 2000.
- [11] WALL D. *Recombinant DNA, Basic Procedures.* In M Schaechter, editor, *Encyclopedia of Microbiology*, pages 271 – 280. Academic Press, Oxford, 2009.
- [12] LIEW CG, et al. *Transient and stable transgene expression in human embryonic stem cells.* Stem Cells, 25(6):1521–1528, Jun 2007.
- [13] NAYLOR LH. *Reporter gene technology: the future looks bright.* Biochem Pharmacol, 58(5):749–757, Sep 1999.
- [14] HANNON G. *RNA interference.* Nature, 418(6894):244–251, 2002.
- [15] MELLO CC et al. *Revealing the world of RNA interference.*

- Nature, 431(7006):338–342, Sep 2004.
- [16] PILLAI RS, et al. *Repression of protein synthesis by miRNAs: how many mechanisms?* Trends Cell Biol, 17(3):118–126, Mar 2007.
- [17] SUI G, et al. *A DNA vector-based RNAi technology to suppress gene expression in mammalian cells.* Proc Natl Acad Sci U S A, 99(8):5515–5520, Apr 2002.
- [18] SHIMADA M, et al. *DNA vaccine expressing HIV-1 gp120/immunoglobulin fusion protein enhances cellular immunity.* Vaccine, 2010.
- [19] VAN BRUMMELEN A, et al. *Establishing malaria parasite transfection technology in South Africa.* 2010.
- [20] LU W, et al. *Tumor Site-Specific Silencing of NF- κ B p65 by Targeted Hollow Gold Nanosphere-Mediated Photothermal Transfection.* Cancer research, 70(8):3177, 2010.
- [21] KIM D, et al. *Generation of human induced pluripotent stem cells by direct delivery of reprogramming proteins.* Cell Stem Cell, 4(6):472–476, Jun 2009.
- [22] BONETTA L. *The inside scoop—evaluating gene delivery methods.* Nature Methods, 2(11):875, 2005.
- [23] BERG K, et al. *Photochemical internalization: a novel technology for delivery of macromolecules into cytosol.* Cancer Res, 59(6):1180–1183, Mar 1999.
- [24] VARKOUHI AK, et al. *Endosomal escape pathways for delivery of biologicals.* J Control Release, Nov 2010.
- [25] GOFF SP et al. *Construction of hybrid viruses containing SV40 and lambda phage DNA segments and their propagation in cultured monkey cells.* Cell, 9(4 PT 2):695–705, Dec 1976.
- [26] CAO F, et al. *Comparison of Gene-Transfer Efficiency in Human Embryonic Stem Cells.* Molecular Imaging and Biology, 12(1):15–24, 2010.
- [27] ATKINSON H et al. *Delivering the goods: viral and non-viral gene therapy systems and the inherent limits on cargo DNA and internal sequences.* Genetica, 138(5):485–498, May 2010.
- [28] ESCORS D et al. *Lentiviral vectors in gene therapy: their current status and future potential.* Arch Immunol Ther Exp (Warsz), 58(2):107–119, Apr 2010.
- [29] ZANTA MA, et al. *Gene delivery: a single nuclear localization signal peptide is sufficient to carry DNA to the cell nucleus.* Proc Natl Acad Sci U S A, 96(1):91–96, Jan 1999.
- [30] DEVROE E et al. *Retrovirus-delivered siRNA.* BMC biotechnology, 2(1):15, 2002.

- [31] LUO D et al. *Synthetic DNA delivery systems*. Nature biotechnology, 18(1):33–37, 2000.
- [32] HOWARD BV, et al. *The uptake of SV40 DNA by nonpermissive cells in the presence of DEAE-dextran*. Biochim Biophys Acta, 228(1):105–116, Jan 1971.
- [33] BLOW N. *Journeys across the membrane*. Nature Methods, 6(4):305–309, 2009.
- [34] GOPALAKRISHNAN B et al. *siRNA and DNA transfer to cultured cells*. Methods Mol Biol, 480:31–52, 2009.
- [35] HASSANE FS, et al. *Cell penetrating peptides: overview and applications to the delivery of oligonucleotides*. Cell Mol Life Sci, 67(5):715–726, Mar 2010.
- [36] MAO H, et al. *Chitosan-DNA nanoparticles as gene carriers: synthesis, characterization and transfection efficiency*. Journal of controlled release, 70(3):399–421, 2001.
- [37] GRAHAM FL et al. *A new technique for the assay of infectivity of human adenovirus 5 DNA*. Virology, 52(2):456–467, Apr 1973.
- [38] FELGNER P, et al. *Lipofection: a highly efficient, lipid-mediated DNA-transfection procedure*. Proceedings of the National Academy of Sciences of the United States of America, 84(21):7413, 1987.
- [39] CHESNOY S et al. *Structure and Function of Lipid-DNA Complexes for Gene Delivery*. Annual review of biophysics and biomolecular structure, 29(1):27–47, 2000.
- [40] KIM TK et al. *Mammalian cell transfection: the present and the future*. Anal Bioanal Chem, 397(8):3173–3178, Aug 2010.
- [41] HART SL. *Multifunctional nanocomplexes for gene transfer and gene therapy*. Cell Biol Toxicol, 26(1):69–81, Feb 2010.
- [42] INOUE Y, et al. *Site-specific gene transfer with high efficiency onto a carbon nanotube-loaded electrode*. J R Soc Interface, 5(25):909–918, Aug 2008.
- [43] SINGH R, et al. *Binding and condensation of plasmid DNA onto functionalized carbon nanotubes: toward the construction of nanotube-based gene delivery vectors*. J Am Chem Soc, 127(12):4388–4396, Mar 2005.
- [44] SANDHU K, et al. *Gold nanoparticle-mediated transfection of mammalian cells*. Bioconjugate Chem, 13(1):3–6, 2002.
- [45] KNEUER C, et al. *A nonviral DNA delivery system based on surface modified silica-nanoparticles can efficiently transfect cells in vitro*. Bioconjug Chem, 11(6):926–932, 2000.
- [46] KUO C, et al. *Surface modified gold nanowires for mammalian cell transfection*. Nanotechnology, 19:025103, 2008.
- [47] SALEM A, et al. *Multifunctional nanorods for gene delivery*.

- Nature Materials, 2(10):668–671, 2003.
- [48] SEGURA T et al. *Surface-tethered DNA complexes for enhanced gene delivery*. *Bioconjug Chem*, 13(3):621–629, 2002.
- [49] LUO D et al. *Enhancement of transfection by physical concentration of DNA at the cell surface*. *Nature biotechnology*, 18(8):893–895, 2000.
- [50] GORDON JW, et al. *Genetic transformation of mouse embryos by microinjection of purified DNA*. *Proc Natl Acad Sci U S A*, 77(12):7380–7384, Dec 1980.
- [51] VAKARELSKI IU, et al. *Penetration of living cell membranes with fortified carbon nanotube tips*. *Langmuir*, 23(22):10893–10896, Oct 2007.
- [52] NEUMANN E, et al. *Gene transfer into mouse lymphoma cells by electroporation in high electric fields*. *EMBO J*, 1(7):841–845, 1982.
- [53] WEAVER J et al. *Theory of electroporation: a review*. *Bioelectrochemistry and Bioenergetics*, 41(2):135–160, 1996.
- [54] KIM JA, et al. *A novel electroporation method using a capillary and wire-type electrode*. *Biosens Bioelectron*, 23(9):1353–1360, Apr 2008.
- [55] BAO S, et al. *Transfection of a reporter plasmid into cultured cells by sonoporation in vitro*. *Ultrasound in medicine & biology*, 23(6):953–959, 1997.
- [56] PEPE J, et al. *Experimental comparison of sonoporation and electroporation in cell transfection applications*. *Acoustics Research Letters Online*, 5:62, 2004.
- [57] LEE PW, et al. *The use of biodegradable polymeric nanoparticles in combination with a low-pressure gene gun for transdermal DNA delivery*. *Biomaterials*, 29(6):742–751, Feb 2008.
- [58] PLANK C, et al. *The magnetofection method: using magnetic force to enhance gene delivery*. *Biol Chem*, 384(5):737–747, May 2003.
- [59] MORISHITA N, et al. *Magnetic nanoparticles with surface modification enhanced gene delivery of HVJ-E vector*. *Biochem Biophys Res Commun*, 334(4):1121–1126, Sep 2005.
- [60] YANG SY, et al. *Ex vivo magnetofection with magnetic nanoparticles: a novel platform for nonviral tissue engineering*. *Artif Organs*, 32(3):195–204, Mar 2008.
- [61] CAI D, et al. *Highly efficient molecular delivery into mammalian cells using carbon nanotube spearing*. *Nat Methods*, 2(6):449–454, Jun 2005.
- [62] KIM W, et al. *Interfacing silicon nanowires with mammalian cells*. *J Am Chem Soc*, 129(23):7228–7229, Jun 2007.
- [63] PECKYS D, et al. *Immobilization and release strategies for DNA delivery using carbon nanofiber arrays and self-assembled monolay-*

- ers. *Nanotechnology*, 20:145304, 2009.
- [64] SHALEK AK, et al. *Vertical silicon nanowires as a universal platform for delivering biomolecules into living cells*. *Proc Natl Acad Sci U S A*, 107(5):1870–1875, Feb 2010.
- [65] NORDE W. *Adsorption of proteins from solution at the solid-liquid interface*. *Adv Colloid Interface Sci*, 25(4):267–340, Sep 1986.
- [66] RUOSLAHTI E et al. *New perspectives in cell adhesion: RGD and integrins*. *Science*, 238(4826):491–497, Oct 1987.
- [67] STUPACK DG, et al. *Apoptosis of adherent cells by recruitment of caspase-8 to unligated integrins*. *J Cell Biol*, 155(3):459–470, Oct 2001.
- [68] FRISCH SM et al. *Disruption of epithelial cell-matrix interactions induces apoptosis*. *J Cell Biol*, 124(4):619–626, Feb 1994.
- [69] ERTEL SI, et al. *In vitro study of the intrinsic toxicity of synthetic surfaces to cells*. *J Biomed Mater Res*, 28(6):667–675, Jun 1994.
- [70] NORDE W. *Driving Forces for Protein Adsorption at Solid Surfaces*. In *Surfactant Science*, pages –. CRC Press, January 2003.
- [71] TIDWELL C, et al. *Endothelial cell growth and protein adsorption on terminally functionalized, self-assembled monolayers of alkanethiolates on gold*. *Langmuir*, 13(13):3404–3413, 1997.
- [72] KILIAN KA, et al. *Geometric cues for directing the differentiation of mesenchymal stem cells*. *Proc Natl Acad Sci U S A*, 107(11):4872–4877, Mar 2010.
- [73] JING G, et al. *Precise cell patterning using cytophobic self-assembled monolayer deposited on top of semi-transparent gold*. *Biomedical microdevices*, pages 1–14, 2010.
- [74] KRISHNAN A, et al. *Mixology of protein solutions and the Vroman effect*. *Langmuir*, 20(12):5071–5078, Jun 2004.
- [75] MCPHERSON T, et al. *Prevention of protein adsorption by tethered poly (ethylene oxide) layers: experiments and single-chain mean-field analysis*. *Langmuir*, 14(1):176–186, 1998.
- [76] ARIMA Y et al. *Effect of wettability and surface functional groups on protein adsorption and cell adhesion using well-defined mixed self-assembled monolayers*. *Biomaterials*, 28(20):3074–3082, Jul 2007.
- [77] LORD M, et al. *Influence of nanoscale surface topography on protein adsorption and cellular response*. *Nano Today*, 5(1):66–78, 2010.
- [78] DUBIEL EA, et al. *Bridging the gap between physicochemistry and*

- interpretation prevalent in cell-surface interactions.* Chem Rev, 111(4):2900–2936, Apr 2011.
- [79] WOZNIAK MA, et al. *Focal adhesion regulation of cell behavior.* Biochim Biophys Acta, 1692(2-3):103–119, Jul 2004.
- [80] SINGHVI R, et al. *Engineering cell shape and function.* Science, 264(5159):696–698, Apr 1994.
- [81] YIM EKF et al. *Significance of synthetic nanostructures in dictating cellular response.* Nanomedicine, 1(1):10–21, Mar 2005.
- [82] HLLSTRM W, et al. *Gallium phosphide nanowires as a substrate for cultured neurons.* Nano Lett, 7(10):2960–2965, Oct 2007.
- [83] ZHAO L, et al. *Mechanism of cell repellence on quasi-aligned nanowire arrays on Ti alloy.* Biomaterials, 31(32):8341–8349, Nov 2010.
- [84] LEE J, et al. *The control of cell adhesion and viability by zinc oxide nanorods.* Biomaterials, 29(27):3743–3749, Sep 2008.
- [85] LEE J, et al. *Randomly oriented, upright SiO₂ coated nanorods for reduced adhesion of mammalian cells.* Biomaterials, 30(27):4488–4493, Sep 2009.
- [86] BERTHING T, et al. *Intact Mammalian cell function on semiconductor nanowire arrays: new perspectives for cell-based biosensing.* Small, 7(5):640–647, Mar 2011.
- [87] XIE C, et al. *Noninvasive neuron pinning with nanopillar arrays.* Nano Lett, 10(10):4020–4024, Oct 2010.
- [88] XIE C, et al. *Vertical nanopillars for highly localized fluorescence imaging.* Proc Natl Acad Sci U S A, 108(10):3894–3899, Mar 2011.
- [89] VERMA P, et al. *Continuum model of mechanical interactions between biological cells and artificial nanostructures.* Biointerphases, 5(2):37–44, Jun 2010.
- [90] PRASAD P. *Introduction to biophotonics*, volume 10. 2005.
- [91] MICHALET X, et al. *Quantum dots for live cells, in vivo imaging, and diagnostics.* Science, 307(5709):538–544, Jan 2005.
- [92] JONES KH et al. *An improved method to determine cell viability by simultaneous staining with fluorescein diacetate-propidium iodide.* J Histochem Cytochem, 33(1):77–79, Jan 1985.
- [93] BRANDON D, et al. *Microstructural characterization of materials.* Wiley New York, 1999.
- [94] GOLDSTEIN J. *Scanning electron microscopy and X-ray microanalysis*, volume 1. Springer Us, 2003.
- [95] BRAY DF, et al. *Comparison of hexamethyldisilazane (HMDS), Peldri II, and critical-point drying methods for scanning electron microscopy of biological specimens.* Microsc Res Tech, 26(6):489–495, Dec 1993.

- [96] ZIAUDDIN J et al. *Microarrays of cells expressing defined cDNAs*. Nature, 411(6833):107–110, May 2001.
- [97] STRZL M, et al. *High throughput screening of gene functions in mammalian cells using reversely transfected cell arrays: review and protocol*. Comb Chem High Throughput Screen, 11(2):159–172, Feb 2008.
- [98] FJELDBO CS, et al. *Functional studies on transfected cell microarray analysed by linear regression modelling*. Nucleic Acids Res, 36(15):e97, Sep 2008.
- [99] YAMAMURA S, et al. *Single-cell microarray for analyzing cellular response*. Anal Chem, 77(24):8050–8056, Dec 2005.
- [100] HORBETT T. *The role of adsorbed proteins in animal cell adhesion*. Colloids and Surfaces B: Biointerfaces, 2(1-3):225–240, 1994.
- [101] CHU P, et al. *Plasma-surface modification of biomaterials*. Materials Science and Engineering: R: Reports, 36(5-6):143–206, 2002.
- [102] OWEN M et al. *Plasma treatment of polydimethylsiloxane*. Journal of adhesion science and technology, 8(10):1063–1075, 1994.
- [103] OZCAN C, et al. *Influence of oxygen plasma modification on surface free energy of PMMA films and cell attachment*. In *Macromolecular symposia*, volume 269, pages 128–137. Wiley Online Library, 2008.
- [104] WALTHER F, et al. *Surface hydrophilization of SU-8 by plasma and wet chemical processes*. Surface and Interface Analysis, 42:1735–1744, 2010.
- [105] ULMAN A. *Formation and structure of self-assembled monolayers*. Chemical reviews, 96(4):1533–1554, 1996.
- [106] LOVE JC, et al. *Self-assembled monolayers of thiolates on metals as a form of nanotechnology*. Chem Rev, 105(4):1103–1169, Apr 2005.
- [107] WASSERMAN S, et al. *Structure and reactivity of alkylsiloxane monolayers formed by reaction of alkyltrichlorosilanes on silicon substrates*. Langmuir, 5(4):1074–1087, 1989.
- [108] WU C, et al. *Effect of polydimethylsiloxane surfaces silanized with different nitrogen-containing groups on the adhesion progress of epithelial cells*. Surface and Coatings Technology, 2010.
- [109] FISSI L, et al. *Amine functionalized SU-8 layer guiding Love mode surface acoustic wave*. Sensors and Actuators B: Chemical, 144(1):23–26, 2010.
- [110] KRASNOSLOBODTSEV A et al. *Effect of water on silanization of silica by trimethoxysilanes*. Langmuir, 18(8):3181–3184, 2002.
- [111] WANG W, et al. *Morphology and Amine Accessibility of*

- (*3-Aminopropyl*) *Triethoxysilane* *Films on Glass Surfaces*. *Scanning*, 30(2):65–77, 2008.
- [112] HSIEH H, et al. *Effective Enhancement of Fluorescence Detection Efficiency in Protein Microarray Assays: Application of a Highly Fluorinated Organosilane as the Blocking Agent on the Background Surface by a Facile Vapor-Phase Deposition Process*. *Analytical chemistry*, 81(19):7908–7916, 2009.
- [113] FAUCHEUX N, et al. *Self-assembled monolayers with different terminating groups as model substrates for cell adhesion studies*. *Biomaterials*, 25(14):2721–2730, Jun 2004.
- [114] LYUBCHENKO YL, et al. *Imaging of nucleic acids with atomic force microscopy*. *Methods*, Feb 2011.
- [115] JOSHI M, et al. *Silanization and antibody immobilization on SU-8*. *Applied surface science*, 253(6):3127–3132, 2007.
- [116] WIRDE M, et al. *Self-assembled monolayers of cystamine and cysteamine on gold studied by XPS and voltammetry*. *Langmuir*, 15(19):6370–6378, 1999.
- [117] HEGNER M, et al. *Immobilizing DNA on gold via thiol modification for atomic force microscopy imaging in buffer solutions*. *FEBS Lett*, 336(3):452–456, Dec 1993.
- [118] ENDERLEIN J. *A theoretical investigation of single-molecule fluorescence detection on thin metallic layers*. *Biophysical Journal*, 78(4):2151–2158, 2000.
- [119] ANGER P, et al. *Enhancement and quenching of single-molecule fluorescence*. *Physical review letters*, 96(11):113002, 2006.
- [120] BEZANILLA M, et al. *Adsorption of DNA to mica, silylated mica, and minerals: characterization by atomic force microscopy*. *Langmuir*, 11(2):655–659, 1995.
- [121] SONG Y, et al. *Self-assembled monolayers of DNA on cysteamine modified Au(111) surface: Atomic force microscopy study*. *Microsc Res Tech*, 73(1):51–57, Jan 2010.
- [122] EL KIRAT K, et al. *Sample preparation procedures for biological atomic force microscopy*. *Journal of microscopy*, 218(3):199–207, 2005.
- [123] NOGUES C et al. *A rapid approach to reproducible, atomically flat gold films on mica*. *Surface science*, 573(3):L383–L389, 2004.
- [124] HEGNER M, et al. *Ultralarge atomically flat template-stripped Au surfaces for scanning probe microscopy*. *Surface science*, 291(1-2):39–46, 1993.
- [125] XIA Y, et al. *One-dimensional nanostructures: synthesis, characterization, and applications*. *Advanced Materials*, 15(5):353–389, 2003.
- [126] FU Y, et al. *Synthesis of Fe₂O₃ nanowires by oxidation of iron*.

- Chemical Physics Letters, 350(5-6):491–494, 2001.
- [127] YAO BD, et al. *Formation of ZnO nanostructures by a simple way of thermal evaporation.* Applied Physics Letters, 81(4):757–759, 2002.
- [128] LI JY, et al. *Synthesis of [beta]-Ga₂O₃ nanorods.* Journal of Alloys and Compounds, 306(1-2):300 – 302, 2000.
- [129] IWANAGA H, et al. *Morphology of SnO₂ whiskers.* Journal of Crystal Growth, 83(4):602 – 605, 1987.
- [130] JIANG X, et al. *CuO nanowires can be synthesized by heating copper substrates in air.* Nano letters, 2(12):1333–1338, 2002.
- [131] HANSEN B, et al. *Transport, Analyte Detection, and Opto-Electronic Response of p-Type CuO Nanowires.* The Journal of Physical Chemistry C, page 353.
- [132] KAUR M, et al. *Growth and branching of CuO nanowires by thermal oxidation of copper.* Journal of Crystal Growth, 289(2):670–675, 2006.
- [133] LIU Y, et al. *From copper nanocrystalline to CuO nanoneedle array: synthesis, growth mechanism, and properties.* 2007.
- [134] XU C, et al. *Formation of CuO nanowires on Cu foil.* Chemical Physics Letters, 399(1-3):62–66, 2004.
- [135] GONÇALVES A, et al. *On the growth and electrical characterization of CuO nanowires by thermal oxidation.* Journal of Applied Physics, 106(3):034303, 2009.
- [136] KUMAR A, et al. *The effect of growth parameters on the aspect ratio and number density of CuO nanorods.* Journal of Physics: Condensed Matter, 16:8531, 2004.
- [137] LI X, et al. *Effect of electric field on CuO nanoneedle growth during thermal oxidation and its growth mechanism.* Journal of Applied Physics, 108:024308, 2010.
- [138] ANANDAN S, et al. *Room temperature growth of CuO nanorod arrays on copper and their application as a cathode in dye-sensitized solar cells.* Materials Chemistry and Physics, 93(1):35–40, 2005.
- [139] HSIEH CT, et al. *Field emission from various CuO nanostructures.* Applied Physics Letters, 83(16):3383–3385, 2003.
- [140] ZHU Y, et al. *Large-scale synthesis and field emission properties of vertically oriented CuO nanowire films.* Nanotechnology, 16:88, 2005.
- [141] VILA M, et al. *Optical and magnetic properties of CuO nanowires grown by thermal oxidation.* Journal of Physics D: Applied Physics, 43:135403, 2010.
- [142] STOHS SJ et al. *Oxidative mechanisms in the toxicity of metal ions.* Free Radic Biol Med, 18(2):321–336, Feb 1995.

- [143] KO C et al. *Effects of pH variation in aqueous solutions on dissolution of copper oxide*. Surface and Interface Analysis, 42(6-7):1128–1130, 2010.
- [144] QUIRK M et al. *Semiconductor manufacturing technology*. Prentice Hall Upper Saddle River, NJ, 2001.
- [145] DUFFY D, et al. *Rapid prototyping of microfluidic systems in poly (dimethylsiloxane)*. Anal. Chem, 70(23):4974–4984, 1998.
- [146] LORENZ H, et al. *High-aspect-ratio, ultrathick, negative-tone near-UV photoresist and its applications for MEMS*. Sensors and Actuators A: Physical, 64(1):33–39, 1998.
- [147] MARIE R, et al. *Immobilisation of DNA to polymerised SU-8 photoresist*. Biosens Bioelectron, 21(7):1327–1332, Jan 2006.
- [148] WALTHER F, et al. *Stability of the hydrophilic behavior of oxygen plasma activated SU-8*. Journal of Micromechanics and Microengineering, 17:524, 2007.
- [149] HENNEMEYER M, et al. *Cell proliferation assays on plasma activated SU-8*. Microelectronic Engineering, 85(5-6):1298–1301, 2008.
- [150] WU C, et al. *SU-8 hydrophilic modification by forming copolymer with hydrophilic epoxy molecule*. In *7th International Conference on Miniaturized Chemical and Biochemical Analytical Systems*, pages 5–9. 2003.
- [151] NORDSTRÖM M, et al. *Rendering SU-8 hydrophilic to facilitate use in micro channel fabrication*. Journal of Micromechanics and Microengineering, 14:1614, 2004.
- [152] PENN L, et al. *Deactivation of epoxide-derivatized surfaces*. Macromolecules, 35(7):2859–2860, 2002.
- [153] STANGEGAARD M, et al. *Whole genome expression profiling using DNA microarray for determining biocompatibility of polymeric surfaces*. Mol Biosyst, 2(9):421–428, Sep 2006.
- [154] SIDLER K. *Fabrication and Characterization of SU-8 Cantilevers with Integrated Tips Designed for Dip-Pen Nanolithography*. Ph.D. thesis, Technical University of Denmark AND Swiss Federal Institute of Technology Zurich, 2006.
- [155] LIU M, et al. *Thickness-dependent mechanical properties of polydimethylsiloxane membranes*. Journal of Micromechanics and Microengineering, 19:035028, 2009.
- [156] LAWTON R, et al. *Air plasma treatment of submicron thick PDMS polymer films: effect of oxidation time and storage conditions*. Colloids and Surfaces A: Physicochemical and Engineering Aspects, 253(1-3):213–215, 2005.
- [157] HILLBORG H, et al. *Crosslinked polydimethylsiloxane exposed to*

- oxygen plasma studied by neutron reflectometry and other surface specific techniques.* Polymer, 41(18):6851–6863, 2000.
- [158] MURAKAMI T, et al. *Dynamics of Polymeric Solid Surfaces Treated with Oxygen Plasma: Effect of Aging Media after Plasma Treatment* 1.* Journal of colloid and interface science, 202(1):37–44, 1998.
- [159] EDDINGTON D, et al. *Thermal aging and reduced hydrophobic recovery of polydimethylsiloxane.* Sensors and Actuators B: Chemical, 114(1):170–172, 2006.
- [160] LEE JN, et al. *Compatibility of mammalian cells on surfaces of poly(dimethylsiloxane).* Langmuir, 20(26):11684–11691, Dec 2004.
- [161] CARRÉ A et al. *Study of surface charge properties of minerals and surface-modified substrates by wettability measurements.* Contact Angle, Wettability and Adhesion, 4:1, 2006.
- [162] LORENZ H, et al. *SU-8: a low-cost negative resist for MEMS.* Journal of Micromechanics and Microengineering, 7:121, 1997.
- [163] PATTIER B, et al. *Cheap and robust ultraflat gold surfaces suitable for high-resolution surface modification.* Langmuir, 24(3):821–825, Feb 2008.
- [164] LOSIC D, et al. *Atomically flat gold for biomolecule immobilization and imaging.* Australian journal of chemistry, 54(10):643–648, 2001.
- [165] BHATIA SK, et al. *Use of thiol-terminal silanes and heterobifunctional crosslinkers for immobilization of antibodies on silica surfaces.* Anal Biochem, 178(2):408–413, May 1989.
- [166] ZHOU J, et al. *Recent developments in PDMS surface modification for microfluidic devices.* Electrophoresis, 31(1):2–16, Jan 2010.
- [167] TAO SL, et al. *Surface modification of SU-8 for enhanced biofunctionality and nonfouling properties.* Langmuir, 24(6):2631–2636, Mar 2008.
- [168] KANE RS, et al. *Patterning proteins and cells using soft lithography.* Biomaterials, 20(23-24):2363–2376, Dec 1999.
- [169] HOOGLIET J et al. *Gold thin-film electrodes: an EQCM study of the influence of chromium and titanium adhesion layers on the response.* Electrochimica acta, 47(4):599–611, 2001.
- [170] YANKER DM et al. *Direct printing of trichlorosilanes on glass for selective protein adsorption and cell growth.* Mol Biosyst, 4(6):502–504, Jun 2008.
- [171] LAN S, et al. *Surface modification of silicon and gold-patterned silicon surfaces for improved biocompatibility and cell patterning selectivity.* Biosens Bioelectron, 20(9):1697–1708, Mar 2005.
- [172] REGEHR KJ, et al. *Biological implications of polydimethylsiloxane-based microfluidic cell culture.*

Lab Chip, 9(15):2132–2139, Aug 2009.

- [173] RAHBARI R, et al. *A novel L1 retrotransposon marker for HeLa cell line identification*. Biotechniques, 46(4):277–284, Apr 2009.
- [174] MOSMANN T. *Rapid colorimetric assay for cellular growth and survival: application to proliferation and cytotoxicity assays*. J Immunol Methods, 65(1-2):55–63, Dec 1983.
- [175] BRAET F, et al. *Drying cells for SEM, AFM and TEM by hexamethyldisilazane: a study on hepatic endothelial cells*. Journal of microscopy, 186(1):84–87, 1997.
- [176] OBATAYA I, et al. *Mechanical sensing of the penetration of various nanoneedles into a living cell using atomic force microscopy*. Biosens Bioelectron, 20(8):1652–1655, Feb 2005.
- [177] CARDENAL-MUNOZ E et al. *Testing of Metafectene Easy in human HeLa cells by immunofluorescence and immunoblotting*. Technical report, Departamento de Genetica, Facultad de Biologia, Universidad de Sevilla, 2011.